Recuperation of H_2SO_4 in the hybrid sulphur process using pervaporation

Marco van Rhyn

B.Eng Chemical

Thesis submitted for the degree of

Master of Engineering

North-West University Potchefstroom Campus

Supervisors: Dr. Marco le Roux
Dr. Percy van der Gryp

Potchefstroom

2012

Innovation through diversity ®

NORTH-WEST UNIVERSITY ®
YUNIBESITI YA BOKONE-BOPHIRIMA
NOORDWES-UNIVERSITEIT
POTCHEFSTROOM CAMPUS

ABSTRACT

In this experimental study the sorption and pervaporation characteristics of commercial Nafion-117 and Nafion-212 membranes with mixtures of water (H_2O) and sulfuric acid (H_2SO_4) were investigated. During experimentation the feed concentration and temperature were varied and quantities such as the flux, selectivity and degree of swelling of the membrane were measured. The main objective of the study was to investigate the separation capabilities of the pervaporation process in order to determine if it can effectively replace the existing sulfuric acid recuperation section in the HyS (Hybrid Sulfur) process. The experimentation was conducted over the entire water sulfuric acid concentration range with the temperatures being varied from 25℃ to 55℃.

Both the Nafion membranes were found to be highly selective towards water, with the permeate selectivity ranging from 25 to approximately 930 and flux values increased from approximately 7 mol/(hour.m^2) at 25℃ to approximately 65 mol/(hour.m^2) at 55℃, showing an approximate increase in flux of 900% as the feed temperature of the mixture to the process is increased.. The water can thus be successfully removed from sulfuric acid mixtures by using pervaporation, as it is preferentially absorbed and permeated through both membranes.

The permeation of the components through the membrane was modeled, using the solution-diffusion model. The predicted values showed good agreement with the experimental measurements obtained. The Suzuki and Onozato model, with an exponential dependence of the diffusivity on concentration, gave the best fit for the experimental data with a standard deviation of 97, compared to that of the Greenlaw and Long models, being 161 and 319, respectively.

The separation capabilties of the pervaporation process were compared with the capabilities of the flash separation section proposed in the reference design completed by Savanah Rivers National Laboratory (SRNL) and found to be as effective. It is recommended that the operational and capital costs for implementing these two processes in industry be studied and investigated in detail in order to make an informed decission between these two processes.

Keywords:

Pervaporation; Water-Sulfuric acid separation; Nafion membranes; Sorption; Solution-Diffusion model; Binary-mixture pervaporation

DECLARATION

I, Marco van Rhyn, the undersigned, hereby declare that this dissertation, Recuperation of H_2SO_4 in the Hybrid Sulfur cycle using Pervaporation, is my own work.

_____

Marco van Rhyn

POTCHEFSTROOM

March 2012

ACKNOWLEDGEMENTS

I wish to express my sincere thanks

First and foremost, to our Lord and Saviour Jesus Christ for giving me the talent, strength and persistance to see this research project through and for all the blessings I receive daily.

To my parents, for giving me the opportunity to study and further develop my knowledge and for listening to all my problems and frustrations.

To my supervisors, Marco le Roux, who kept me on the right path throughout and encouraged me to work harder and guided me through the entire learning process, and to Percy van der Gryp for assisting me in matters of which I had little understanding and was always available for some much needed advice.

To my girlfriend and best friend, Laetitia, who served as great encouragement and stood by me in the difficult times, especially the last tedious part of corrections and editing, I am very thankful.

To each and everyone of my friends in Veritas men's residence who accompanied me to the labs in the early hours of the morning to start my experimental runs.

TABLE OF CONTENT

ABSTRACT i

DECLARATION ii

ACKNOWLEDGEMENTS iii

TABLE OF CONTENT iv

NOMENCLATURE vii

LIST OF FIGURES ix

LIST OF TABLES xi

Chapter 1: Introduction **1**

Overview 1

1.1 Background and motivation 1

1.1.1 Hydrogen energy 1

1.1.2 Market and future prospects 2

1.1.3 Hydrogen Production 3

1.1.4 The Hybrid Sulfur cycle 6

1.1.5 Current separation sections 7

1.2 Motivation 9

1.3 Main objectives 9

1.3.1 Hypotheses 10

1.3.2 Scope of investigation 10

Chapter 2: Literature Study **12**

Overview 12

2.1. Pervaporation 12

2.1.1 Background 12

2.1.2 Process description 13

2.1.3 Industrial applications 14

2.1.4 Advantages and disadvantages of Pervaporation 15

2.1.5 Process variables 16

2.2 Characterization of membranes 18

2.2.1 Membrane definition 18

2.2.2 Types of membranes 19

2.2.3 Membrane performance parameters 21

2.2.4 Side effects of membrane use 22

2.2.5 Membrane swelling 23

2.3 Mass transfer through membranes 24
2.3.1 Overview 24
2.3.2 Theory and assumptions of the Solution-Diffusion model 27
2.4 Pervaporation applied for separation of water and sulfuric acid 30
2.4.1 Water and sulfuric acid separation 30
2.4.2 Pervaporation of water and acid mixtures 30

Chapter 3: Experimental 32
Overview 32
3.1 Membranes used 32
3.2 Chemicals used 37
3.3 Pervaporation experiments 37
3.3.1 Apparatus and methodology 37
3.3.2 Experimental equipment 39
3.3.3 Analytical equipment 40
3.4 Experimental planning and design 41
3.4.1 Assumptions regarding pervaporation experiments 41
3.4.2 Experimental design 41
3.4.3 Membrane screening 41
3.4.4 Sorption experiments 43
3.4.5 Pervaporation experiments 43
3.5 Proof of Steady-state and Experimental error 44
3.6 Reproducibility 46

Chapter 4: Experimental Results and Discussions 49
Overview 49
4.1 Pervaporation characteristics of the membranes 49
4.1.1 Influence of operating temperature 49
4.1.2 Influence of feed composition 55
4.2 Sorption characteristics of the membranes 60
4.2.1 Influence of feed composition and temperature 60
4.3 Modeling of pervaporation results 61
4.4 Comparison of separation capabilities 66

Chapter 5: Conclusions and recommendations 70
Overview 70
5.1 Main objective 70
5.2 Pervaporation characteristics 70
5.3 Sorption characteristics 71
5.4 Modeling 71
5.5 Recommendations 72

References **73**

Appendix A: Raw data **82**
A.1 Pure component pervaporation experiments 82
A.1.1 Pure water 82
A.1.2 Pure sulfuric acid 84
A.1.3 Proof of steady-state experiments 86
A.1.4 Pure component repeatability experiments 87
A.2 Binary components pervaporation experiments 90
A.2.1 Sodium hydroxide Titration 91
A.2.2 Binary mixture repeatability experiments 92
A.3 Sorption experiments 93

Appendix B: Calculated data **95**
B.1 Pure component pervaporation experiments 95
B.1.1 Pure water 95
B.1.2 Proof of Steady-state experiments 98
B.1.3 Pure Sulfuric acid 99
B.1.4 Pure component selectivity 101
B.1.5 Pure component repeatability calculations 104
B.2 Binary solution pervaporation experiments 106
B.2.1 Flux determination 106
B.2.2 Sodium Hydroxide titration 107
B.2.3 Binary composition selectivity calculations 109
B.2.4 Binary mixture repeatability experiments 116
B.3 Sorption experiments 116

Appendix C: Statistical inference and experimental error **119**
Overview 119
C.1 Uncertainties and confidence intervals in measurement 119
C.2 Calculations of pervaporation experimental error 121

Appendix D: Modeling of pervaporation results 126

Appendix E: Separation capabilities calculations **129**
E.1 Vapor-liquid equilibrium data 129
E.2 Pervaporation efficiency data 130
E.3 Concentration of sulfuric acid 132

NOMENCLATURE

Symbol	Description	Unit
D_i	diffusion coefficient of component i	m^2/s
DS	degree of swelling	g/g
g_{ij}	binary interaction parameter	-
J	flux	$mol/(hr.m^2)$
k	Darcy's constant	m^2
L	membrane thickness	µm
M	swelling ratio	g/g
n_i	mole fraction of component i	-
P	permeability	$m^3m/(m^2s).Pa.m$
T	temperature	˚C
V_i	molar volume of component i	m^3/mol
W	mass of the swollen or unswollen membrane	g
x	mass fraction of component in feed	g/g
y	mass fraction of component in permeate	g/g

Greek symbol	Description	Unit
α	selectivity (separation factor)	-
β	enrichment factor	-
µ	viscosity	$N.s/m^2$
ε	deviation coefficient	-
μ_i	chemical potential of component i	J/mol
ρ	density	kg/m^3
Ø	volume fraction in ternary phase	-

Abbreviations	Description
Btu	British thermal unit
D	Diffusivity
DOE	Department of Energy
HyS	Hybrid sulfur
HySA	Hydrogen South-Africa
M	molar
MO	Metal-oxide
NHI	Nuclear Hydrogen initiative
PV	Pervaporation
SDE	SO_2-depolarized electrolyzer
TAME	tert-amyl methyl ether
vol	volume
wt	weight

Subscripts	Description
aq	aqueous
g	gas
H_2O	Water
H_2SO_4	Sulfuric acid
i or *j*	component in mixture
ox	oxidation
red	reduction
x	mass fraction of component in feed
y	mass fraction of component in permeate
∞	initial

LIST OF FIGURES

FIGURE 1.1: GROWING US TRANSPORTATION OIL GAP 2
FIGURE 1.2: PRIMARY ENERGY USE BY FUEL (QUADRILLION BTU) 3
FIGURE 1.3: SCHEMATIC OF TWO-STEP HYS CYCLE. 7
FIGURE 1.4: CURRENT H_2SO_4 RECUPERATION SECTION. 8

FIGURE 2.1: SCHEMATIC DIAGRAM OF PERVAPORATION PROCESS 13
FIGURE 2.2: TWO PHASE SYSTEM SEPARATED BY A MEMBRANE PROCESS 19
FIGURE 2.3: PERMEATION OF A ONE-COMPONENT SOLUTION THROUGH A MEMBRANE ACCORDING TO SOLUTION-DIFFUSION MODEL 26
FIGURE 2.4: PERMEATION OF A ONE-COMPONENT SOLUTION THROUGH A MEMBRANE ACCORDING TO PORE FLOW MODEL 26

FIGURE 3.1: SEM IMAGE OF NAFION-117 MEMBRANE 33
FIGURE 3.2: SEM IMAGE OF THE NAFION-212 MEMBRANE 34
FIGURE 3.3: SEM IMAGE OF HIGH TEMPERATURE ALKALINE PBI MEMBRANE 1 35
FIGURE 3.4: SEM IMAGE OF HIGH TEMPERATURE ALKALINE PBI MEMBRANE 2 35
FIGURE 3.5: SEM IMAGE OF LOW TEMPERATURE ACIDIC PBI MEMBRANE 1 36
FIGURE 3.6: SEM IMAGE OF LOW TEMPERATURE ACIDIC PBI MEMBRANE 2 36
FIGURE 3.7: SCHEMATIC DIAGRAM OF STANDARD PERVAPORATION SET-UP 38
FIGURE 3.8: PHOTO OF PERVAPORATION APPARATUS 39
FIGURE 3.9: COLOUR CHANGE OF PHENOLPHTHALEIN DURING TITRATION. ON THE LEFT THE COLOURLESS SOLUTION BEFORE END POINT AND ON THE RIGHT PINK SOLUTION AFTER ENDPOINT. 40
FIGURE 3.10: COMPARISON OF THE RESULTS OBTAINED FROM SCREENING PROCEDURE. 42
FIGURE 3.11: STEADY-STATE DETERMINATION FOR NAFION-212 AT 25˚C. 45
FIGURE 3.12: STEADY-STATE DETERMINATION FOR NAFION-117 AT 25˚C. 46

FIGURE 4.1: INFLUENCE OF OPERATING TEMPERATURE ON TOTAL FLUX THROUGH THE NAFION-212 MEMBRANE USING A PURE WATER FEED. 50
FIGURE 4.2: INFLUENCE OF OPERATING TEMPERATURE ON TOTAL FLUX THROUGH THE NAFION-117 MEMBRANE USING A PURE WATER FEED. 51
FIGURE 4.3: INFLUENCE OF OPERATING TEMPERATURE ON TOTAL FLUX THROUGH THE NAFION-212 MEMBRANE USING A PURE SULFURIC ACID FEED. 52
FIGURE 4.4: INFLUENCE OF OPERATING TEMPERATURE ON TOTAL FLUX THROUGH THE NAFION-117 MEMBRANE USING A PURE SULFURIC ACID FEED. 53

FIGURE 4.5: INFLUENCE OF OPERATING TEMPERATURE ON THE PURE COMPONENT SELECTIVITY FOR BOTH MEMBRANES. 54
FIGURE 4.6: INFLUENCE OF OPERATING TEMPERATURE ON TOTAL FLUX WITH BINARY MIXTURE EXPERIMENTS. 55
FIGURE 4.7: INFLUENCE OF FEED COMPOSITION ON MEMBRANE SELECTIVITY FOR NAFION-212. 56
FIGURE 4.8: INFLUENCE OF FEED COMPOSITION ON MEMBRANE SELECTIVITY FOR NAFION-117. 57
FIGURE 4.9: CALCULATED SPECIES DISTRIBUTION AS A FUNCTION OF PH FOR SULFURIC ACID IN WATER (CASAS *ET AL.*, 2000) 58
FIGURE 4.10: SWELLING RATIOS FOR BOTH NAFION MEMBRANES AT 25˚C AND 55˚C. 60
FIGURE 4.11: COMPARISON OF THE EXPERIMENTAL PERMEATE FLUX AT 55℃ WITH THE GREENLAW MODEL. 62
FIGURE 4.12: COMPARISON OF THE EXPERIMENTAL PERMEATE FLUX AT 55℃ WITH THE LONG MODEL. 63
FIGURE 4.13: COMPARISON OF THE EXPERIMENTAL PERMEATE FLUX AT 55℃ WITH THE SUZUKI AND ONOZATO MODEL. 63
FIGURE 4.14: VAPOR/LIQUID EQUILIBRIUM DIAGRAM USING FLASH SEPARATION. 60

LIST OF TABLES

TABLE 3.1: PROPERTIES OF NAFION 117 AND NAFION 212 MEMBRANES 34
TABLE 3.2: EXPERIMENTAL EQUIPMENT WITH SPECIFICATIONS 39
TABLE 3.3: PLANNING REGARDING REPEATABILITY OF EXPERIMENTAL RESULTS 47

TABLE 4.1: COMPARISON OF STANDARD DEVIATION AND R^2-VALUES OF APPLIED MODELS 64
TABLE4.2: COMPARISON OF LIMITING DIFFUSION COEFFICIENTS AND PLASTICIZATION COEFFICIENTS FOR WATER 64
TABLE 4.3: COMPARISON OF LIMITING DIFFUSION COEFFICIENTS AND PLASTICIZATION COEFFICIENTS .. 65
TABLE 4.4: PERCENTAGE SULFURIC ACID PRESENT IN TOTAL PERMEATE FOR NAFION-212 AT 55˚C 67
TABLE 4.5: CONCENTRATION OF SULFURIC ACID STREAM OBTAINED FOR BOTH THE REFERENCE DESIGN AND PERVAPORATION PROCESS 68

TABLE A.1: PURE WATER DATA FOR NAFION-212 MEMBRANE 82
TABLE A.2: PURE WATER DATA FOR NAFION-117 MEMBRANE 83
TABLE A.3: PURE SULFURIC ACID DATA FOR NAFION-212 MEMBRANE 84
TABLE A.4: PURE SULFURIC ACID DATA FOR NAFION-117 MEMBRANE 85
TABLE A.5: PROOF OF STEADY-STATE EXPERIMENT FOR NAFION-212 MEMBRANE 86
TABLE A.6: PROOF OF STEADY-STATE EXPERIMENT FOR NAFION-117 MEMBRANE 87
TABLE A.7: REPEATABILITY EXPERIMENTS FOR NAFION-212 AND PURE WATER 87
TABLE A.8: REPEATABILITY EXPERIMENTS FOR NAFION-212 AND PURE ACID 88
TABLE A.9: REPEATABILITY EXPERIMENTS FOR NAFION-117 AND PURE WATER 88
TABLE A.10: REPEATABILITY EXPERIMENTS FOR NAFION-117 AND PURE ACID 89
TABLE A.11: TOTAL PERMEATE (G) FOR NAFION-212 MEMBRANE WITH BINARY COMPONENTS 90
TABLE A.12: TOTAL PERMEATE (G) FOR NAFION-117 MEMBRANE WITH BINARY COMPONENTS 90
TABLE A.13: NAOH (G) USED IN SULFURIC ACID TITRATION FOR NAFION-MEMBRANE 91
TABLE A.14: NAOH (G) USED IN SULFURIC ACID TITRATION FOR NAFION-MEMBRANE 92
TABLE A.15: BINARY MIXTURE EXPERIMENTS AT 40 VOL% WATER IN FEED AND 55˚C 92
TABLE A.16: MEASURED RESULTS OF SORPTION EXPERIMENTS FOR NAFION-212 93
TABLE A.17: MEASURED RESULTS OF SORPTION EXPERIMENTS FOR NAFION-117 94

TABLE B.1: CALCULATED PERMEATE FLUX FOR NAFION-212 MEMBRANE WITH PURE WATER 95
TABLE B.2: CALCULATED PERMEATE FLUX FOR NAFION-117 MEMBRANE WITH PURE WATER 97
TABLE B.3: STEADY-STATE CALCULATIONS FOR NAFION-212 MEMBRANE AT 25˚C 98
TABLE B.4: STEADY-STATE CALCULATIONS FOR NAFION-117 MEMBRANE AT 25˚C 98
TABLE B.5: CALCULATED PERMEATE FLUX FOR NAFION-212 MEMBRANE WITH PURE SULFURIC ACID ... 99
TABLE B.6: CALCULATED PERMEATE FLUX FOR NAFION-117 MEMBRANE WITH PURE SULFURIC ACID . 100

TABLE B.7: PURE COMPONENT SELECTIVITY VALUES FOR NAFION-212 MEMBRANE 102
TABLE B.8: PURE COMPONENT SELECTIVITY VALUES FOR NAFION-117 MEMBRANE 103
TABLE B.9: REPEATABILITY EXPERIMENTS FOR NAFION-212 AND PURE COMPONENTS 104
TABLE B.10: REPEATABILITY EXPERIMENTS FOR NAFION-117 AND PURE COMPONENTS 105
TABLE B.11: BINARY FLUX DATA FOR NAFION-212 MEMBRANE..... 106
TABLE B.12: BINARY FLUX DATA FOR NAFION-117 MEMBRANE..... 107
TABLE B.13: H_2SO_4 (X 10^{-3} MOL) PRESENT IN BINARY PERMEATE FOR NAFION-212 MEMBRANE 108
TABLE B.14: H_2SO_4 (X 10^{-3} MOL) PRESENT IN BINARY PERMEATE FOR NAFION-117 MEMBRANE 109
TABLE B.15: H_2SO_4 (G) PRESENT IN BINARY PERMEATE FOR NAFION-212 MEMBRANE..... 110
TABLE B.16: WEIGHT (G) OF WATER IN THE BINARY FLUX FOR THE NAFION-212 MEMBRANE..... 110
TABLE B.17: WEIGHT FRACTION OF WATER IN THE BINARY FEED 111
TABLE B.18: WEIGHT FRACTION WATER IN BINARY PERMEATE FOR THE NAFION-212 MEMBRANE 112
TABLE B.19: MEMBRANE SELECTIVITY FOR A BINARY SOLUTION USING NAFION-212 MEMBRANE 113
TABLE B.20: H_2SO_4 (G) PRESENT IN BINARY PERMEATE FOR NAFION-117 MEMBRANE..... 113
TABLE B.21: WEIGHT (G) OF WATER IN THE BINARY FLUX FOR THE NAFION-117 MEMBRANE..... 114
TABLE B.22: WEIGHT FRACTION WATER IN BINARY PERMEATE FOR THE NAFION-117 MEMBRANE 115
TABLE B.23: MEMBRANE SELECTIVITY FOR A BINARY SOLUTION USING NAFION-117 MEMBRANE 115
TABLE B.24: FLUX VALUES (MOL/HOUR.M^2) FOR THE REPEATABILITY EXPERIMENTS OF THE BINARY MIXTURE 116
TABLE B.25: CALCULATED SWELLING RATIO RESULTS FOR NAFION-212 MEMBRANE..... 117
TABLE B.26: CALCULATED SWELLING RATIO RESULTS FOR NAFION-212 MEMBRANE..... 118

TABLE C.1: Z-VALUES TO BE USED IN TWO-SIDED LARGE-N INTERVALS FOR μ..... 121
TABLEC.2: PURE COMPONENT PERVAPORATION EXPERIMENTAL REPRODUCIBILITY DATA FOR BOTH MEMBRANES..... 121
TABLE C.3: PURE COMPONENT STEADY-STATE μ RESULTS FOR BOTH MEMBRANES 123
TABLEC.4: BINARY MIXTURE PERVAPORATION EXPERIMENTAL REPRODUCIBILITY DATA FOR BOTH MEMBRANES 124
TABLE C5: BINARY MIXTURE STEADY-STATE μ RESULTS FOR BOTH MEMBRANES 125

TABLE D.1: EXPERIMENTAL RESULTS OBTAINED FROM PERVAPORATION EXPERIMENTS 126
TABLE D.2: PREDICTED VALUES OF THE THREE FITTED MODELS..... 127
TABLE D.3: VALUES FOR SD AND MODELING CONSTANTS CALCULATED FOR THE THREE MODELS..... 128

TABLE E.1: VLE DATA FOR THE FLASH SEPARATION OF WATER AND SULFURIC ACID 129
TABLE E.2: PERCENTAGE SULFURIC ACID PRESENT IN TOTAL PERMEATE FOR NAFION-212 AT 25˚C... 130
TABLE E.3: PERCENTAGE SULFURIC ACID PRESENT IN TOTAL PERMEATE FOR NAFION-212 AT 55˚C.. 131
TABLE E.4: PERCENTAGE SULFURIC ACID PRESENT IN TOTAL PERMEATE FOR NAFION-117 AT 25˚C.. 131

TABLE E.5: PERCENTAGE SULFURIC ACID PRESENT IN TOTAL PERMEATE FOR NAFION-117 AT 55˚C .. 131
TABLE E.6: MASS BALANCE CALCULATION FOR NAFION-212 AT 25℃ 132
TABLE E.7: MASS BALANCE CALCULATION FOR NAFION-212 AT 55℃ 132
TABLE E.8: MASS BALANCE CALCULATION FOR NAFION-117 AT 25℃ 133
TABLE E.9: MASS BALANCE CALCULATION FOR NAFION-117 AT 55℃ 133

Chapter 1: Introduction

Overview

In Chapter 1 a general introduction is provided to give the reader a clear indication of what the motivation for this research project was. The chapter will be subdivided into three sections, namely the background, motivation and the main objectives of the research project.

1.1 Background and motivation

1.1.1 Hydrogen energy

In the current climate of ongoing concerns about the future energy demands and the decreasing fossil fuel supply, coupled with the concerns surrounding global warming, great emphasis is placed on finding a cleaner and, more importantly, sustainable, energy source. With the current recognition that the easily obtained fossil fuel resources are limited and steadily decreasing, and that the consumption of these resources for energy needs may have devastating effects on the global climate, alternative pathways to meet this ever increasing demand globally are assuming increased importance (Orme *et al.*, 2009).

On a global scale, the supply of petroleum will be in increasingly higher demand as highly populated and developing countries expand their economies and become more energy intensive (United States Department of Energy, 2006). Government entities around the world are focusing their intention on finding alternative energy sources for the promise that it can be used instead of the fossil fuel resources for various applications. In South Africa one of the main focus areas for an alternative energy source is hydrogen energy. Apart from the advantage that hydrogen energy will decrease the dependency on fossil fuels, it will also play an important part in the fight against global warming. In any scenario where restrictions are in place to minimize the release of carbon dioxide to the atmosphere, the demand for hydrogen will likely increase if non-greenhouse hydrogen production technologies are available at reasonable costs (Forsberg, 2007).

Clean forms of energy are needed to support sustainable global economic growth while minimizing or eliminating impacts on air quality and the potential effects of greenhouse gas emissions (United States Department of Energy, 2006). The effort of researching and developing hydrogen as a viable energy source is led by the United States Department of

Energy (DOE). The primary objective of the DOE is to develop the hydrogen production technologies to produce hydrogen at a cost that can be competitive with alternative fuels while minimizing or eliminating the production of greenhouse gases (Gorensek & Summers, 2009). Hydrogen produced from renewable sources might be considered as the ultimate clean and climate neutral energy system (Gosselink, 2002).

1.1.2 Market and future prospects

For the conversion from a fossil fuel economy to a hydrogen economy, the amount of hydrogen being produced, must be increased significantly (Orme & Jones, 2005). The potential markets that exist for the large-scale production of hydrogen include:

- Production of liquid fuels (gasoline, diesel, jet) including liquid fuels with no net greenhouse emissions (Forsberg, 2007)
- Peak electricity production
- Fertilizer production
- Oil refining
- In future, use as transportation fuel, replacing petroleum (Gorensek & Summers, 2009)

As the demand for clean and affordable hydrogen energy increases, the market for large-scale production of hydrogen will keep expanding. Figure 1.1 shows the actual and projected use of oil for transport purposes in the USA versus the production of oil per day.

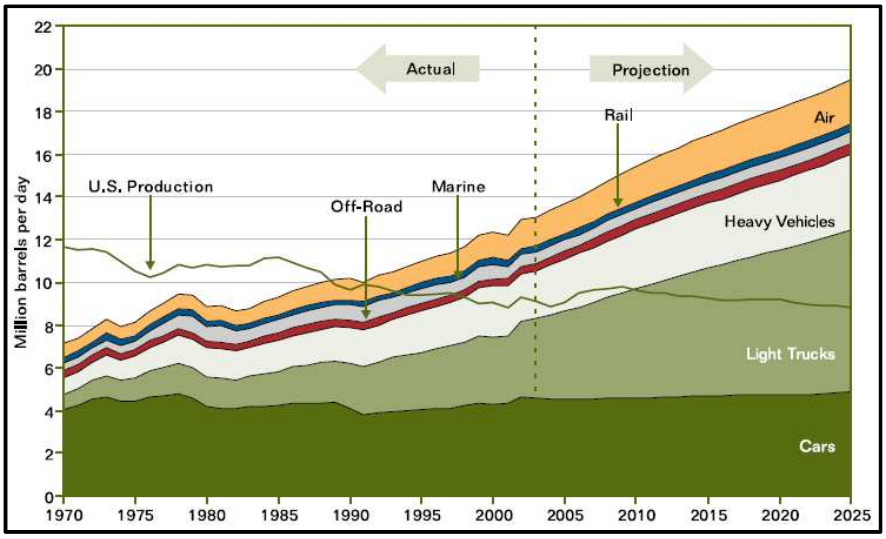

Figure 1.1: Growing US transportation oil gap (United States Department of Energy, 2006)

As can be seen in Figure 1.1 the production of oil will be increasingly insufficient as the demand increases in the near future. The abovementioned phenomenon is also referred to as peak oil. Peak oil can be seen as a certain point in time when the maximum rate of

petroleum extraction will be reached globally, from where on the production rate will enter a phase of terminal decline. Optimistic estimations forecast that the global decline in peak oil production will begin in 2020 (United States Department of Energy, 2006).

Figure 1.2 shows the projection of fuel usage, in quadrillion Btu, as energy source in the United States of America for the next 25 years.

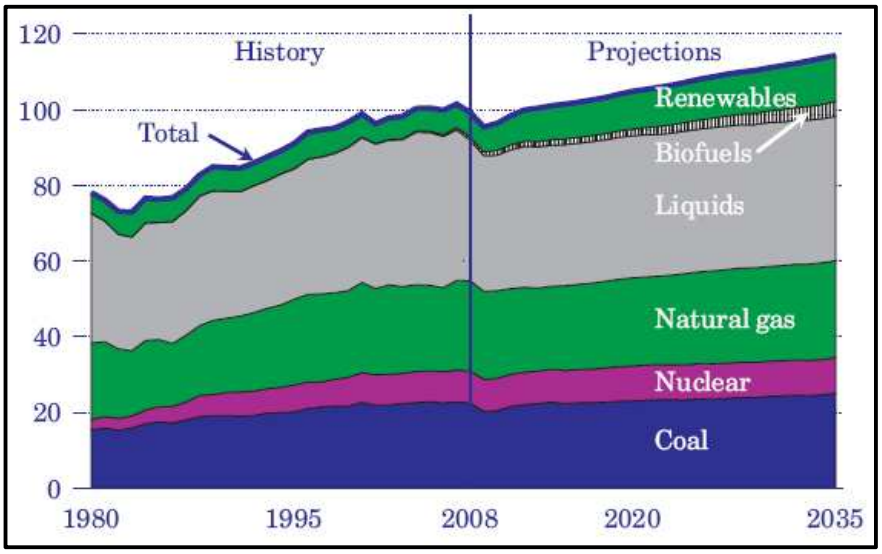

Figure 1.2: Primary energy use by fuel (quadrillion Btu) (Annual energy outlook, 2010)

Figure 1.2 also shows that the projected use of fuel reserves will keep increasing in the future. This data emphasizes the need to find a suitable and affordable replacement for fossil fuels and thus opens up a large market for hydrogen production.

1.1.3 Hydrogen Production

Globally great emphasis is placed on researching alternative pathways for the large-scale production of hydrogen and making it a financially viable energy source (Forsberg, 2007; Gosselink, 2002; United States Department of Energy, 2002). It is not only the processes used for production that are being investigated, but also the energy source needed in the production process that is enjoying great attention. One of the options considered, is the use of nuclear energy as the primary source.

It was proposed by the US Department of Energy's Nuclear Hydrogen Initiative (NHI) that the use of fossil fuels for hydrogen production be replaced by the use of water-splitting, powered by nuclear energy (Gorensek & Summers, 2009). The advantages of nuclear driven hydrogen production include the inherent renewable nature of hydrogen, the reliance of the process on local resources and the absence of CO_2 emissions (Orme & Jones, 2005). Nuclear power plants produce heat as a by-product that can be used directly or converted to electricity in order to produce hydrogen. There is also a considerable amount of research in

progress to finding an energy source that is both sustainable as well as renewable, and solar energy is enjoying much of the attention. When producing hydrogen, there are four main classes of production processes that either already exist or are currently being developed. These include (Forsberg, 2007):

- Traditional electrolysis
- High temperature electrolysis
- Thermochemical cycles
- Hybrid cycles

The electrolysis of water, at low or high temperatures, is a sufficient process for hydrogen production, but is rarely used in industrial applications as a process on its own for large-scale hydrogen production. This is due to the fact that the energy efficiency of water electrolysis is not as good as expected, reported to be in the region of 50-80%. Thermochemical cycles are expected to be more efficient than electrolysis for the production of hydrogen as their energy efficiency is not limited by the conversion of heat to electricity (Charvin *et al.,*2008).

Thermochemical cycles consist of the multi-step thermal dissociation of water into the elemental hydrogen and oxygen. Chemical intermediates are involved in exothermic reactions that generate hydrogen by water-splitting, and in endothermic reactions that release oxygen (Charvin & Abanades, 2008). These exothermic and endothermic reactions can be illustrated by the following equations:

$$MO_{RED} + H_2O \rightarrow MO_{OX} + H_2 \quad (1\text{-}1)$$

$$MO_{OX} + \text{thermal energy} \rightarrow MO_{RED} + {}^{1}/_{2}O_2 \quad (1\text{-}2)$$

Abanades *et al.* (2005) state that a database comprising 280 thermochemical water-splitting cycles was developed at PROMES-CNRS. From this database roughly 30 potential cycles for hydrogen production, consisting mainly of two-step and three-step cycles were identified. These cycles were indentified because of the ease of operation of these two or three step cycles, the reduction of operating costs, as well as the potential of incorporating them with renewable energy sources, such as solar energy.

Hybrid cycles

The term “hybrid” describes a mixture of two or more components used in conjunction, and in terms of the production cycle it refers to the electrochemical nature of one of the steps, which requires electrical as well as thermal energy to be supplied to the process (Gorensek & Summers, 2009). Thus a hybrid cycle is essentially a thermochemical cycle where electrical energy is used in one of the processing steps.

There are a few hybrid thermochemical cycles currently under development, which include the following:

- Copper-chlorine thermochemical cycle: This cycle consists of three thermal reactions and one electrochemical reaction, and is thus a hybrid cycle. The cycle consists of five steps, with a chemical reaction occurring in each step, except for drying (Orhan *et al.*, 2010). The electrochemical step is the third step of the cycle where solid copper monochloride and water react endothermically, and solid copper and a copper chloride-water solution are produced. In the fifth step, which is the hydrogen production step, copper and hydrochloric acid enter and are converted to gaseous hydrogen and solid copper monochloride (CuCl) (Orhan *et al.*, 2010).
- Copper oxide-copper sulfate water splitting thermochemical cycle: This cycle consists of two principle steps, namely hydrogen production from the electrolysis of water, SO_2 and CuO and the second step, namely the thermal decomposition of $CuSO_4$ to form O_2 and SO_2, which are recycled (Gonzales *et al.*, 2009). This cycle uses three reagents and only produces hydrogen and oxygen as products.
- Sulfur-iodine cycle: The sulfur-iodine cycle, which is a purely thermochemical cycle, consists of two oxidation-reduction cycles based on sulfur and iodine. This cycle is made up of three chemical reactions (Orme *et al.*, 2009):
  - $SO_2 + I_2 + 2H_20 \rightarrow H_2SO_4 + 2HI$ (1-3)
  - $2HI \rightarrow H_2 + I_2$ (1-4)
  - $2H_2SO_4 \rightarrow 2H_2O + 2SO_2 + O_2$ (1-5)
- Hybrid-sulfur cycle: An electrochemical variant of the sulfur-iodine cycle, where hydrogen is generated through the electrolysis of water in the presence of SO_2 and sulfuric acid is produced (Orme *et al.*, 2009).

In the current energy climate reigning in South Africa great emphasis is placed on developing cleaner and sustainable energy sources, with hydrogen energy being one of the most promising. Hydrogen South Africa (HySA) has developed an infrastructure which aims to create a knowledge base on hydrogen production in South Africa. The aim is not only to further investigate and develop the existing Hybrid Sulfur (HyS) cycle but for the people

involved to gather the “know-how” and use this knowledge, working towards the goal of converting to a hydrogen economy. The HySA infrastructure initiated a 5-year plan in cooperation with the North-West University with the goal in mind to gather the necessary knowledge and skills to make hydrogen energy a reality in South Africa. In the following section the Hybrid Sulfur Cycle will be investigated thoroughly.

1.1.4 The Hybrid Sulfur cycle

The hybrid sulfur cycle (HyS) was first proposed in 1975 by Brecher and Wu at the Westinghouse Electric Corporation. The process was then developed further in the 1970s and 1980s by Farbman (1976), Lu and Ammon (1980) and Parker (1983). As a result of the research done by the corporation the HyS cycle came to be known as the Westinghouse process (Brecker *et al.*, 1977).

The HyS cycle is one of the simplest thermochemical cycles, comprising only two steps and only fluid reactants. The hybrid acknowledges the electrochemical nature of one of the steps, where both electrical and thermal energy need to be supplied to the process (Gorensek & Summers, 2009). The HyS cycle is categorized as a sulfur cycle, as it entails sulfur oxidation and reduction.

Process description

In the first step of the HyS cycle, which takes place in all sulfur cycles, sulfuric acid is decomposed to water and sulfur dioxide,

$$H_2SO_4 \rightarrow H_2O + SO_2 + {}^1/_2O_2 \qquad (1\text{-}6)$$

This reaction is the result of two separate reactions. As the sulfuric acid is vaporized and superheated in the acid decomposition reactor, it spontaneously decomposes into H_20 and SO_3,

$$H_2SO_4\,(aq) \rightarrow H_2O\,(g) + SO_3\,(g) \qquad (1\text{-}7)$$

Further heating to temperatures in excess of 800˚C in the presence of a catalyst drives the endothermic decomposition of SO_3 into O_2 and SO_2 (Gorensek & Summers, 2009),

$$SO_3\,(g) \rightarrow SO_2\,(g) + {}^1/_2O_2\,(g) \qquad (1\text{-}8)$$

In Figure 1.3, taken from Gorensek and Summers (2009), a simple schematic of the HyS cycle is shown.

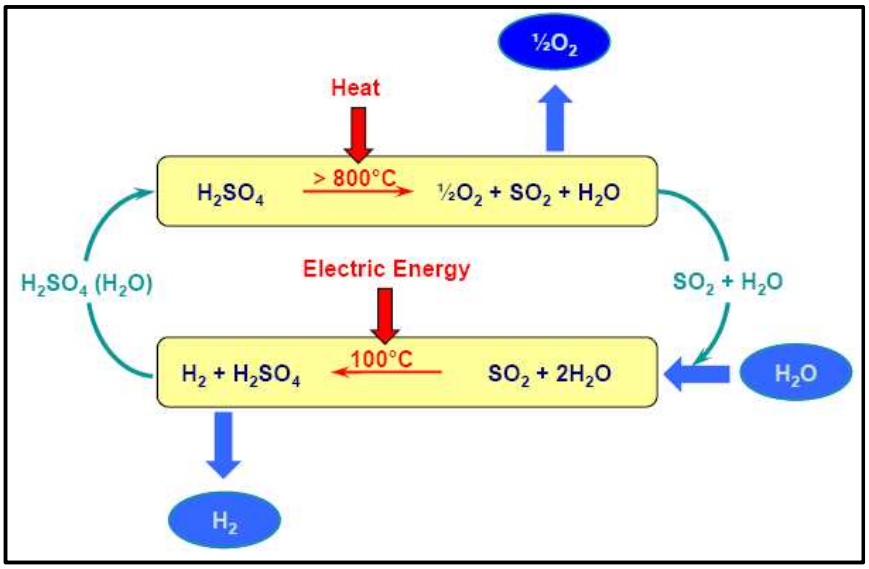

Figure 1.3: Schematic of two-step HyS cycle (Gorensek & Summers, 2009).

As can be seen in Figure 1.3, after the first step oxygen is removed from the process as co-product. After the removal of the co-product, the SO_2 and H_2O are combined with make-up water and recycled H_2SO_4 and fed to the anode side of the SO_2-depolarized electrolyzer, where the second reaction takes place (Gorensek & Summers, 2009). This is the electrolysis of water,

$$2H_2O + SO_2 \rightarrow H_2SO_4 + H_2 \qquad (1\text{-}9)$$

SO_2 is electrochemically oxidized at the anode to form H_2SO_4, electrons and protons,

$$SO_2\ (aq) + 2H_2O \rightarrow H_2SO_4\ (aq) + 2H^+ + 2e^- \qquad (1\text{-}10)$$

The protons that are formed are conducted across the electrolyte separator to the cathode side where they are recombined with the electrons that pass through an external circuit to form H_2 (Leybros *et al.*, 2010),

$$2H^+ + 2e^- \rightarrow H_2\ (g) \qquad (1\text{-}11)$$

The H_2SO_4 produced in the second step by the electrolyzer is then recycled back to the high temperature reactor from the first step to make this a closed cycle. The hydrogen produced at the SO_2-depolarized electrolyzer is removed from the process as the principle product.

1.1.5 Current separation sections

During the reference design conducted on the HyS cycle by Savannah River National Laboratory, it was proposed that the sulfuric acid that is produced during the electrolysis step of SO_2 and H_2O be recuperated, using a series of vapor-liquid separation steps. The sulfuric

acid that is recuperated, can then be circulated back to the decomposition reactor for anolyte production, thus entailing a self-proficient cycle.

The main purpose of the recuperation section is to first and foremost produce a purified feed stream to be sent to the decomposition step, which consists of 75 wt % H_2SO_4 and 25 wt % H_2O (Le Roux & Hattingh, 2010). For these specifications to be met, SO_2, O_2 and H_2O must subsequently be removed. The difference in boiling point between these substances favors the use of vapor liquid separation techniques such as distillation and flash drums. In the proposed recuperation section the O_2 and SO_2 are almost entirely removed in the first flash separation process, thus for the purpose of this research project, only the separation of H_2O and H_2SO_4 is considered.

Figure 1.4 below shows the current H_2SO_4 recuperation section as proposed for the HyS cycle.

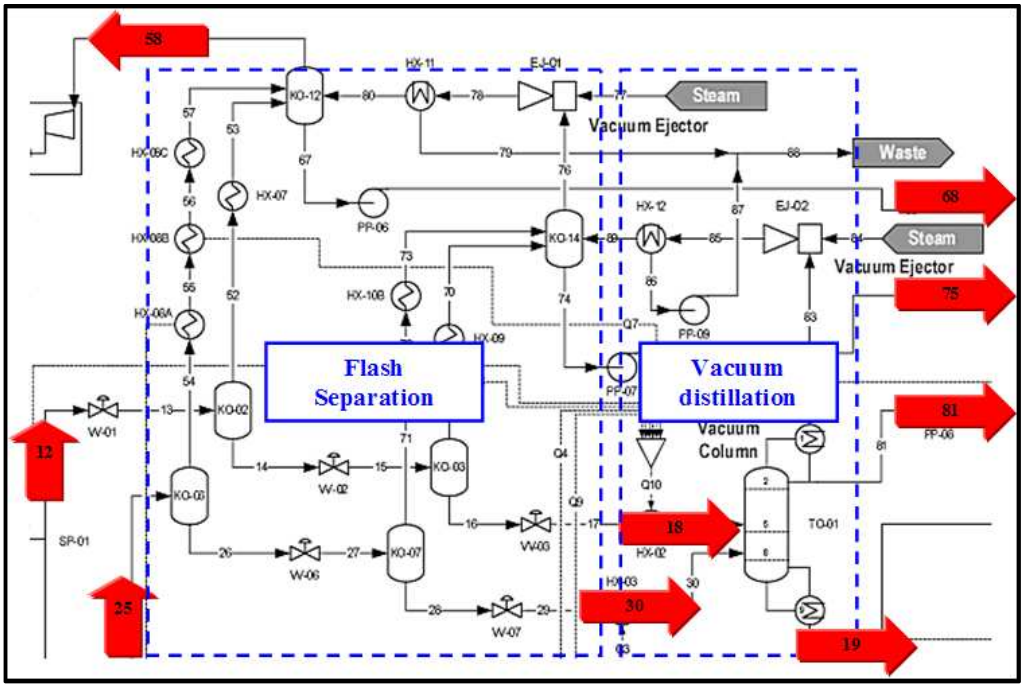

Figure 1.4: Current H_2SO_4 recuperation section. Adapted from (Gorensek & Summers, 2009).

As can be seen in Figure 1.4, the recuperation section can be divided into a flash separation section and a vacuum distillation section. This current design consists of a very large number of processing equipment and is operated under extreme temperatures and pressures, which all contribute to making this a very costly and energy intensive process.

One of the options investigated for replacing the current recuperation section is to use membrane separation techniques. A few membrane technologies have been identified that

could be incorporated into the recuperation section, with pervaporation for H_2SO_4 recovery being one of the more promising options.

1.2 Motivation

One of the projects proposed, was to investigate the feasibility of using membrane technology in the sulfuric acid recuperation section. Using pervaporation as a process application is increasingly becoming more popular. The pervaporation process will be discussed in great detail in Chapter 2. The process has been used for similar applications and the following advantages for using pervaporation for these specific applications have been identified:

- Excellent efficiency for H_2SO_4/H_2O separation can be obtained with more than 80% of water removal.
- Membranes are being developed that resist degradation due to the presence of H_2SO_4.
- It can effectively replace vacuum distillation in the recuperation phase and can be operated at ambient conditions compared to the high temperatures and pressures of the proposed process.

1.3 Main objectives

The main purpose of this study is to investigate the possibility of concentrating a binary mixture of sulfuric acid and water by selectively removing the water from the mixture using a pervaporation process. The efficiency of different membranes are tested using the pervaporation process as well as determining which operating conditions tend to give the best results and what trends can be seen from these results. From the obtained results the technical feasibility of using pervaporation for this specific application are analyzed by comparing the results obtained to the data from the proposed separation section which uses flash drums. Furthermore, an economical feasibility study is completed to compare the existing separation to the proposed application, taking into account energy and operating costs.

The two main parameters being investigated with pervaporation are the flux and the membrane selectivity. The parameters are determined for different membranes and operating conditions. The operating conditions which play a role in the functioning of the

pervaporation process include temperature, as well as the concentration of the main permeant in the feed, and the effect of these conditions on the main parameters are monitored.

1.3.1 Hypotheses

Pervaporation has been applied in industrial applications for several separation or concentration purposes. There is little information available on the use of pervaporation for the specific application as it is used in this research project. From literature certain trends in the results obtained from extensive experimentation can be observed, and these trends are found to be applicable to a wide range of membranes and feed mixtures used. Thus the hypothesis of this research project is that the following results will be obtained from the experimentation:

- The permeate flux increases with the increase in weight percent water in the feed mixture.
- The membrane selectivity decreases with the increase in weight percent water in the feed mixture.
- The flux and the selectivity will increase with the increase in temperature.

1.3.2 Scope of investigation

The dissertation is subdivided into five chapters consisting of the following:

- Chapter 2 gives an overview of the terminology and current literature on the pervaporation process, and all other relevant subjects. The purpose of this chapter is to acquire the necessary background knowledge and to investigate previous work done on similar applications.
- In Chapter 3 the experimental methodology used is discussed in great detail, including the apparatus and the set-up used for all experimentation. The two aspects of the experimental procedure, namely the pervaporation and the sorption experiments, are discussed.
- The results obtained from the extensive experimentation for both the pervaporation and sorption experiments are discussed in Chapter 4. The results are analyzed in order to verify if the pervaporation application is suitable for the specified purpose. The obtained results are also verified by modeling the data and comparing it to existing mathematical models. Lastly the pervaporation results achieved is compared to results obtainable from using the proposed flash separation process.

- Finally, in Chapter 5 the discussion and main conclusions are drawn with some recommendations given for further studies.

Chapter 2: Literature Study

Overview

In Chapter 2 of the dissertation the literature concerning the research project is studied in detail. All the necessary background knowledge to fully understand the scope of the dissertation is given and explained. In Section 2.1 of the chapter the pervaporation process is discussed in detail, focusing on the process description, applications, advantages and disadvantages, process variables and certain membrane properties.

In Section 2.2 the characterization of membranes is discussed, including definitions, performance parameters, side effects of membrane use, membrane swelling and different types of membranes. Section 2.3 explains the mass transport through membranes. In Section 2.4 the application of pervaporation for the separation of water and sulfuric acid mixtures found in literature is studied. Finally, Section 2.5 investigates the theory and assumptions concerning the solution diffusion model, focusing on mass transport and diffusion coefficients.

2.1. Pervaporation

2.1.1 Background

Although the research on pervaporation and all its applications have received great attention in the past decade, the original concept has been around for a long time. The idea of pervaporation was first observed by Kober (1917) when his assistant noted that liquid kept in a collodion bag which was suspended in the air, evaporated. He coined the phrase pervaporation, which is a combination of two separate words, namely permeation and evaporation. His finding was that collodion and parchment membrane containers permit water to evaporate through the walls as if no membrane was present (Kober, 1917).

The first quantitative work on pervaporation was published by Heisler (1956). His work was done on aqueous alcoholic solutions and the effects of temperature and solute concentration on the pervaporation experiments. However, the great potential of pervaporation for industrial applications was only recognized after the publication of Binning *et al.* (1961). Binning *et al.* did their work on the liquid phase permeation through thin plastic films for the separation of azeotropes and other organic mixtures.

The advances that have been made in the pervaporation as well as the membrane technologies during the past decades have ensured that they have become an indispensable part of the chemical industry. The first industrial applications of pervaporation were aimed at water/alcohol separation. The first pilot plant was commissioned in Brazil in 1982, where the goal was to remove water from ethanol. Pervaporation as a membrane-based technology is widely used for purification and concentration of fluid mixtures. Today pervaporation is considered as an operating unit with various environmental, energy and chemical processes (Marx *et al.*, 2002).

2.1.2 Process description

In literature there are numerous descriptions of the definition of the pervaporation process (Lipnizki *et al.*, 1999). Pervaporation is a membrane separation technique where the phase state on one side of the membrane is different than that on the other side (Seader & Henley, 2006). In pervaporation the liquid feed mixture that needs to be separated, is contacted with one side of a permselective membrane, and the permeated product is removed as low pressure vapor on the other side of the membrane (Feng & Haung, 1997).

Figure 2.1, adapted from Feng & Haung (1997), shows a simple illustration of the basic working of the pervaporation process.

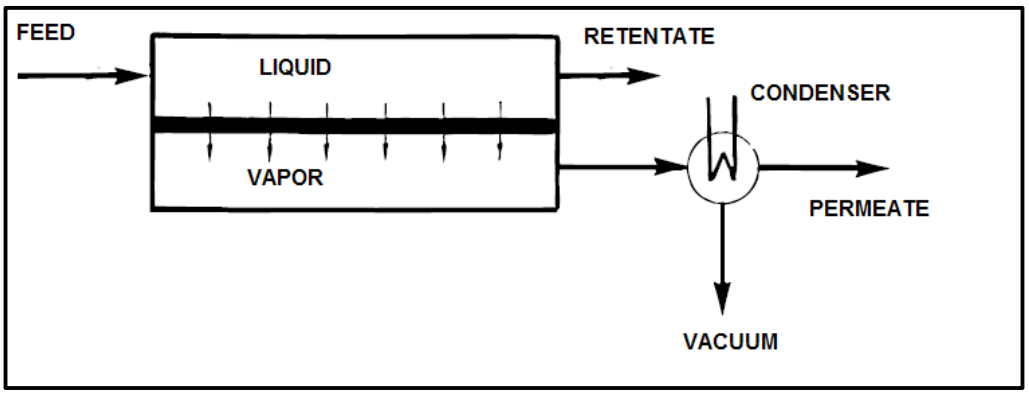

Figure 2.1: Schematic diagram of pervaporation process

The liquid feed is fed to the membrane module where the permeate side is kept at a constant pressure below the partial pressure of the feed liquid. Therefore a vapor pressure difference is established between the feed and permeate side, which acts as the driving force of separation between species. The driving force can be obtained by applying a vacuum pump or an inert purge on the permeate side.

When separating mixtures using pervaporation, the separation is not dependent on the volatility of the components in the mixture that needs to be separated, but rather on the relative affinity of the membrane for one of the components in the mixture (Marx, 2002).

Theoretically, separation of any kind of liquid mixture is obtainable by changing the properties and nature of the membrane, thus making it permselective towards one of the components in the mixture. Pervaporation works most effectively when the feed to the process is dilute in the main permeant. If too much permeant is present in the feed, it may require a number of membrane stages, with only a small amount of permeate produced per stage (Seader & Henley, 2006).

According to Binning (1961), permeation involves three steps:

- Solution of liquid in the film surface in contact with the liquid charge mixture.
- Migration through the body of the film.
- Vaporization of the permeating material at the downstream interface where permeate product is immediately swept away (Binning, Lee, & Jennings, 1961).

For further general reading of the applications of pervaporation, see for example Dutta *et al*. (1997), Sun & Haung (1995) and Zhang and Drioli (1995).

2.1.3 Industrial applications

In the section above the process described is commonly referred to as vacuum pervaporation or standard pervaporation. This is the most widely used mode of pervaporation. The other form of pervaporation regularly used, is inert purge pervaporation, which is applied if the permeate can be discharged without condensation. Apart from the abovementioned processes, there are numerous other processes, including:

- Thermal pervaporation
- Perstraction or osmotic distillation
- Saturated vapor permeation
- Pressure driven pervaporation (Feng & Haung, 1997).

The application of pervaporation can be classified in three main categories (van der Gryp, 2003):

- Hydrophilic pervaporation (dehydration of organic solvent)
- Hydrophobic pervaporation (removal of organic compounds from aqueous solutions)
- Organophilic pervaporation (removal of organic compound from an organic mixture)

Each of these applications will be overviewed briefly.

Hydrophilic pervaporation

One of the main applications of pervaporation is the dehydration of organics, including ethanol, isopropanol and ethylene glycol. The purpose of this class of pervaporation is to

remove water from aqueous-organic mixtures by preferentially permeating the compound through the membrane. This form of pervaporation is applied in several fields, including the breaking of azeotropic or binary mixtures, batch wise dehydration in discontinuous processes and dehydration of multicomponent mixtures. At the end of the 1990s there were approximately seventy commercial plants for alcohol dehydration operating around the world (Dutta *et al.*, 1997).

Hydrophobic pervaporation

In hydrophobic pervaporation the aim is to remove the organic compounds from aqueous-organic mixtures by preferentially permeating the organic compound through the membrane. Although pervaporation is mainly applied in the chemical processing industry, it can also be used for other applications such as removal of organic traces from ground or drinking water, removal of alcohol from beer or wine and the separation of compounds from a fermentation broth in biotechnology.

One area where hydrophobic pervaporation is also used, is in environmental applications for the removal of volatile organic compounds (VOCs) from wastewater (Mulder, 1996). Previous methods of wastewater treatment such as adsorption or bioremediation can be quite expensive, thus pervaporation can be a viable alternative.

Organophilic pervaporation

Organophilic pervaporation generally works on the same concept as the hydrophilic pervaporation in that it aims to preferentially remove organic compounds. The only difference is that it removes these organic compounds from organic-organic mixtures rather than from aqueous-organic mixtures. Its main application is to remove alcohols that form azeotropes with other compounds such as aromatics, ether and esters.

2.1.4 Advantages and disadvantages of Pervaporation

One of the greatest advantages of the pervaporation process is that the energy consumption of the process is minimized. Furthermore, pervaporation has shown to be very effective in separating close-boiling or azeotropic mixtures which create problems in other separation methods. The operating unit itself is simple and easy to operate and maintain and it takes up less space than operating units like distillation columns.

The drawbacks that can be experienced when using a pervaporation process include (Mulder, 1996):

- Membranes for specific applications that are a good trade-off between high flux rates and sufficient separation factors are not always readily available.
- The maintenance of the vacuum unit can be expensive.

- A large number of membrane modules might be needed to handle larger loads in industrial applications.
- Membranes can be prone to degradation which will lead to a short membrane lifetime, thus increasing the operational cost of applying pervaporation in industry.

2.1.5 Process variables

When conducting pervaporation experiments it is of the utmost importance to understand the effects that the operating conditions may have on permeation flux and separation factor values. The process variables that influence the obtained values are feed composition and temperature, the permeate pressure and the membrane properties.

Feed composition

The feed composition is one of the most important determining factors of the permeation flux and selectivity when working with pervaporation experiments. When there is a fluid mixture to be pervaporated, there is always one component that will preferentially permeate through the membrane, and the concentration of this component in the feed determines the flux and selectivity values.

In experiments conducted by Orme *et al.* (2009), where they concentrated a HI/water feed, they noted that there was a positive correlation between the flux of water and the concentration of water in the feed. Furthermore, the inverse was observed for the separation factor, which decreased as the water concentration increased. The same trend was observed when a HI/Iodine feed was used (Ginosar & Stewart, 2007). Park *et al.* (1995), who conducted work on the separation of methanol from MTBE, where methanol preferentially permeated through the membrane, found that the permeate flux decreased with an increase in poly(vinyl alcohol) concentration, and selectivity increased accordingly.

Thus, from the abovementioned literature, it can be concluded that the permeation flux increases with the increase in concentration of the component which preferentially permeates while the selectivity decreases.

Temperature

Since the liquid feed stream is the only carrier that provides thermal energy to the pervaporation process, there is great incentive to operate the pervaporation experiments at elevated temperatures (van der Gryp, 2003). Goldblatt and Gooding (1986) stated that a higher temperature feed stream led to higher diffusion rates and higher fluxes, which they presumed was caused by the increased thermal motion of the polymer chains and diffusing species.

In general, an increase in temperature causes an increase in permeation flux and a slight decrease in selectivity (Binning *et al.*, 1961). The same trend was noted by Orme *et al.* (2009). In their work on the separation of methanol from a methanol/TAME mixture using pervaporation, Marx *et al.* (2002) found that the total flux of methanol permeating through the membrane increased, as well as the partial fluxes. The experiments conducted by Park *et al.* (1995) on the methanol/MTBE separation also showed an increase in flux with an increase in temperature, but the selectivity stayed constant.

Thus it can be concluded from the literature mentioned that the increase in temperature is normally accompanied by an increase in total permeation flux and that the selectivity will slightly decrease or remain constant.

Permeate pressure

As the main driving force in pervaporation is the pressure gradient, it is obvious that an increase in permeate pressure will have a decrease in flux as result. In other words, the permeation rate of any single feed component will increase as its partial permeate pressure is lowered. The effect that the permeate pressure has on the efficiency of the pervaporation process is dictated by the magnitude of the respective vapor pressures, as well as the difference in vapor pressures between them (van der Gryp, 2003).

The optimum permeate pressure for a specific application is chosen in such a manner that the driving force for the permeation is maximized, while still keeping the process economically feasible.

Membrane properties

There are two properties of membranes that play an important role in the functioning of pervaporation processes, namely the thickness and the molecular structure. It is generally accepted that flux is inversely proportional to the membrane thickness, thus thin membranes will generate higher flux values. This was confirmed by Orme *et al.* (2009) when they concentrated HI from an aqueous solution using two different thickness Nafion membranes. Although the membranes had the exact same molecular structure, the thinner membrane produced superior flux rates.

How a membrane behaves, can depend greatly on the orientation of the membrane with respect to the permeate flow. It is generally observed that the selectivity values are the highest when the dense selective layer faces the feed mixture (Neel, 1991).

One other area that also influences the performance of pervaporation is membrane pretreatment. Since the swelling of a particular membrane plays an important role in determining the flux, pre-swelling the membrane with feed mixture or a suitable solvent may

increase the flux considerably (van der Gryp, 2003). In experiments conducted by Orme and Jones (2005), they found that by pretreating the membrane, they could effectively control the pore size. By reducing the pore size they decreased the flux, but the separation factor was increased by an order of magnitude.

In the following section the specific characteristics of membranes will be investigated to shed a greater light on how they may influence the working of the pervaporation processes.

2.2 Characterization of membranes

Membrane based technology is fast becoming a new frontier of chemical engineering processes during the past decade and the use of membranes in a variety of industries has become an indispensable component in the processing industry. Membrane applications include concentration, purification, desalination and the fractioning of fluid mixtures (Feng & Haung, 1997).

2.2.1 Membrane definition

According to Mulder (1996) a membrane can be defined as a permselective barrier between two separate phases (Strathman, 2005). The phase from which the mass transfer occurs, is commonly referred to as the donor, feed or upstream phase, while the phase that receives the flow is called the acceptor, permeate or downstream phase (Pinto & Laespada, 1999). Figure 2.2 shows a schematic representation of a typical membrane separation process.

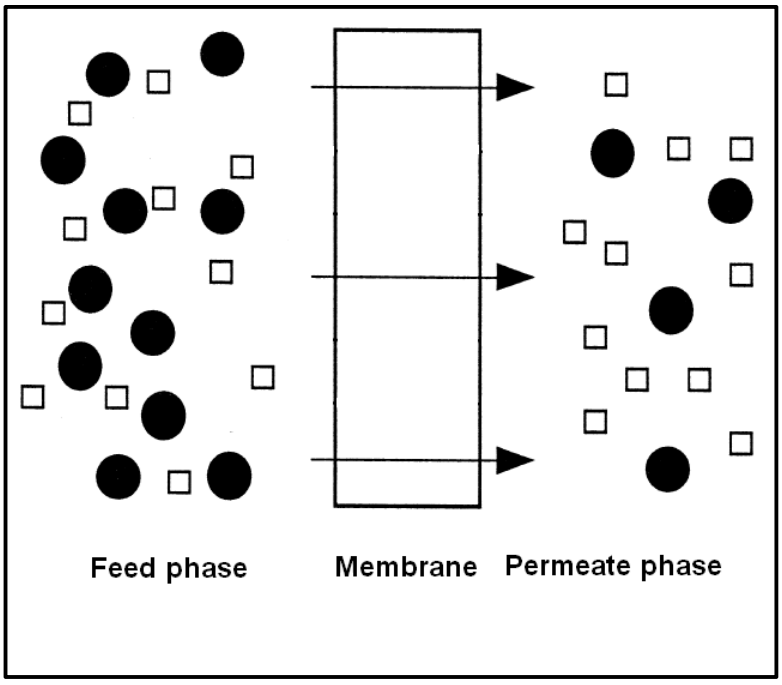

Figure 2.2: Two-phase system separated by a membrane process. Adapted from (Pinto & Laespada, 1999)

In a two-phase or even multi-phase system, separation through membrane processes is achieved through the use of a certain driving force. With the help of a specific driving force across the membrane, the membrane has the ability to transport one of the components in the donor or feed side more readily than the other components that may be present in the feed, thus making it permselective. These driving forces can include the partial pressure difference, concentration difference or the chemical potential difference.

The magnitude of the driving force across the membrane is determined by the difference in potential across the membrane, divided by the thickness of the specific membrane. It is possible for one or several of the abovementioned driving forces to contribute to the overall driving force over the membrane.

2.2.2 Types of membranes

As membrane technology has become an increasingly integral part of the processing industry, the amount of membranes produced has increased dramatically as the need for membranes for specific applications is ever growing. There are several aspects to take into consideration when choosing the specific material for the membrane, including application, economic considerations and the environment in which it will be applied. Membranes can be made from organic or inorganic materials which include metals or ceramics, homogenous films (polymers), heterogeneous solids (polymeric mixes) and liquids (Perry & Green, 1997).

Ceramic membranes are generally produced from inorganic materials such as silicon carbides, aluminum and zirconium oxides. One of the advantages of using ceramic membranes is that they are very resistant to the aggressive media or harsh environments such as acids, strong solvents or high temperatures. These membranes are also chemically, thermally and mechanically stable and have long working lives. On the downside they might have substantial capital costs with regard to production and lower selectivity in certain applications.

Liquid membranes refer to a type of synthetic membrane that is made of non-rigid materials. There are several types of liquid membranes currently produced, including immobilized (supported) liquid membranes, emulsion membranes, molten salts and hollow-fiber contained membranes (Perry & Green, 1997). These abovementioned membranes are studied intensively but there aren't many commercial applications at present.

Polymeric membranes

Polymeric membranes have so far dominated the membrane separation industry as they are very competitive in both performance as well as economic considerations. These membranes are applied in various industrial applications such as desalination of sea water, gas separation, food and beverage processing, hemodialysis and slow release (van der Gryp, 2003). The main applications for polymeric membranes include ultra filtration, dialysis, microfiltration and importantly, pervaporation.

To choose a specific membrane polymer is not an easy task, as the polymer has to have the appropriate characteristics for the intended application. Some of the aspects to be taken into consideration may include the following (Zeman & Zydney, 1996):

- Polymer has to offer low binding affinity for separated molecules (biotechnology).
- May be able to withstand harsh cleaning conditions.
- Must be compatible with the membrane fabrication process.
- The polymer has to have a suitable form in terms of its chain rigidity, chain interactions and the polarity of its functional groups.
- It has to be easily obtainable and reasonably priced.

Not all the abovementioned aspects need to be taken into consideration for every application, but they act as a guideline for choosing a certain polymer. The most common polymers used for membrane synthesis are cellulose acetates, nitrates, polysulfone (PS), polyether sulfone (PES), polyethylene and polypropylene (PE and PP) and polyvinylchloride (PVC) (Zeman & Zydney, 1996).

For the use in pervaporation, dense polymeric membranes are required, preferably with an anisotropic morphology, as well as an asymmetric structure containing a dense top layer and open porous sublayers (Mulder, 1996). Previous research showed that, in general, polar molecules permeate faster through polar membranes than non-polar molecules, and *vice versa* (Park *et al*., 1995). Thus polar polymers such as polyvinylalcohol, cellulose acetate and more importantly, Nafion, were found to be selectively permeable for polar molecules.

Nafion membranes are non-reinforced films based on Nafion PFSA polymer, a perfluorosulfonic acid/PTFE copolymer in the acid (H+) form.

2.2.3 Membrane performance parameters

The performance of a membrane is rated on the basis of two criteria: firstly on the amount of permeate it produces, and secondly on its ability to distinguish between compounds in a feed which it retains and those which it allows to pass through. Thus the effectiveness of the membrane to separate compounds in a liquid mixture can be characterized by the flux and selectivity, respectively (Dutta *et al.*, 1997).

The productivity of the membrane, or as mentioned above the permeation flux, is a measure of the amount of component that will permeate through a specific membrane surface area in a given time unit (Marx *et al*, 2002). The flux is most commonly expressed in the following units (kg/m^2.hr or kmol/m^2.hr). The selectivity of the membrane can be quantified by two alternative dimensionless parameters, namely the selectivity (α) and the enrichment factor (β). The selectivity ratio can be quantified by the following dimensionless ratio (Neel, 1995)

$$\alpha_i = \frac{y_i/(1-y_i)}{x_i/(1-x_i)} \qquad (2\text{-}1)$$

where i represents the preferentially permeating species and x and y represent the mass fraction of each of the components in the feed and permeate, respectively.

On the other hand, the enrichment factor (β) indicates the ratio of concentrations in the feed and permeate of the preferentially permeating species (Dutta *et al.*, 1997)

$$\beta_i = \frac{y_i}{x_i} \qquad (2\text{-}2)$$

The values of the abovementioned parameters can be related to one another by using the following relationship

$$\alpha_i = \beta \frac{(1-x_i)}{1-\beta x_i} \qquad (2\text{-}3)$$

This parameter is more commonly used and is similar to the membrane selectivity or separation factor. It is clear that these parameters are of no use if the feed composition to the membrane is not specified.

2.2.4 Side effects of membrane use

When using membrane processes for separation, there exist different occurrences which may influence the overall performance of the membranes, and can have negative effects on the entire process.

Fouling

When membrane processes are used for separation of liquid feeds, fouling is one of the problems that is most frequently encountered. According to Humphrey (1997) fouling can be seen as a process where the membrane surface is coated or blocked by a solid or gelatinous material, and this blockage creates a barrier through which the permeating species must pass. Because of this fouling or blockage of the membrane surface, the effect on the performance is a decrease in flux through the membrane. Other effects may include the formation of a second, nonselective resistance which may have the effect of decreasing the overall selectivity of the membrane (van der Gryp, 2003).

Plasticizing effect

When separating liquid feeds with membrane processes, the liquids may exhibit a high solubility in polymeric membranes. When there is a high concentration of permeant in the membrane, it can greatly influence the diffusion coefficients of the permeant. The high concentration of permeant present in the membrane may then be responsible for an increase in mobility of certain polymeric chains in the membrane – thus it may occur that the flux of the unwanted component may be significantly higher than expected (Cao, Shi, & Chen, 1999)

Concentration polarization

Concentration polarization is a phenomenon which occurs commonly in membrane processes, especially where liquid feeds are used. This phenomenon is similar to fouling as a restrictive layer is formed near the surface of the membrane, which has a concentration different from that of the bulk of the fluid. This process consists of a buildup of concentration of the non- or slower permeating components in the feed while the faster permeating species passes through the membrane. The effect of this buildup is a lower rate of permeation of the faster or preferred permeating component, while the permeation rate of the slower permeating species can increase. Thus concentration polarization not only decreases the permeation flux, but also the overall membrane selectivity (Humphrey, 1997).

Coupling effect

When multiple components are transported through membranes, a coupling effect may occur due to strong permeant-permeant as well as permeant-membrane interactions (Marx *et al*, 2002). Because mass transport in pervaporation processes is essentially the motion of individual molecules, Drioli *et al.* (1993) introduced the deviation coefficient (ε) along with a molar normalized permeation rate (J^n) to help describe the coupling effect.

The following equation was proposed

$$\varepsilon = \frac{J_i}{J_i^0 x_i} = \frac{J_i^n}{J_i^0} \qquad (2\text{-}4)$$

with $J_i^n = \frac{J_i}{x_i}$ being the normalized permeation rates, J_i is the flux of component i in the mixture and J_i^0 is the pure component flux. This deviation coefficient, which is dimensionless, can be used to describe the actual permeation of a binary liquid mixture. When the coefficient is 1, $J^n = J^0$, it means that the pervaporation is in the ideal permeation situation. When $\varepsilon > 1$, the coupling interaction between membrane and permeants increases the permeation of the permeants. Conversely, when $\varepsilon < 1$, the interaction decreases the permeation (Marx *et al*, 2002).

2.2.5 Membrane swelling

The phenomenon of swelling of the membrane is a feature unique to the pervaporation process. This occurs when polymeric membranes are used. The liquid which is fed to the membrane dissolves in the membrane which causes it to swell, thus altering the properties of the membrane. Generally the swelling leads to higher permeability but a lower overall selectivity.

When swelling occurs because of the permeating mixture, the swelling is vectored in the direction of the permeating flow; in other words, the swelling decreases from the upstream to the downstream side of the membrane (Neel, 1995). Boddeker (1990) also describes the swelling as ranging from fully swollen on the feed side to essentially dry on the permeate side that is kept under constant vacuum.

There are two parameters used to describe the swollen state of the membrane, namely the degree of swelling and the swelling ratio. The degree of swelling (DS) can be defined as the amount of solution absorbed into the membrane at equilibrium (W_∞), compared to the mass of the unswollen membrane (W_0). The following equation, given as a mass percentage uptake, was proposed (Nam *et al.*, 1999)

$$DS = \left[\frac{W_\infty - W_0}{W_0}\right] x\ 100 \qquad (2\text{-}5)$$

The other parameter, the swelling ratio (M_∞), relates the amount of equilibration solution absorbed to the total mass of the membrane and equilibration solution (Yang *et al.*, 1998)

$$M_\infty = \left[\frac{W_\infty - W_0}{W_0}\right] = \emptyset_1 + \emptyset_2 \qquad (2\text{-}6)$$

with $\emptyset_i$ being the volume fraction in the ternary (membrane) phase.

2.3 Mass transfer through membranes

2.3.1 Overview

The main characteristic of membranes used in separation processes is their ability to control the permeation of different species. Two models are widely used to describe the permeation process in membranes, namely the solution-diffusion model and the pore flow model.

The first model, the solution diffusion model, became popular after the 1940s when it was used to describe the transport of gases through polymeric membranes. Since then it has been widely considered as the appropriate model for describing all mass transport through membranes. The solution-diffusion model involves the permeants dissolving into the membrane material and then diffusing through the membrane material down a concentration gradient (Wijmans & Baker, 1995). According to the model, separation is achieved between the different permeants because of a difference in the amount of material dissolved into the membrane, as well as the rate at which the specific material diffuses through the membrane.

The second model, the pore flow model, is based on permeants separated by pressure-driven convective flow through tiny pores. Thus the separation is achieved because one of the permeants is excluded from some of the pores through which the other permeants are able to move (Wijmans & Baker, 1995). Chang *et al.* (2007) also report that the most widely accepted mathematical models for the description of pervaporation are the solution diffusion model, using concentration as driving force, and the pore model, using pressure as driving force.

Schaetzel *et al.* (2004) proposed a simplified solution diffusion model which they called the total solvent volume fraction model. This model is based on the assumption that the diffusivity of each component depends on the total volume fraction occupied by each of the permeant molecules. This model was also proposed by Bouallouche *et al.* (2010) where they referred to it as the key component model. In this model they state that one of the

components, the key component, is absorbed much more than the other components – thus the diffusivity of each species in the polymer depends only on the volume fraction of the key component.

The starting point for determining a mathematical description of permeation in membranes is the proposition that the driving forces such as temperature, concentration and pressure are all interrelated and that the overall driving force responsible for movement of a permeant is its chemical potential gradient (Wijmans & Baker, 1995).

Thus, accordingly, the flux (J) of a certain component (*i*) can be described by

$$J_i = -L_i \frac{d\mu_i}{dx} \qquad (2\text{-}7)$$

where $d\mu_i/dx$ is the chemical potential gradient of component i and L_i is the proportionality coefficient linking the chemical potential driving force with flux (Wijmans & Baker, 1995). All of the driving forces commonly used, can be reduced to chemical potential gradients and their effect on the overall flux can be described easily by this equation.

The two abovementioned models differ in the way that the chemical potential gradient in the membrane is described (Paul, 1974):

- The solution-diffusion model assumes that the pressure in the membrane is uniform throughout the membrane and that the chemical potential gradient is only expressed as a concentration gradient.
- The pore-flow model assumes that the concentrations of the solvent and solute are uniform in the membrane – thus the chemical potential gradient across the membrane is only expressed as a pressure gradient.

In Figures 2.3 and Figure 2.4 the difference in these two approaches is illustrated:

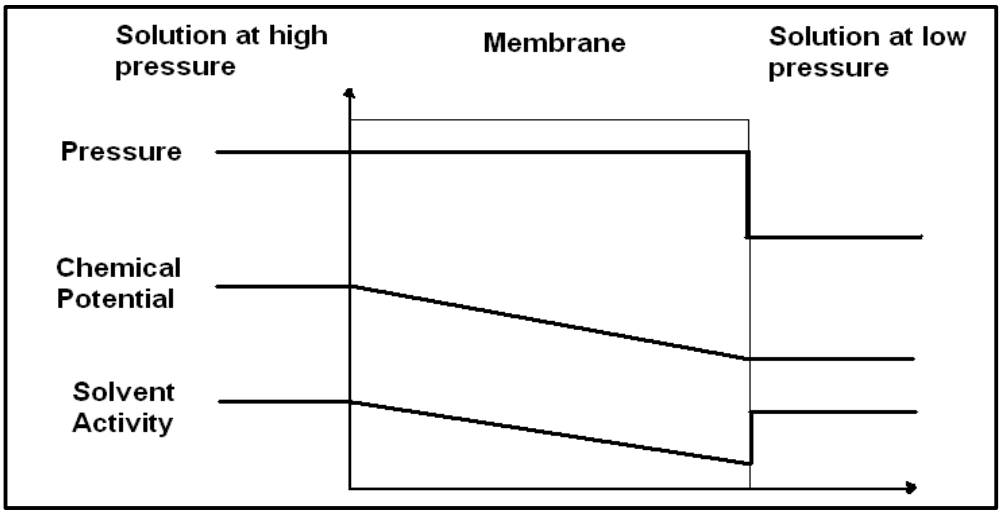

Figure 2.3: Permeation of a one-component solution through a membrane according to solution-diffusion model (Wijmans & Baker, 1995)

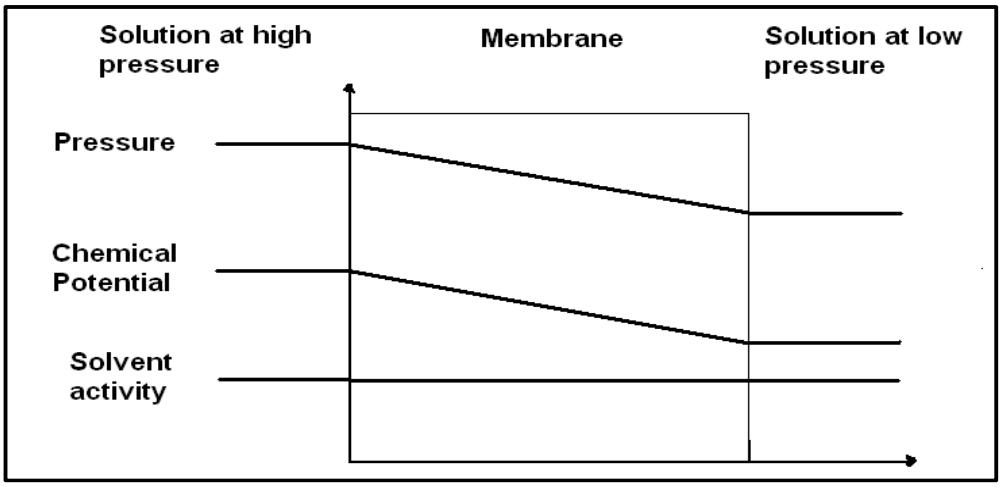

Figure 2.4: Permeation of a one-component solution through a membrane according to pore flow model (Wijmans & Baker, 1995)

In both of the two models, the pressure difference across the membrane produces a gradient in chemical potential. In the pore-flow model the gradient pressure is assumed to have a smooth gradient through the membrane, but the solvent activity ($\gamma_i c_i$) remains constant throughout the membrane. Conversely, it is assumed in the solution diffusion model that when a pressure is applied across a membrane, the pressure everywhere within the membrane is constant at the high-pressure value (Wijmans & Baker, 1995). Thus the solution diffusion model assumes the membranes transmit the pressure in the same way as liquids.

When considering the pore flow model, and equation 2.7 given above, the equation can be integrated across the membrane to give Darcy's law

$$J = \frac{k(p_0 - p_l)}{l} \quad (2\text{-}8)$$

where k is Darcy's law coefficient and l the membrane thickness. When the solution-diffusion model is considered, again using equation 2.7 and integrating over the thickness of the membrane, it has the same form as Fick's law

$$J_i = \frac{D_i(c_{i0} - c_{il})}{l} \quad (2\text{-}9)$$

where D_i is Fick's diffusion coefficient, c_i the component concentration and l the membrane thickness. The solution diffusion model will be investigated in more detail in the following section.

2.3.2 Theory and assumptions of the Solution-Diffusion model

As explained previously in the chapter, when pervaporation is used for separation of a liquid mixture, the mixture is in direct contact with the membrane on one side while the permeated product is removed on the low pressure side as a vapor. During this process transport of molecules through the membrane takes place which can be described by the solution-diffusion model. Feng and Haung (1997) described the pervaporation in three steps:

1. The sorption of the permeating species from the feed mixture into the membrane.
2. Diffusion of the permeant through the membrane according to the chemical potential gradient.
3. Desorption into the vapor phase of the permeated species in the low pressure side.

When working with the solution-diffusion model, there are numerous assumptions made when fitting this model to the experimental data obtained. This includes (Mulder & Smolders, 1984):

- The application of this model is restricted to membranes that are homogeneous or composite membranes.
- The flow of the permeants through the membrane is described as one-dimensional steady-state diffusion.
- The chemical potential of the components as well as the permeation rates is independent of time.
- There are no structural changes of the membrane when steady-state is reached.
- The chemical potential of a component in the upstream phase, or in other words the feed, is equal to the potential of the component just inside the membrane.

2.3.2.1 Mass transport in pervaporation

As mentioned above, the easiest way of describing the relation between the flux of a certain component *i* in a polymer membrane and the driving force is using Fick's first law which gives (Dutta *et al.*, 1997)

$$J_i = \mu C_i - D_i \frac{dC_i}{dZ} \quad (2\text{-}10)$$

with J_i being the permeant flux, μ the average molar velocity of the components and C_i is the concentration of the component at a certain depth characterized by the coordinate z. In this equation the coefficient μC_i accounts for the convective contribution to the total flux, but it can be neglected if the diffusional process is dominant. Thus, with the convective contribution neglected, the relation becomes

$$J_i = -D_i \frac{dC_i}{dZ} \quad (2\text{-}11)$$

At isothermal conditions, the concentration of the component *i* in the membrane, C_i, can be given in terms of the mass fraction (y_i) of this component in the membrane

$$C_i = \rho_m y_i \quad (2\text{-}12)$$

with ρ_m being the density of the membrane. Substituting this relation into Fick's law it becomes

$$J_i = -D_i \frac{dC_i}{dZ} = \rho_m D_i \frac{dy_i}{dZ} \quad (2\text{-}13)$$

Fick's law as given above can take the mutual effects of the sorption into the membrane and the diffusion through the membrane into account. It remains the most widely used model although relatively few systems fit the ideal conditions required for this model exactly (Jonquieres *et al.*, 1996). The difference in the models using Fick's law is in the way it describes the variation of the diffusion coefficient across the membrane. Thus for the Solution-diffusion model to effectively describe the obtained experimental data, it has to express the diffusion coefficient as a function of the concentration, as well as accounting for the swelling gradient (van der Gryp, 2003).

2.3.2.2 Diffusion coefficient

How well penetrants diffuse in polymer material is usually strongly dependent on the concentration of the said permeant in the material; thus it is necessary for the characterization of pervaporative mass transfer to describe the variation of diffusion coefficients. Expressions for the diffusivity of concentration-dependant coefficients can either be a linear dependence on the concentration of the individual components, (Greenlaw

1997), or an exponential dependence, as is the case with Long (1965) and Suzuki and Onozato (1982).

The linear dependence of the diffusivity on the concentration of the individual components proposed by Greenlaw *et al*. (1997) is given by

$$D_i = \rho_m D_i^0 (y_i + \beta_{ij} y_j) \quad (2\text{-}14)$$

with D_i^0 the limiting diffusion coefficient of the i^{th} component at zero concentration and β_{ij} is the effect of "plasticization" exerted by the j^{th} component on the diffusion of the i^{th} component. Substitution of this equation into Equation 2.13 and integrating over the membrane thickness gives the i^{th} component's flux

$$J_i = \frac{D_i^0 \rho_m}{L} \{\frac{(y_i)^2}{2} + \beta_{ij} y_i (1 - y_i)\} \quad (2\text{-}15)$$

An exponential dependence of the diffusivity on the concentration of the i^{th} component, referred to as the Long model, is given by

$$D_i = \rho_m D_i^0 \exp(\beta_{ij} y_j) \quad (2\text{-}16)$$

After substituting this equation into Equation 2.13 and integrating over the membrane thickness it yields the flux of the i^{th} component as

$$J_i = \frac{D_i^0 \rho_m}{L} \{\exp(\beta_{ij} y_i) - 1\} \quad (2\text{-}17)$$

A similar empirical relationship was proposed by Suzuki and Onozato (1982) with the diffusion given as

$$D_i = \rho_m D_i^0 (\beta_{ii} y_j + \beta_{ij} y_j) \quad (2\text{-}18)$$

Again, substitution into Equation 2.13 and integrating over the membrane thickness give the flux as

$$J_i = \frac{D_i^0 \rho_m}{L} (\frac{-1}{\beta_{ij} - \beta_{ii}}) \{\exp\left(\beta_{ii} y_i + \beta_{ij} (1 - y_i)\right) - \exp(\beta_{ij})\} \quad (2\text{-}19)$$

These models are the most commonly used models to fit experimental data and depending on the experimental points and degrees of freedom one will choose either a linear or exponential model.

2.4 Pervaporation applied for separation of water and sulfuric acid

In this section the application of pervaporation for the separation of water and sulfuric acid mixtures, found in literature, will be investigated.

2.4.1 Water and sulfuric acid separation

As sulfuric acid is a major commodity in the chemical industry, the concentration of sulfuric acid by the removal of water is a very important practice. Typically in industrial applications the acid is concentrated by distillation in which the feed stream temperature is raised to boiling point and the water subsequently removed, which leaves a more concentrated acid product (Orme & Stewart, 2009). One of the problems with using distillation for the concentration process is that boiling sulfuric acid is highly oxidizing and corrosive and aggressively corrodes materials, especially at the vapor liquid interface Thus it is advantageous to operate at temperatures less than boiling point. Pervaporation is such an application where operation at temperatures lower than boiling point is used.

2.4.2 Pervaporation of water and acid mixtures

Nafion and Nafion-type membranes were previously used for the concentration of acid in numerous processes. Nafion ionomers as pervaporation membranes were applied for the selective removal of water from acetic acid mixtures (Kusumocahyo & Sudoh, 1999). Fully sulfonated Nafion membranes were shown to be effective for the removal of water from solutions with hydriodic acid at temperatures reaching 135℃ (Orme & Stewart, 2007). In the latter mentioned case, the performance of the Nafion membranes was found to be a function of the thickness of the membrane, with higher flux values observed for thinner membranes, and of the temperature, where higher temperatures yielded higher flux values. This is in accordance with the hypothesis of this research project. Orme and Jones (2009) applied Nafion membranes for the concentration of sulfuric acid by selectively removing water from the mixture. These initial experiments were conducted at 100℃ using Nafion-117 membranes. Results obtained from these experiments found that, as the acid concentration increased, the water fluxes obtained through the membrane decreased. This can be expected as water is preferentially permeated through the membrane and the decrease in availability of water in the feed will have a decrease in permeate produced as a result. The flux of acid was found to be in the region of three orders of magnitude lower than the corresponding water flux at similar acid concentrations.

From literature it was observed that pervaporation processes have been applied for the separation of water and acid mixtures for several different mixture combinations, but for the

specific application of separating water and sulfuric acid mixtures, few examples could be found. Thus it was decided to investigate this option further as this is a relatively unexplored field and it is possible to operate under lower temperatures using pervaporation than in the flash separation units, which will help decrease the corrosive effects of the sulfuric acid at high temperatures.

Summary

Chapter 2 gave a good overview of all the different aspects needed to be understood in order to successfully complete this study. In short, the most important aspects of the chapter can be summarized as follows:

- Pervaporation is a membrane separation technique where the phase state on one side of the membrane is different than that on the other side.
- The greatest advantages of the pervaporation process is that the energy consumption of the process is minimized. Furthermore, pervaporation has shown to be very effective in separating close-boiling or azeotropic mixtures which create problems in other separation methods.
- The permeation flux increases with the increase in concentration of the component which preferentially permeates while the selectivity decreases.
- The increase in temperature is normally accompanied by an increase in total permeation flux and that the selectivity will slightly decrease or remain constant.
- Fouling or blockage of the membrane surface is one of the drawbacks of applying membrane processes, as its effect on the performance of the process is a decrease in flux through the membrane.
- The solution-diffusion model is most commonly used for the description of mass transfer through the membrane surface.
- Pervaporation of water and sulfuric acid mixtures have not been thoroughly investigated by many researchers and thus emphasizing the need to investigate the possibility of applying it for this specific application.

Chapter 3: Experimental

Overview

In the following chapter all the experimental work done in this research project is discussed in greater detail. The chapter is subdivided into the following sections:

- Membranes used
- Chemicals used
- Pervaporation experiments apparatus and methodology
- Experimental planning and design
- Screening results
- Sorption experiments
- Proof of steady-state and experimental error
- Reproducibility

3.1 Membranes used

When pervaporation experiments are conducted, the specific characteristics of the membrane used, greatly influence the performance of the experimental procedure. Thus the choice of the correct membrane is of utmost importance. For the purpose of this investigation, six membranes were considered. The membranes under investigation were all hydrophillic (Orme & Stewart, 2009), meaning that they were selective towards the permeability of water. Furthermore, they were shown to be resistant towards degradation brought on by contact with strong acids, in this case sulfuric acid. The membranes considered were:

- Nafion 117 and Nafion 212 membranes
- Two high temperature, alkaline PBI (Poly-bibenzimidazole) membranes
- Two low temperature , acidic based PBI membranes

Nafion-117 membranes, produced by DuPont, are non-reinforced films based on perfluorosulfonic acid/PTFE copolymer in the acid (H^+) form. The Nafion PFSA NRE-212 membranes are non-reinforced dispersion cast films based on chemically stabilized perfluorosulfonic acid/PTFE copolymer in the acid (H^+) form (DuPont fuel cells data sheet,

2005). The physical properties remain the same for the chemically stabilized and non-stabilized membranes, but the stabilized membrane exhibits substantially lower fluoride ion release compared to the non-stabilized polymer. In Figure 3.1 the Nafion-117 membrane is shown and it can be seen clearly that it is non-supported and non-reinforced.

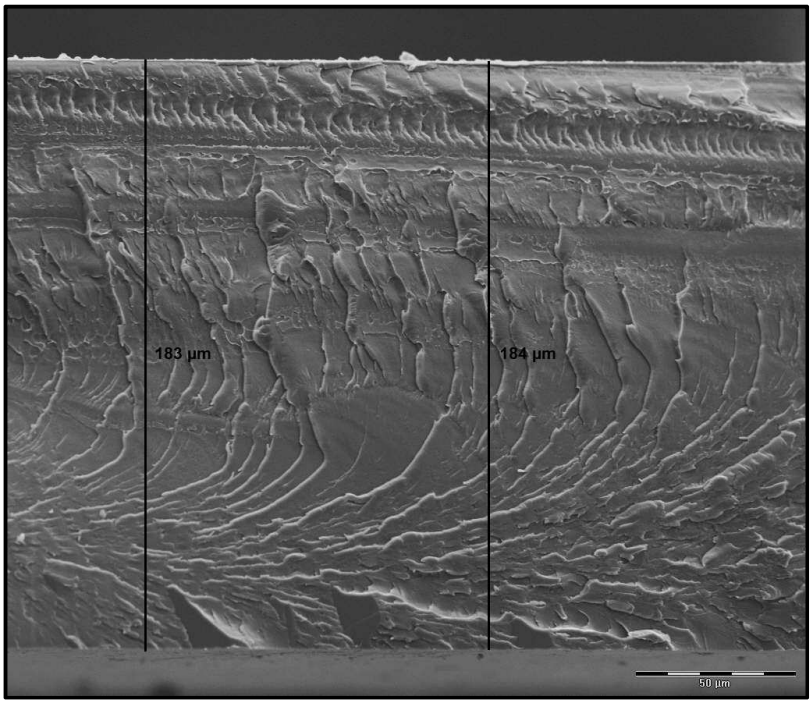

Figure 3.1: Cross-section SEM image of Nafion-117 membrane

Nafion membranes are the first of a class of synthetic polymers which exhibit ionic properties called ionomers (Mauritz & Moore, 2004). The unique ionic properties of these membranes can be attributed to the incorporation of perfluorovinyl ether groups that are terminated with sulfonate groups attached to a tetrafluoroethylene (Teflon®) backbone (Heitner-Wirguin, 1996). Nafion membranes have enjoyed a considerable amount of attention as a proton conductor in proton exchange membrane (PEM) fuel cells because they have excellent thermal as well as mechanical stability.

There are a few properties that make Nafion suitable for use in this specific application. Firstly, it is highly conductive towards cations, thus it can be used in numerous membrane applications. It is also very resistant to chemical attack, with only alkali metals being degrading to the membrane's chemical structure under normal operating temperatures and pressures. Furthermore, the Teflon backbone interlaced with ionic sulfonate groups makes it suitable for use under high operating temperatures. Lastly, but most importantly, it is selective and highly permeable towards water. In Figure 3.2 the SEM image for the Nafion-212 membrane is shown.

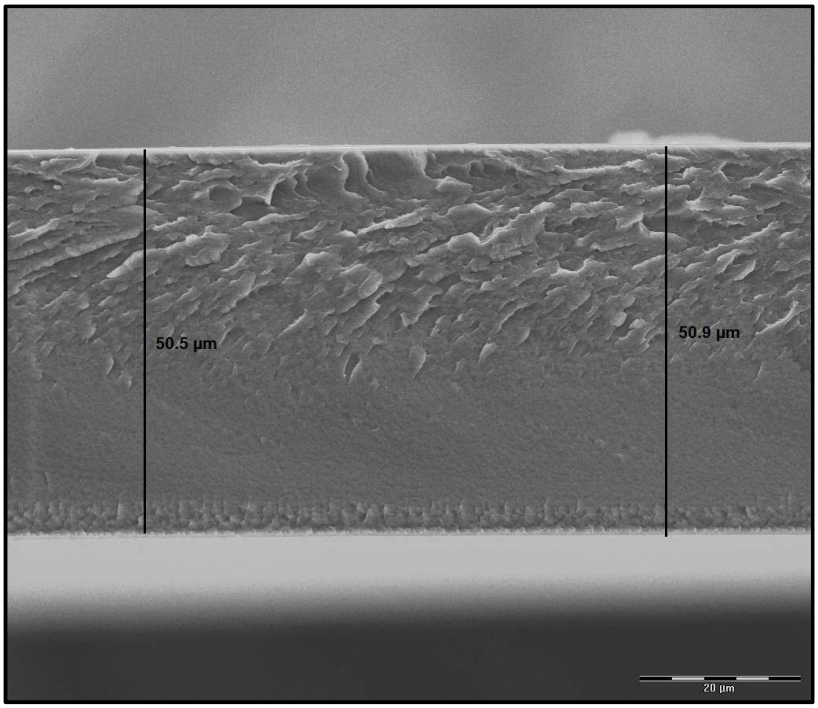

Figure 3.2: Cross-section SEM image of the Nafion-212 membrane

When comparing Figures 3.1 and Figure 3.2 it can be seen that structurally they are the same, with both being non-reinforced films. Thus, the only significant difference between the two membranes is their thickness. Table 3.1 shows some of the most important characteristics of the two membranes, as well as minor differences.

Table 3.1: Properties of Nafion 117 and Nafion 212 membranes (DuPont fuel cells data sheet, 2005)

	Nafion 117	**Nafion 212**
Typical thickness (micrometers)	183	50.8
Basic weight (g/m^2)	360	100
Specific gravity	1.98	1.97
Water content (% water)	5	5
Water uptake (% water)	38	50

The other membranes also considered for the application are the two high temperature alkaline membranes (Figures 3.3 and 3.4) as well as the two low temperature acid based membranes (Figures 3.5 and 3.6).

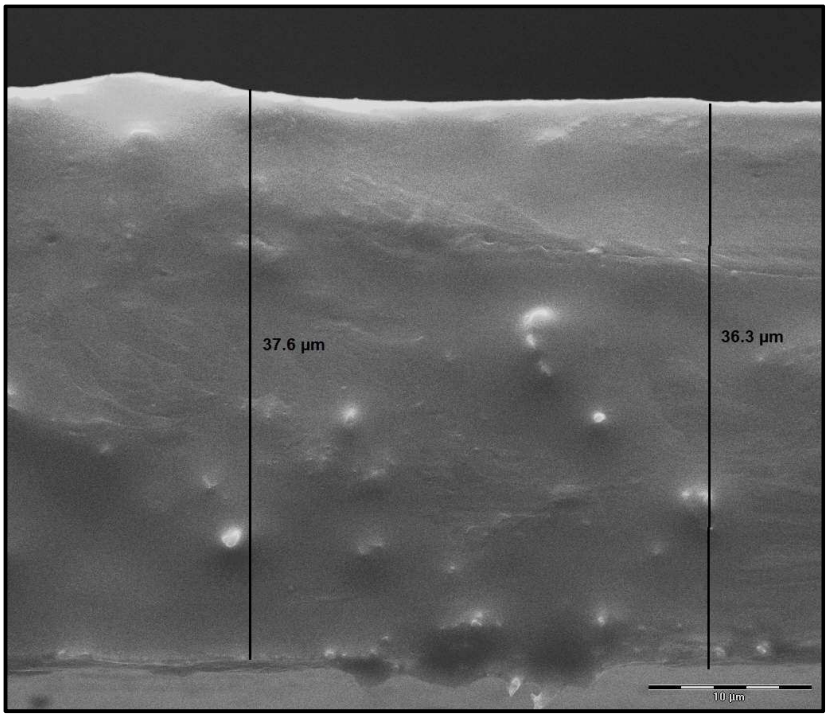

Figure 3.3: Cross-section SEM image of high temperature alkaline PBI membrane 1

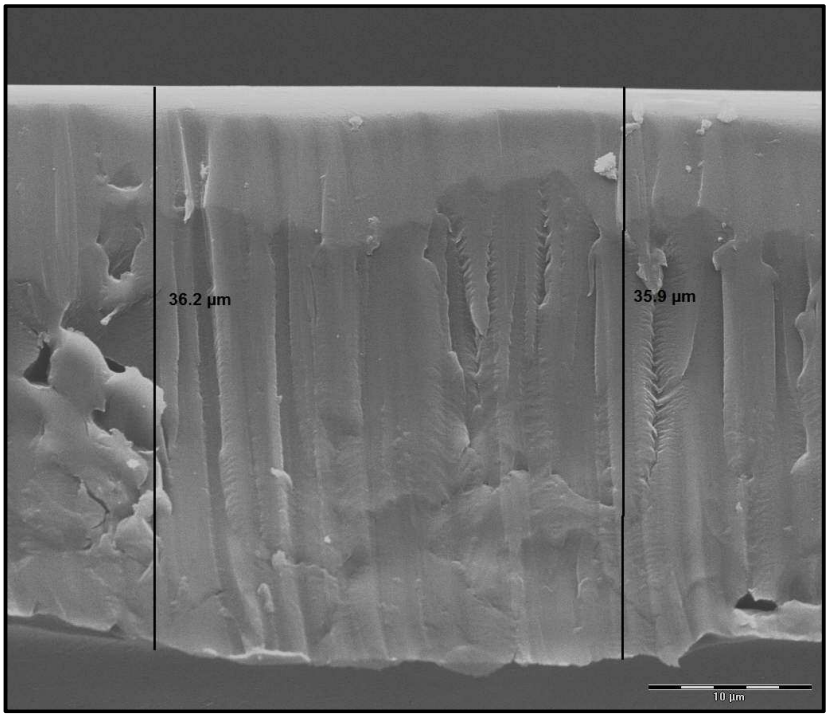

Figure 3.4: Cross-section SEM image of high temperature alkaline PBI membrane 2

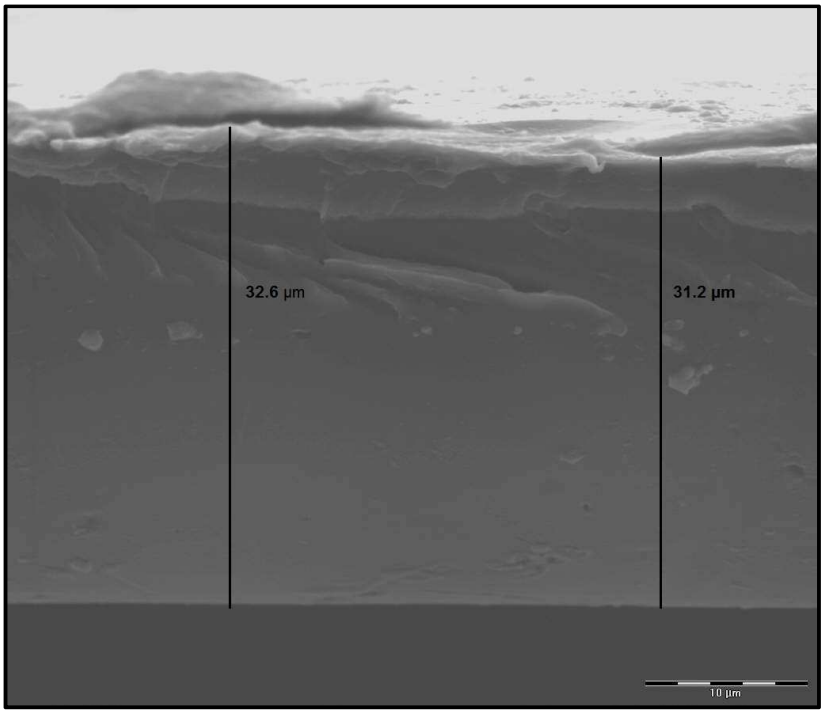

Figure 3.5: Cross-section SEM image of low temperature acidic PBI membrane 1

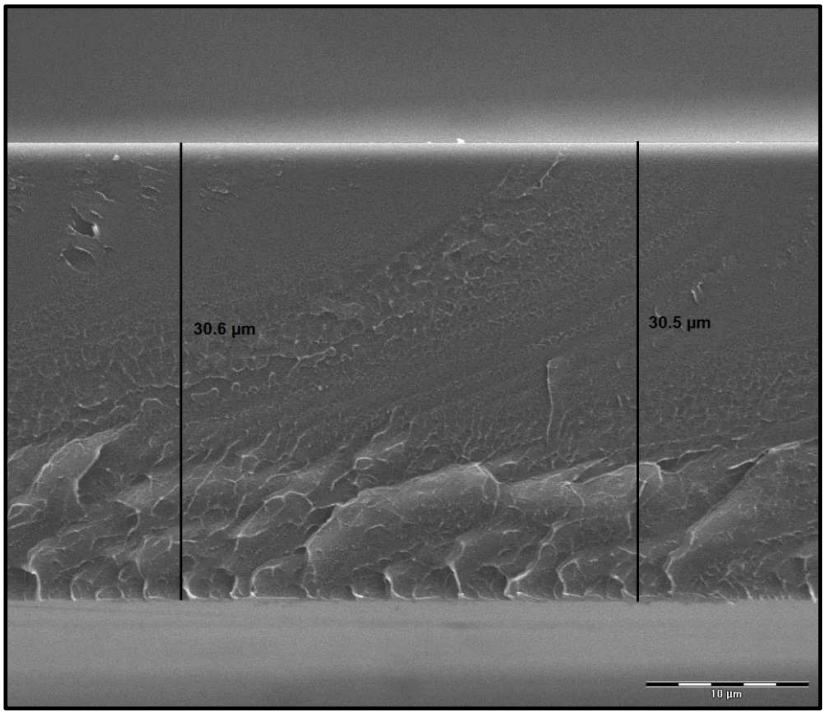

Figure 3.6: Cross-section SEM image of low temperature acidic PBI membrane 2

All the PBI membranes are single-layer, unsupported membranes as can be seen from the figures. These PBI (Polybenzimidazole) membranes are fully aromatic heterocyclic polymers. They consist of three benzene rings in a repeating unit that contributes to the

polymer's properties such as good thermal stability, stiffness and toughness (Li *et al.* 2004). Furthermore, they have also proven to have good chemical resistance. Most importantly, these membranes are shown to be permselective towards water which makes them suitable for this application (Wang *et al.*, 2007).

3.2 Chemicals used

Sulfuric acid (H_2SO_4) 98 wt% was used throughout all the pervaporation and sorption experiments. For the purpose of the dissertation the 98 wt% sulfuric acid will be referred to as pure sulfuric acid hence forth. Also in the case where the feed to the pervaporation module consists only of water or sulfuric acid, the stream will be referred to as pure water of sulfuric acid, respectively. It was purchased from ACE's (Associated chemical enterprise) platinum line, and used as received. In the selectivity analysis where a standardized titration procedure was performed, sodium hydroxide (NaOH) pellets with a minimum of 98 wt% purity were used, also purchased from the ACE's platinum line. Phenolphthalein ($C_{20}H_{14}O_4$) solution was used as indicator and purchased from ACE's gold line.

All the chemicals were used without any further purification. Any minor impurities in these chemicals were assumed negligibly small and would not influence the experimental results.

3.3 Pervaporation experiments

3.3.1 Apparatus and methodology

Pervaporation is a widely used process for separation and the standard pervaporation set-up with all the required equipment are all well described in literature (Cao *et al.,* 1999). Figure 3.7 shows a schematic diagram of the pervaporation set-up used in the study.

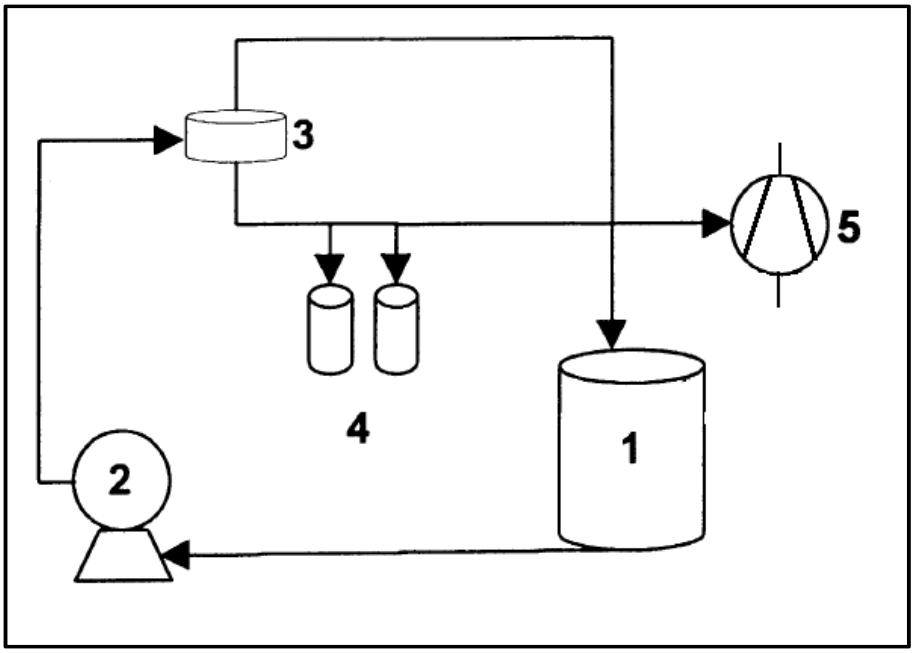

Figure 3.7: Schematic diagram of standard pervaporation set-up. Adapted from (Marx *et al*, 2002)

The feed solution was kept at a constant temperature using a heat jacket around the feed vessel (1) connected to a thermocouple which measured and controlled the temperature. From the feed vessel the feed solution is fed directly to the active side of the flat sheet, polymer membrane model (3) using a magnetic pump (2). The permeate side of the membrane cell is kept at a constant pressure at maximum vacuum (0.4 kPa) using a vacuum pump (5). The vapor that forms on the permeate side is captured using cold traps (4) submerged in an ice bath. In Figure 3.8 an illustration of the set-up used, is shown.

The total permeation flux was determined by measuring the weight collected in the cold traps over a certain period of time at steady state. The separation factor was determined analytically using a standardized sodium hydroxide titration procedure.

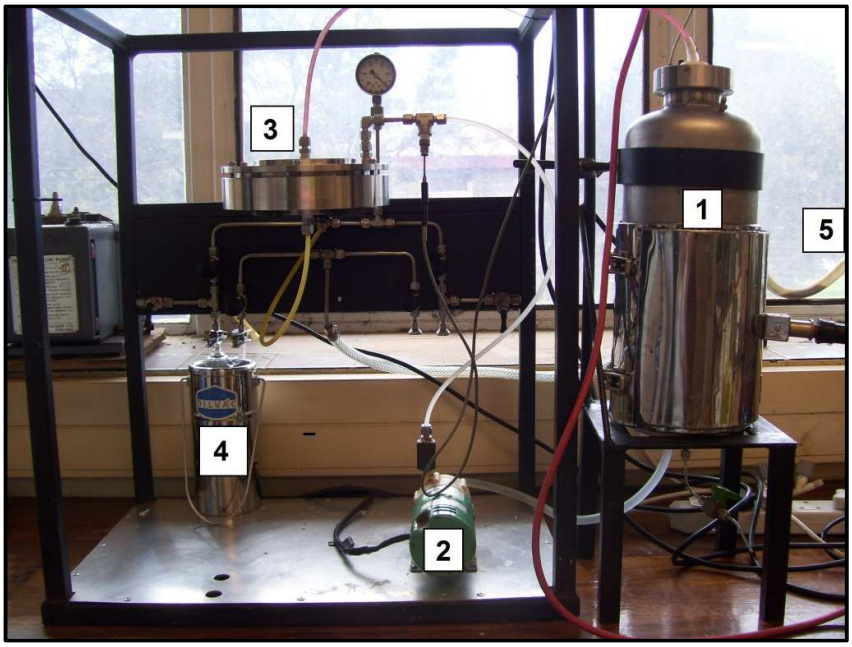

Figure 3.8: Photo of pervaporation apparatus

3.3.2 Experimental equipment

The pieces of equipment used during the pervaporation experiments are listed in Table 3.2.

Table 3.2: Experimental equipment with specifications

Equipment	Number	Type/supplier	Operating conditions
Feed vessel	1	5 Litre Stainless steel tank	2.5 Litre ± 0.05 Litre
Feed pump	2	Nikkiso seven pump, model CP-1G Nikkiso pumps America, Inc	Maximum flow rate 15 litre/min
Vacuum pump	5	Edwards, 2-stage high vacuum pump from Wirsam	Highest vacuum 1 x 10^{-3} Pa
Pressure meter		Vacuum pressure meter - Wika instruments	0 – 100 kPa

3.3.3 Analytical equipment

Since the only two compounds present in the feed solution to the pervaporation process are water and sulfuric acid, the simplest and most effective procedure to determine the selectivity of the permeate flux is a standardized sodium hydroxide titration.

To perform the titration procedure a 0.100 M (molar) sodium hydroxide solution was prepared. The procedure followed can be summarized as:

- Pipette the permeate liquid that was produced into an Erlenmeyer flask.
- Add 2-3 drops of the phenolphthalein solution to the flask.
- Titrate with the prepared sodium hydroxide solution until the first colour chance occurs. The colour change is shown in Figure 3.9.

Figure 3.9: Colour change of phenolphthalein during titration. On the left the colourless solution before end point and on the right pink solution after endpoint.

The reaction that takes place during the titration procedure is

$$H_2SO_4 + 2NaOH \rightarrow Na_2SO_4 + 2H_2O \qquad (3\text{-}1)$$

According to this reaction sulfuric acid reacts with the sodium hydroxide on a 1:2 basis, which means that the number of moles of sulfuric acid is half the number of moles of sodium hydroxide added.

3.4 Experimental planning and design

3.4.1 Assumptions regarding pervaporation experiments

- The pervaporation system is a closed loop, in other words no material can enter or leave the system except through the membrane. Because the membrane area is small and only minor amounts of the material leave the system by means of pervaporation (approximately 1%), it can be considered that the loss of material is very small compared to the feed solution, thus making it a closed loop,ensuring steady-state conditions during sampling.
- As the feed rate to the membrane module is not used as a variable in the experimental design, the feed to the membrane module via the feed pump is considered to be constant throughout the entire experiment.

3.4.2 Experimental design

The experimental design can be subdivided into three different sections. To start off the six membranes chosen undergone a membrane screening procedure. After the results of the screening procedure were analyzed the most suitable membranes for the specific application were determined. The chosen membranes were then used in the pervaporation experiments. During the pervaporation experiments the two parameters monitored throughout are the permeate flux and the selectivity. The influence that the operating temperature as well as the feed concentration has on these parameters is determined and thoroughly investigated. These membranes also undergone sorption experiments. Each of these sections are discussed in further detail in the following sections.

3.4.3 Membrane screening

The membrane screening was the preliminary testing phase where the six membranes considered for this application were tested. In order to compare the performance of these membranes they were all tested under similar process conditions to determine which were the most suitable.

All the tests were completed at 25˚C and a constant pressure differential. The membranes were tested with both pure water (H_2O) and pure sulfuric acid (H_2SO_4) in order to determine the flux and selectivity of the various membranes. Before the pervaporation experiment was commenced, the membrane had been presoaked under the same process conditions for a period of 8 hours. This was done to ensure that the membrane was fully swolen. When this time period elapsed the vacuum pump was switched on and the experiment commenced. It

was run for 4 hours after which the total permeate flux was measured and the selectivity determined.

Screening results

From the results of the screening procedure it was observed that the flux of water through the membranes was significantly higher than that of the sulfuric acid. In all of the cases the permeated sulfuric acid was almost neglectably small. The results obtained from the membrane screening experimentation are shown in Figure 3.10, where a comparison is drawn between the six membranes tested.

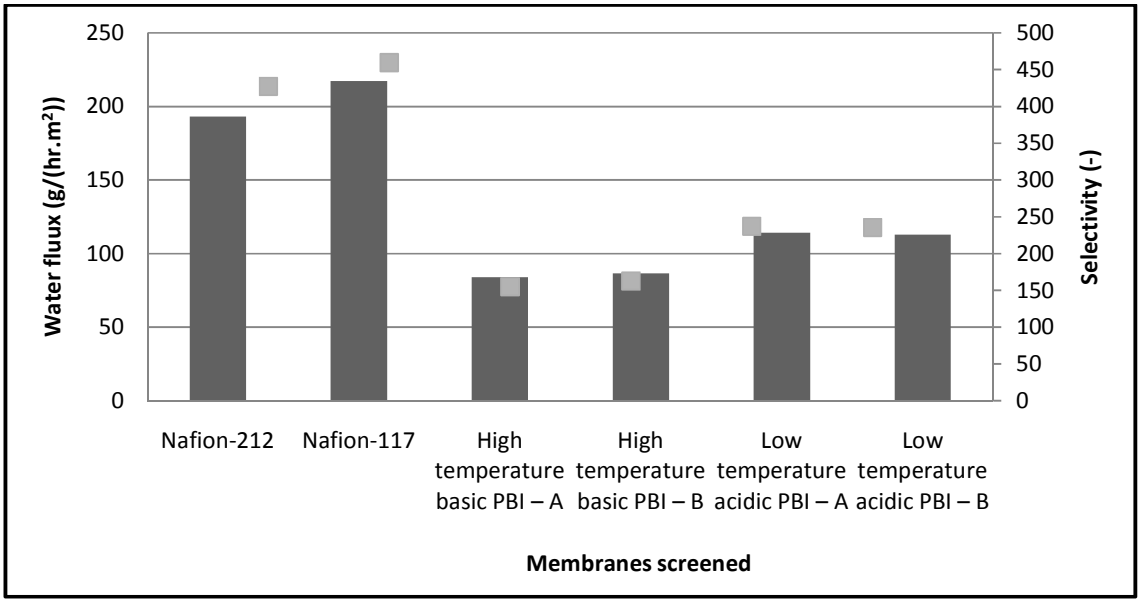

Figure 3.10: Comparison of the results obtained from screening procedure. Water flux is given as (■) and the selectivity as (■).

The flux values given in Figure 3.10 are given as g/(hour.m^2) and the selectivity is calculated by dividing the water flux obtained through each membrane by the respective acid flux through the same membrane – thus a higher selectivity value is indicative of a superior selectivity. Thus it should be noted that ideal selectivities is calculated for each of the given membranes and shown in Figure 3.10.

From the results shown in Figure 3.10 it can be seen that the two Nafion membranes have a far greater flux value as well as selectivity values compared to the PBI membranes. The low temperature PBI membranes performed better than the high temperature membranes which can be expected as these experiments were conducted at 25˚C.

In Section 3.1 the SEM images for the Nafion-117 and Nafion-212 membranes were shown and a conclusion was drawn that the only significant difference between these two membranes was their thicknesses (Section 3.1), with both being unsupported and having the

same chemical structures. The same applies to the PBI membranes – all of them were unsupported, single layer membranes with a uniform and homogenous structure. Thus it can be concluded that the difference in performance between the PBI and the Nafion membranes can be attributed to the different chemical structures of the respective membranes.

From the results obtained in the membrane screening procedure the Nafion-117 and Nafion-212 membranes were chosen for further investigation. Conventionally, only one membrane is identified and used for further investigation, but the results obtained from the initial membrane screening for the two Nafion mebranes were so close, it was decided that both membranes should be investigated further.

3.4.4 Sorption experiments

For the sorption experiments, a standard methodology was followed (Aminabhavi *et al.*, 1997). A small piece of membrane with a fixed area of 1cm^2 was used in all the experiments. The dry weight of the membrane strip was determined by weighing it before the experiments commenced. The strip of membrane was then immersed in a flask which contained a binary mixture of water and sulfuric acid, with the concentration of water being varied from 0 to 100% with 20% intervals, the same intervals used during the pervaporation experiments.

The temperature was also varied, with two temperatures, namely 25˚C and 55˚C – the same temperatures as used in the pervaporation experiments. The contact time interval was set at 10 seconds. After each time interval, the membrane was removed, placed between two paper towels, gently patted dry and then weighed. This procedure was repeated until no further mass increase occurred, which indicated that sorption equilibrium had been reached.

3.4.5 Pervaporation experiments

After the initial screening experiments were conducted, the chosen membranes were used for further experimentation. The pervaporation experiments were conducted in two sections.

Firstly, the temperature was varied as the independent variable in order to investigate the effect it had on the pervaporation characteristics. The feed temperature was varied from 25˚C to 55˚C with 10˚C intervals; thus 4 temperatures were tested. At these temperatures both of the membranes were tested with pure components of water and sulfuric acid and a constant permeate pressure vacuum (0.4kPa). The membranes were again pre-soaked at the specific operating condition for 8 hours after which the experiment commenced. From the start of the experiment a sample was taken every 2 hours and the total flux measured. This procedure was repeated for a period of 10 hours.

From the data gathered the total permeate flux and selectivity could be determined, as well as the ideal temperature which produced the best flux values as well as selectivity.

In the second part of the pervaporation experiments the feed composition was used as the independent variable to investigate its effects on the dependent variables. The feed composition was varied between 0 and 100 wt.% H_2SO_4 at intervals of 20%. This was done for both membranes at 25 ˚C as well as 55 ˚C and a constant permeate pressure. Again the pervaporation experiments were conducted over a 10 hour period with samples taken every 2 hours. The sample was used to determine the total flux and the selectivity was calculated using the standard titration process.

3.5 Proof of Steady-state and Experimental error

In pervaporation experiments it is important to reach steady-state as these values are used during the calculations of the experimental error, as well as all further calculations and modeling. Steady-state is reached when the experimental values obtained for the flux through the membrane have reached a constant level. To determine when steady-state was reached for each of the membranes, 3 experimental runs were completed at 25˚C over a period of 14 hours. In Figure 3.11 the results obtained for the Nafion-212 membrane are shown.

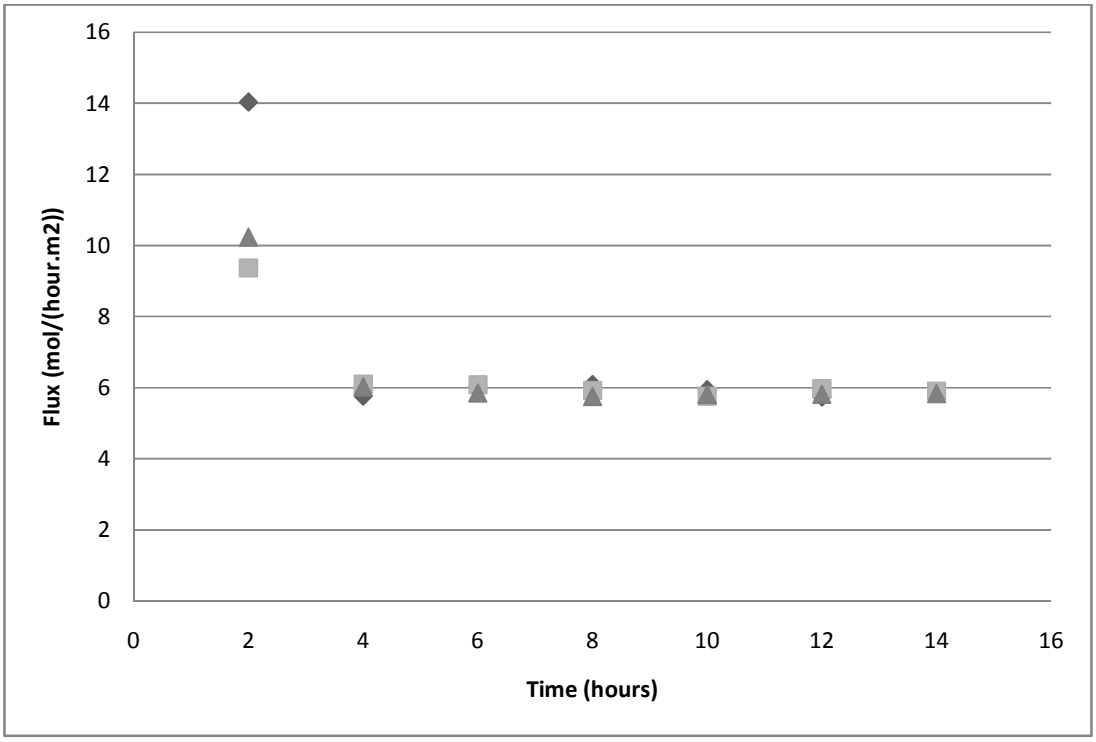

Figure 3.11: Steady-state determination for Nafion-212 at 25˚C. The data is represented by run 1 (♦), run 2 (■) and run 3 (▲).

From the results shown in Figure 3.11, it can be concluded that steady-state was reached after 4 hours, thus for the Nafion-212 membrane this data will be used in further calculations. The average of the steady-state values was taken to calculate the experimental error, which was calculated as 2.1% for the Nafion-212 membrane. All the calculations are given in Appendix C.

In Figure 3.12 below the results obtained from the same experiment conducted on the Nafion-117 membrane are shown.

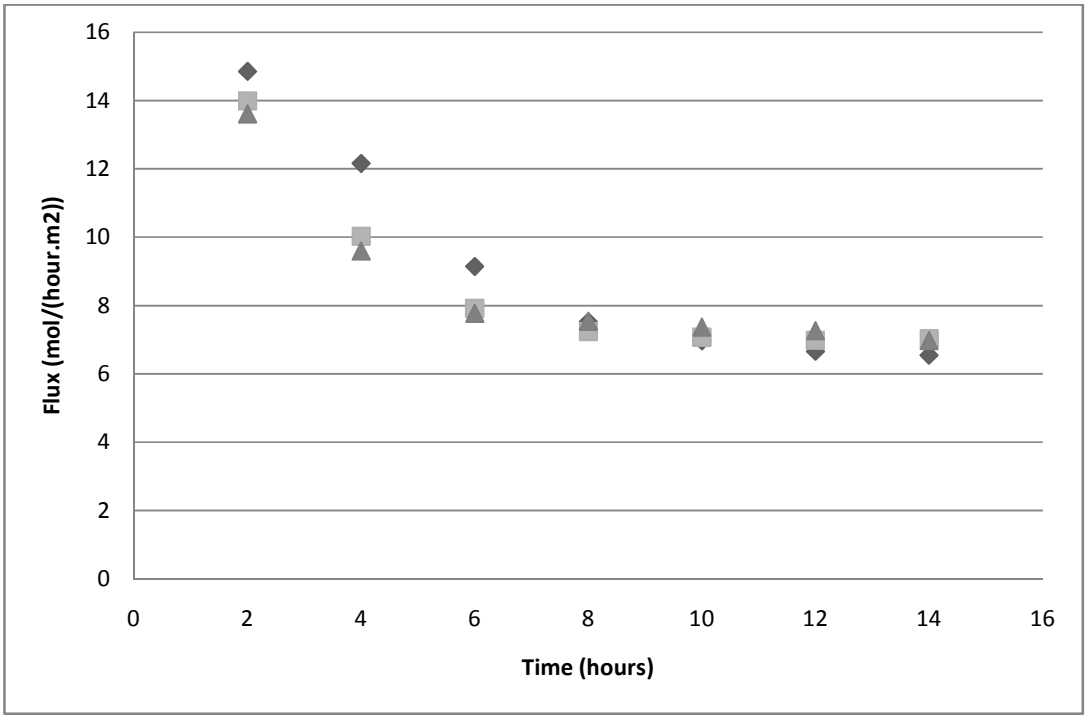

Figure 3.12: Steady-state determination for Nafion-117 at 25˚C. The data is represented by run 1 (♦), run 2 (■) and run 3 (▲).

Figure 3.12 shows that the Nafion-117 membrane results differ somewhat from the results obtained for the Nafion-212 membrane in that it took approximately 6 hours to reach steady state, compared to the 4 hours for the Nafion-212 membrane under similar conditions. Thus for further experimentation using the Nafion-117 membrane, steady-state was assumed to be established after 6 hours and this values was used to determine the experimental error. The experimental error was calculated as 2.3% for the Nafion-117 membrane.

3.6 Reproducibility

It is important when doing experimental work that the results obtained are reproducible, as it helps to validate the experimental conclusions and protect against unconscious experimental blunders.

For the pervaporation experiments, the reproducibility was confirmed for the pure component experiments for both the water and sulfuric acid over the entire temperature range. The experimental planning regarding the reproducibility is shown in Table 3.3.

Table 3.3: Planning regarding repeatability of experimental results

Nafion-212	Temperature	Pure water (# of repeats)	Pure sulfuric acid (# of repeats)
	25˚C	1	2
	35˚C	2	1
	45˚C	1	2
	55˚C	2	1
Nafion-117	25˚C	2	1
	35˚C	1	2
	45˚C	2	1
	55˚C	1	2

In Table 3.3 the stated numbers show the number of times the specific experiment was repeated. In the binary mixture experiment, the 40 vol% water experiment was chosen to be repeated for both of the membranes at 55˚C. This specific experiment was chosen because it fitted the HyS objective the best, where a stream consisting of approximately 60-65 vol% sulfuric acid is received from previous processing units and then concentrated. The experiment was repeated 3 times for both the nafion-212 membrane and the Nafion-117 membrane. The experiments conducted on the Nafion 212-membrane had an experimental error of 1.7% while the experimental error for the Nafion-117 membrane was 2.2%. All the experimental error calculations are given in Appendix C.

Summary

In Chapter 3 the experimental design of the project was discussed in great detail, with the critical observations summarised as:

- Nafion membranes are highly selective and highly permeable towards water, making it suitable for the specific application.
- From theresults of the initial screening procedure it was observed that the flux of water through the membranes was significantly higher than that of the sulfuric acid. In all of the cases the permeated sulfuric acid was almost neglectably small.

- The two Nafion membranes have a far greater flux value as well as selectivity values compared to the PBI membranes.
- It was concluded that steady state is reached after 4 hours for the Nafion-212 membrane and after 6 hours for the Nafion-117 membrane.
- The average of the steady-state values was taken to calculate the experimental error, which was calculated as 2.1% for the Nafion-212 membrane and 2.3% for Nafion-117.

Chapter 4: Experimental Results and Discussions

Overview

In this chapter the results obtained for both the pervaporation and sorption experiments are given and discussed in detail. The chapter is subdivided into 4 sections, with Section 4.1 the pervaporation characteristics of the membrane. The dependence of the total permeate flux, as well as the selectivity on the feed concentration and the operating temperature are discussed.

In Section 4.2 the sorption experimental results are given and the swelling properties of the membrane addressed. The modeling of the pervaporation data is then discussed and analyzed in Section 4.3. The aim of the section is to determine whether a simplified model which is based on solution-diffusion mechanism can be developed, in order to correctly describe the obtained experimental results and predict similar pervaporation results. Lastly, in Section 4.4 the separation capabilities of the pervaporation process are compared to that of the existing reference design proposed, including a flash separation section, by SRNL.

4.1 Pervaporation characteristics of the membranes

Section 4.1.1 investigates the dependence of the total flux and selectivity on the temperature range for both the pure component experiments as well as the binary mixture experiments. Section 4.1.2 will look at the dependence of the fluxes and selectivity on the concentration range of water in the feed mixture.

4.1.1 Influence of operating temperature

The influence of operating temperature on the performance of the pervaporation experiments was investigated for both pure component as well as the binary mixture experiments. In the pure component pervaporation experiments, pure water and sulfuric acid were fed to pervaporation set-up, with the temperature being varied from 25˚C to 55˚C in 10℃ increments for both of the Nafion membranes. Figure 4.1 shows the results obtained for Nafion-212 and Figure 4.2 for Nafion-117, using pure water as feed in both instances. As given in Section 3.5,

for the Nafion-212 membrane the margin of error was calculated as 2.1% and for the Nafion-117 membrane as 2.3%.

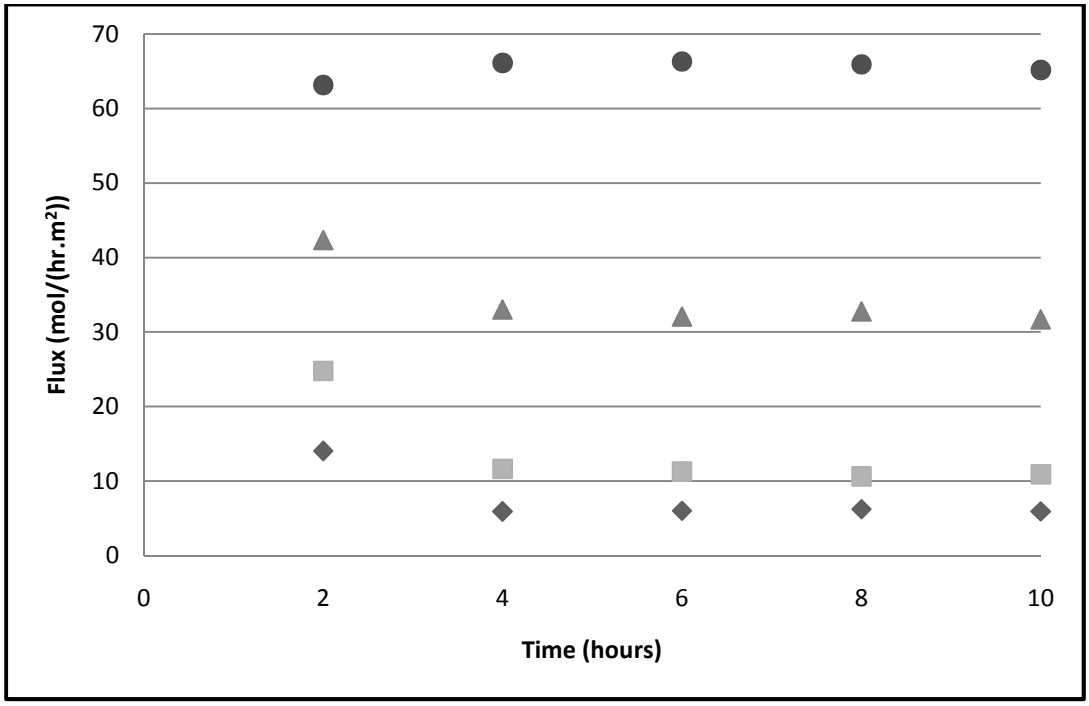

Figure 4.1: Influence of operating temperature on total flux through the Nafion-212 membrane using a pure water feed. In the graph (♦) represents 25℃, (■) 35℃, (▲) 45℃ and (●) 55℃.

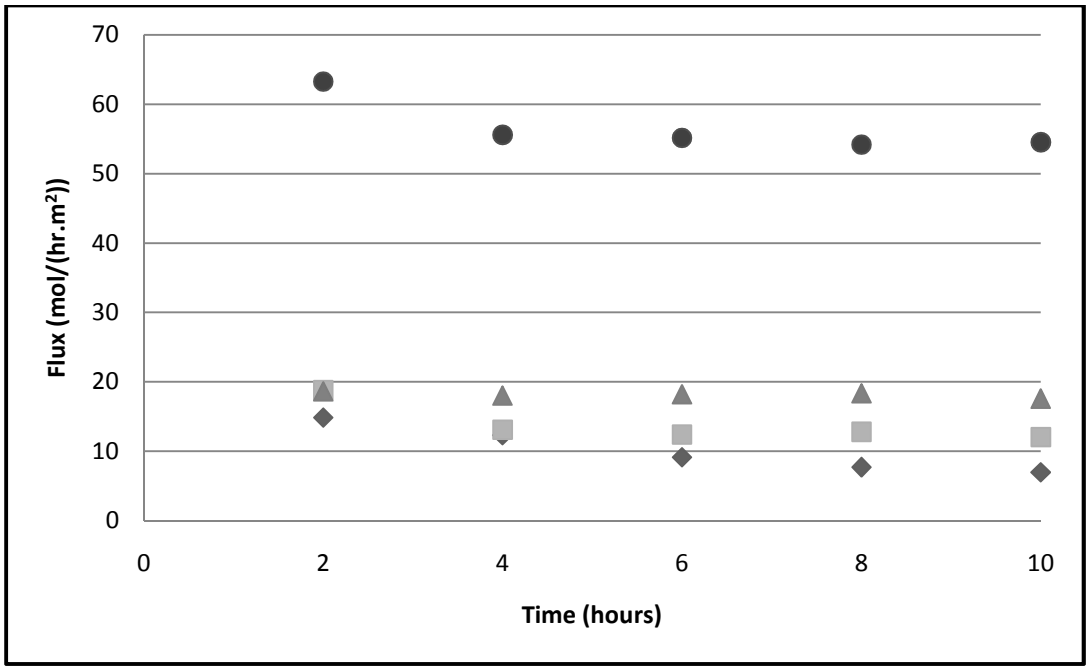

Figure 4.2: Influence of operating temperature on total flux through the Nafion-117 membrane using a pure water feed. In the graph (♦) represents 25℃, (■) 35℃, (▲) 45℃ and (●) 55℃.

All the calculations to determine the flux values are given in Appendix B. In Section 3.5 it was proven that for the Nafion-212 membrane steady-state was reached after 4 hours and for Nafion-117 after 6 hours. This fact is proven if Figures 4.1 and 4.2 is studied in which it can be seen that this was the case over the entire temperature range investigated.

In Figures 4.1 and 4.2 it can be seen clearly that the total flux increases for both of the membranes as the feed temperature increases. Other researchers (Mulder et al., 1985; Orme et al., 2009) reported similar results. This phenomenon may be ascribed to an increase in the mobility of the molecules as the temperature is raised and the diffusivity of water increases in the membrane, also noted by Luo *et al.* (1997). In both membranes the total flux increases as the temperature increases, with the Nafion-212 membrane having a higher flux than the Nafion-117 membrane at the higher temperatures. The Nafion-212 membrane has a more gradual increase in flux values as the temperature rises while for the Nafion-117 membrane the increase is more exponential.

The higher flux values of the Nafion-212 compared to the Nafion-117 membrane may be attributed to the difference in thickness of the membranes. Both of the membranes have the same chemical structure end density, with the only difference being their thicknesses, with Nafion-212 (50.8 µm) being thinner than Nafion-117 (183 µm), illustrated in Section 3.1 where the SEM images were shown. Thus, as the temperature increases and the mobility of the

molecules increases, the molecules can more easily diffuse through the thinner Nafion-212 membrane. The end result is higher flux values under similar feed conditions for this membrane than for the Nafion-117, as indicated in Figures 4.1 and 4.2.

The same results are seen in the pure sulfuric acid experiments, where the total flux also slightly increases as the temperature increases, but the flux values obtained from these experiments are insignificantly small compared to the fluxes obtained in the pure water experiments, shown in Figures 4.3 and 4.4. This can be expected as both of the Nafion membranes are permselective towards water (Orme *et al*., 2009).

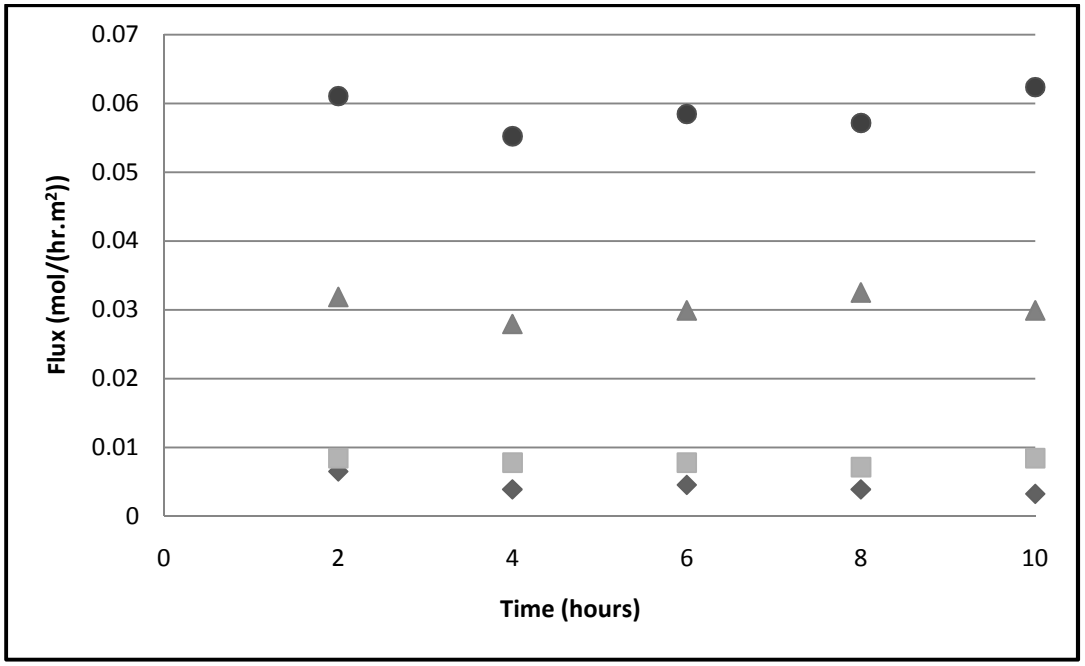

Figure 4.3: Influence of operating temperature on total flux through the Nafion-212 membrane using a pure sulfuric acid feed. In the graph (♦) represents 25℃, (■) 35℃, (▲) 45℃ and (●) 55℃.

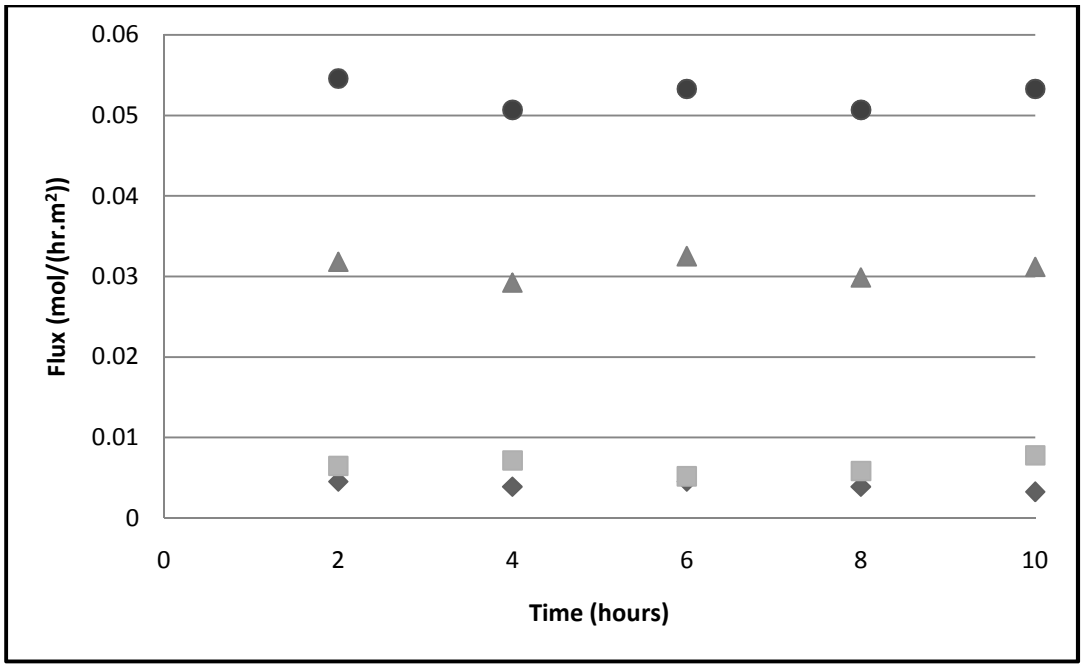

Figure 4.4: Influence of operating temperature on total flux through the Nafion-117 membrane using a pure sulfuric acid feed. In the graph (♦) represents 25℃, (■) 35℃, (▲) 45℃ and (●) 55℃.

The pure component selectivity was calculated using Equation 4.1:

$$\alpha = \frac{J_{water}}{J_{acid}} \qquad (4\text{-}1)$$

where J_{water} is the obtained water flux and J_{acid} the acid flux through the membrane, respectively. Details of these calculations are given in Appendix B and the effect of temperature is shown in Figure 4.5.

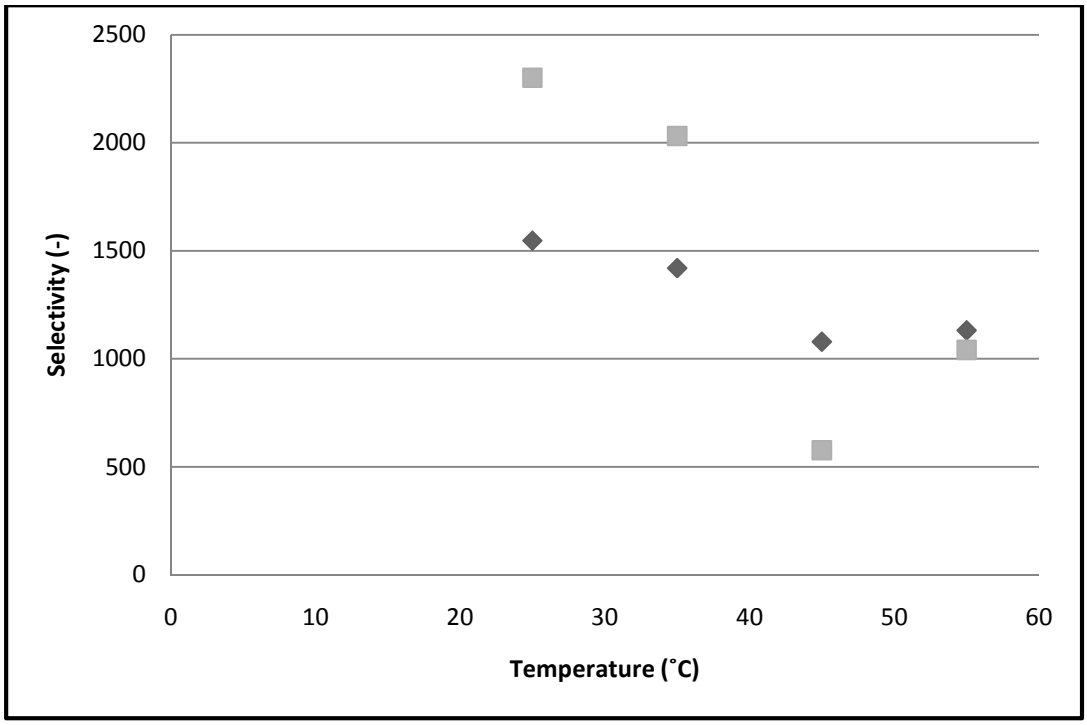

Figure 4.5: Influence of operating temperature on the pure component selectivity for both membranes. Nafion-212 is represented by (♦) and Nafion-117 by (■).

In Figure 4.5 it can be seen that as the temperature increases the pure component selectivity of both membranes decreases. At the first two temperatures, namely 25˚C and 35˚C, the flux of sulfuric acid is almost infinitesimally small, which is the reason for the higher selectivities observed for both membranes, even if the water flux is significantly smaller than at 55˚C. The selectivity at 55˚C is higher for both membranes than at 45˚C, which indicates more favorable flux values at the higher temperatures. The low values observed at 45˚C for both membranes, especially for Nafion-117 can be attributed to the fact that the water flux values only increases slightly from 25˚C up to 45˚C and then more significantly at 55˚C. The sulfuruic acid flux on the other hand increases more steadily over the temperature range, thus at 45˚C the selectivity is effected negatively as the water flux did not increase portionally as much as the sulfuric acid did compared to the results observed at 55˚C. The phenomenon of the selectivity decreasing with increasing temperature was observed by Burshe *et al.* (1999) as well as Luo *et al.* (1997).

Figure 4.6 shows the results obtained for the total flux in the binary mixture experiments for both membranes.

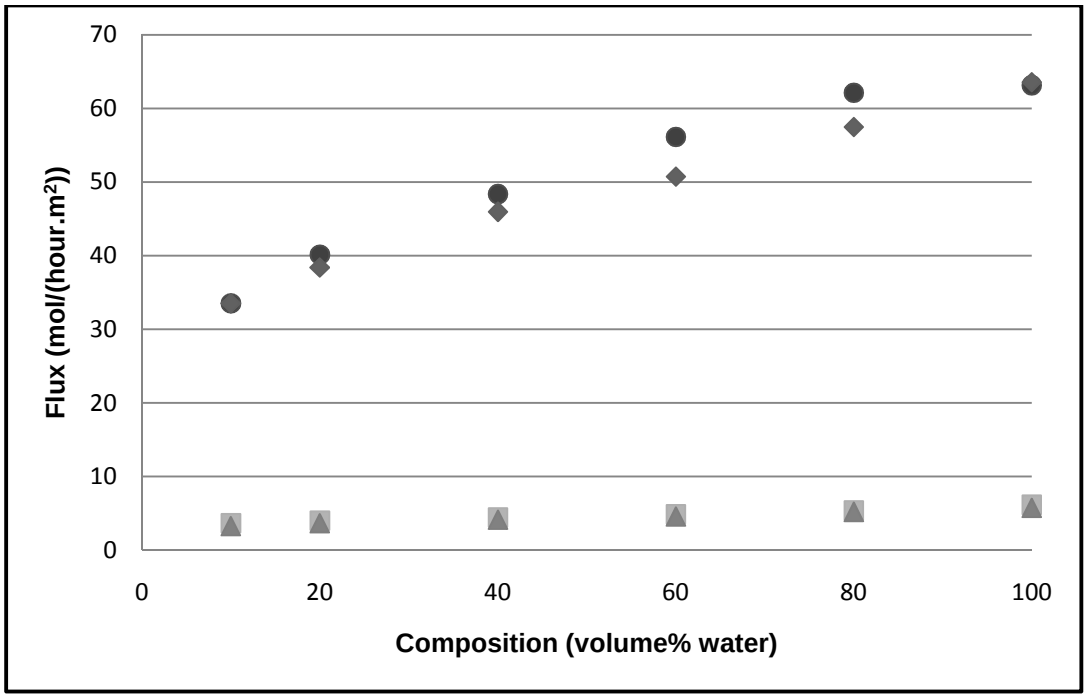

Figure 4.6: Influence of operating temperature on total flux with binary mixture experiments. (■) shows Nafion-212 at 25℃, (▲) Nafion-117 at 25℃, (●) Nafion-212 at 55℃ and (♦) Nafion-117 at 55℃.

In Figure 4.6 the same trends that were obtained in the pure component experiments can be observed, with a significant increase in flux values for both membranes as the temperature was increased. Again the Nafion-212 produced higher flux values than the Nafion-117 membrane at the higher temperatures. From the pure component experiments as well as the binary composition experiments it seems to indicate that water has the greatest influence on the total amount of permeants produced. This can only be confirmed after the selectivity experiments are completed. The selectivity of the binary mixture experiments will be investigated in the next section where the effect of feed composition will be analyzed.

4.1.2 Influence of feed composition

The influence of the feed composition range on the selectivity of the two Nafion membranes was investigated by varying the volume percentage water in the feed to the process at two chosen temperatures. The flux data obtained were used for the determination and calculations of the binary mixture selectivity of both of the membranes. To calculate the binary selectivity of the membranes Eq 2.1 given in Section 2.2.2 is used, which states

$$\alpha = \frac{\mathbf{y_{water}}/(\mathbf{1}-\mathbf{y_{water}})}{\mathbf{x_{water}}/(\mathbf{1}-\mathbf{x_{water}})}$$

where x and y represent the mass fraction of each of the components in the feed and permeate, respectively, and water is the preferentially permeating species. Details of all the relevant calculations are given in Appendix B. The results obtained from the experiments are given in Figure 4.7 which shows the selectivity of the Nafion-212 membrane and Figure 4.8 the selectivity for Nafion-117.

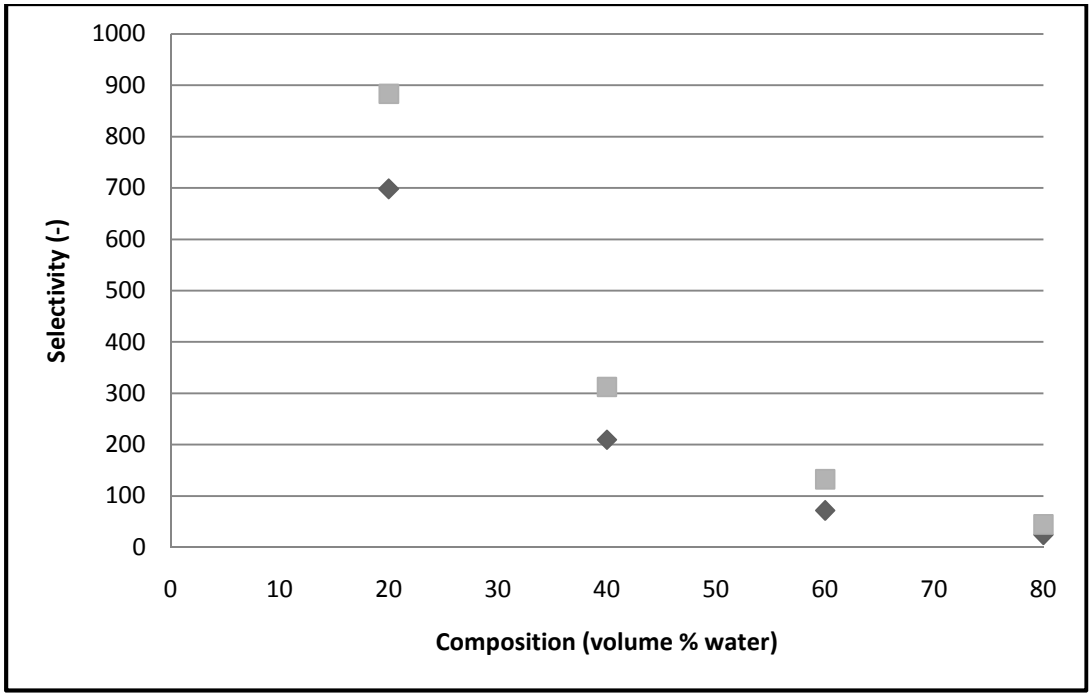

Figure 4.7: Influence of feed composition on membrane selectivity for Nafion-212. (♦) represents 25℃ and (■) 55℃.

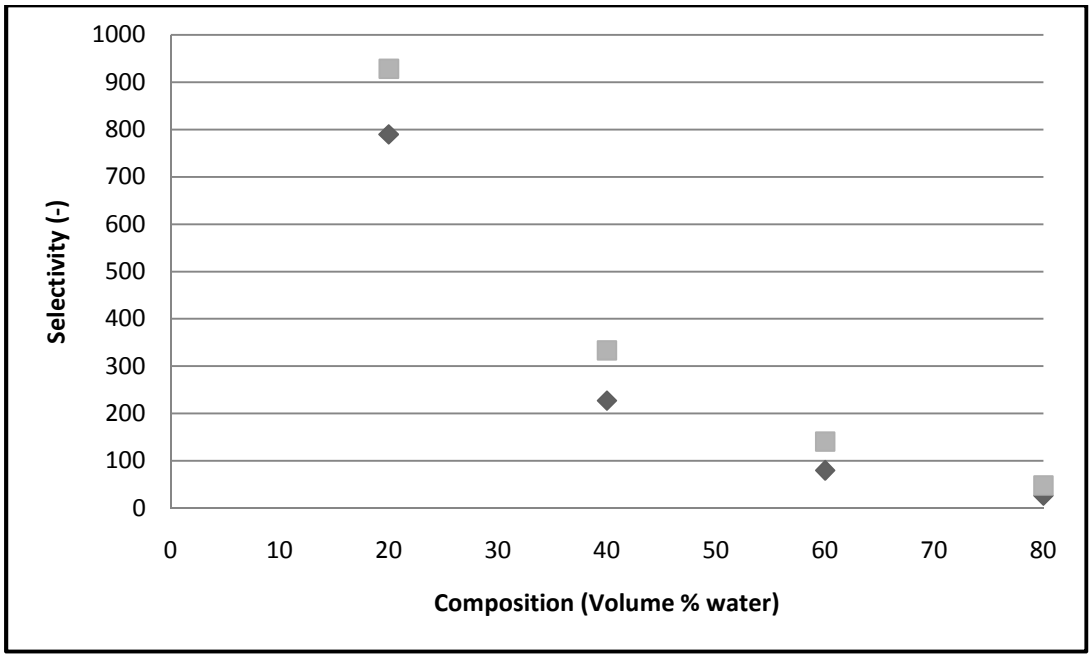

Figure 4.8: Influence of feed composition on membrane selectivity for Nafion-117. (♦) represents 25℃ and (■) 55℃.

In Figure 4.6 in the previous section it can be seen that the total flux increases as the fraction of water in the feed increases, while in Figure 4.7 and Figure 4.8 it is clear that, for both membranes, the selectivity decreases. The same results were reported by numerous other researchers (Mulder *et al*., 1985; Orme *et al*., 2009; Cao *et al*., 1999). The permeation flux can be seen as a cumulative effect of diffusion and sorption. Both of these steps depend on variables such as the size of the penetrants, free volume of the membrane and polar-polar interactions.

There are a few factors that can influence the diffusivity of the permeants through the membrane which in turn influences the performance. One of the factors that may have a great influence when working with liquid feeds is speciation. Speciation occurs when a fluid, in this case sulfuric acid, dissociates in water and forms different ionic species. When sulfuric acid dissociates in water it forms sulfate (SO_4^{2-}), bisulfate (HSO_4^-) and H^+ ions, and the concentration of these different ions depends on the concentration of sulfuric acid in the water. *Casas et al.* (2000) investigated the dissociation of sulfuric acid in water and obtained the results shown in Figure 4.9.

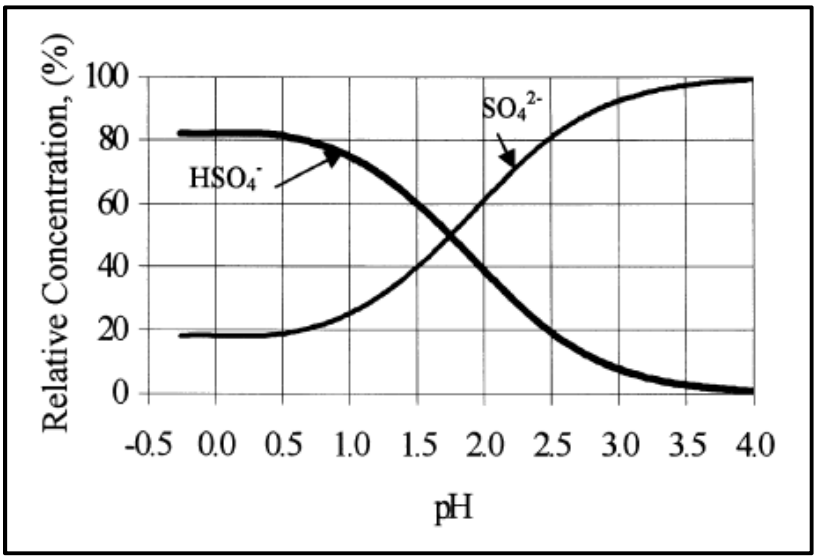

Figure 4.9: Calculated species distribution as a function of pH for sulfuric acid in water (Casas *et al.*, 2000)

In Figure 4.9 it can be noted that the equivalence point (where the sulfate and bisulfate ions have similar concentrations) is at a pH of 1.75. When the pH level is between 1.75 and 4 the sulfuric acid is partially dissociated into SO_4^{2-} and HSO_4^- with the majority being SO_4^{2-} ions. At pH levels between 1.75 and 0.5 partial dissociation also occurs, but the HSO_4^- ions are favored with more forming than SO_4^{2-} ions. When the pH reaches levels below 0.5 the concentration stabilizes with 80% HSO_4^- ions and 20% SO_4^{2-}. At pH levels higher than 4, sulfuric acid is fully dissociated with only SO_4^{2-} and H^+ ions being formed. Thus, as the percentage of water in the feed increases, the pH levels will increase and favor the dissociation of sulfuric acid into SO_4^{2-} and H^+ ions.

In a study completed by Larson *et al.* (1982) in which the relative volumes of the anions associated with the dissociation of some commonly used acids were investigated, the volumes of sulfate ions and bisulfate ions respectively, were measured. They found that HSO_4^- had a relative molecular volume of 35.2 cm^3/mol and SO_4^{2-} a relative volume of 14 cm^3/mol. The sulfate ion therefore has a significantly smaller volume than the bisulfate ion. Thus it can be concluded that speciation may play an important role in influencing the diffusivity of the permeants through the membrane. As the fraction of water in the feed increases, the pH level increases, which favors the formation of sulfate ions which can diffuse through the membranes more easily.

This phenomenon will not only increase the total flux of the acid through the membrane, but it can also explain the observed results for the membrane selectivity as shown in Figures 4.7 and

4.8. As the water fraction increases and sulfate ions diffuse through the membrane, it can bond with the H^+ ions which also diffuse through the membrane to form sulfuric acid. Thus, as more sulfate ions diffuse through the membrane, more sulfuric acid is formed on the permeate side which has a decrease in selectivity as effect.

Another factor that should be taken into consideration when explaining the results shown in Figure 4.5 and 4.6 for the membrane selectivity is a coupling effect. When working with a feed consisting of multiple components, a coupling effect can occur due to strong permeant-permeant interactions, as well as strong permeant-membrane interactions as explained in Chapter 2. When there is interaction between the species in the feed, which is the case as sulfuric acid dissociates in water, the obtained flux can deviate from the ideal situation. Both the Nafion membranes are permselective towards water, thus as the concentration of water increases and the flux increases correspondently, the sulfuric acid may diffuse more easily through the membrane along with the water. This may explain the decrease in membrane selectivity: as the water concentration increases, more sulfuric acid is diffused, which lowers the selectivity calculated for both the membranes.

Permeant-permeant interactions can influence the pervaporation properties, but also the interaction between the permeants and the polymeric membrane, and this effect is referred to as plasticization. Zhou *et al.* (1996) used this phenomenon to explain the results obtained for the decrease in selectivity. As the water concentration is increased, the membrane becomes more swollen due to the strong interaction between the water and the membrane. As the membrane becomes more swollen, the polymer chains in the membrane becomes more flexible, which can decrease the resistance of the membrane towards the diffusive transport of the permeants. The result of this plasticization effect is an increase in the total flux, which can be seen from the results obtained, explained by an easier passage through the membrane for the molecules. Furthermore, the selectivity will decrease accordingly as the mobility of both the water and sulfuric acid molecules is increased, which leads to an increase in sulfuric acid flux values. Thus, plasticization effects can readily explain the results obtained from the experimentations.

4.2 Sorption characteristics of the membranes

In this section the sorption characteristics of the Nafion membranes with a binary mixture of water and sulfuric acid are addressed. The aspect that is under investigation during the sorption experiments is the swelling properties; in other words, the mass absorbed by the membrane. The dependence of the membrane swelling on both the temperature and concentration of the water is shown and discussed.

4.2.1 Influence of feed composition and temperature

The influence of the temperature range of the solution, as well as the feed composition range on the sorption characteristics of both membranes was investigated. This was done by varying the concentration of water in the feed solution over the same range as it was varied in the pervaporation experiments at two different temperatures. The mass uptake was measured continually and from this data the swelling ratio of both membranes could be calculated. All the details concerning these calculations can be seen in Appendix B. Figure 4.10 shows the swelling ratio results obtained for both membranes.

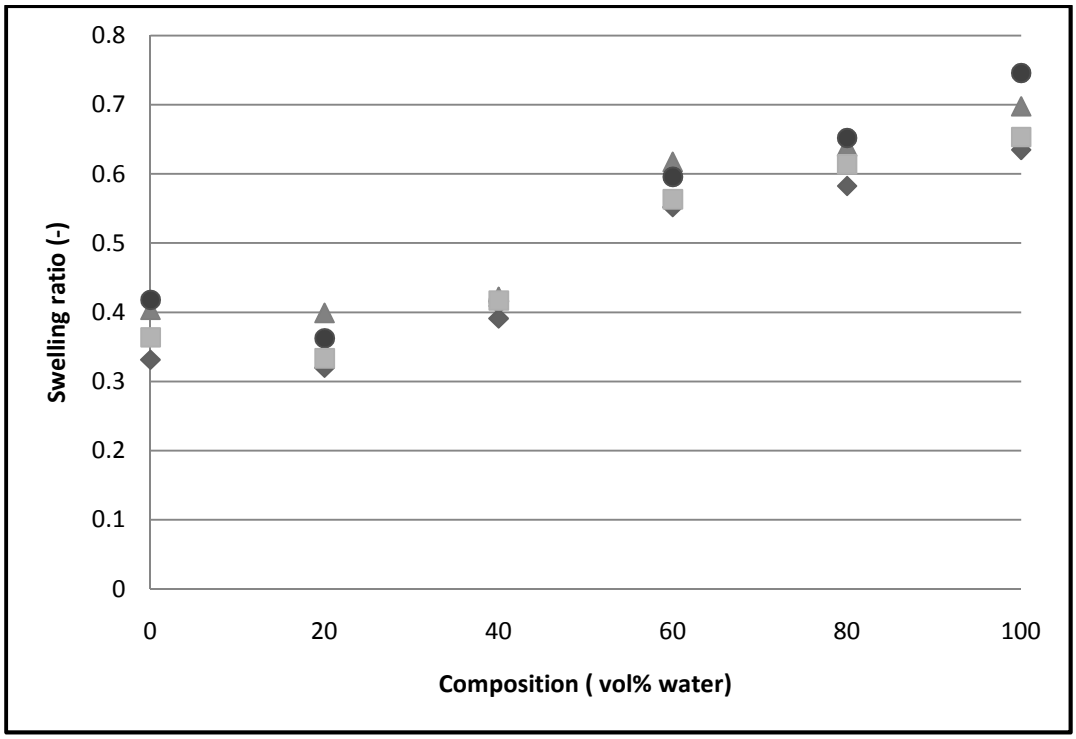

Figure 4.10: Swelling ratios for both Nafion membranes at 25˚C and 55˚C. (▲) shows Nafion-212 at 25℃, (♦) Nafion-117 at 25℃, (●) Nafion-212 at 55℃ and (■) Nafion-117 at 55℃.

The swelling ratio (M_∞) shown in Figure 4.10 above is a measure of the amount of solution that is absorbed into the membrane when equilibrium is reached between the feed solution and the membrane, compared to the dry membrane strip's initial mass. This was discussed in Chapter 2, and the equation was given as (eq. 2.6)

$$M_\infty = \frac{W\infty - Wo}{Wo}$$

In Figure 4.10 it can be seen that there is a steady increase in the swelling ratio across the concentration range. Thus, as the amount of water in the feed solution is increased, the amount of liquid absorbed in the membrane also increases. At the lower water concentrations, in the 0 to 20 vol% water region, the swelling ratio decreases before slightly increasing to the 40 vol% water range, from whereon it increases more significantly. It can also be observed that higher swelling ratio's is obtained at higher temperatures within the same membrane. This phenomenon confirms the higher flux values, as well as the definite decrease in membrane selectivity as the concentration of water increases.

In Section 4.1 the effects of plasticization were explained, where as the membrane became more swollen, the polymer chains in the membranes could become more flexible, which could decrease the resistance of the membrane towards the diffusive transport of the permeants, including the diffusion of sulfuric acid. It can be concluded from the results shown above that this is a definite possibility as there is a significant increase in membrane swelling at the higher water concentrations. Other researchers (Majstrik *et al.,* 2007; Randova *et al.,* 2009) also found a steady increase in the amount of liquid absorbed as the concentration of the preferentially permeating species increased, but no literature was found on a water/sulfuric acid system to compare the results with.

4.3 Modeling of pervaporation results

The aim of this section is to determine whether a simplified model based on solution-diffusion mechanism can be developed in order to describe the obtained experimental results correctly. In Section 2.4.1 it was noted that for the solution-diffusion model to effectively describe the experimental data, it had to express the diffusion coefficient as a function of concentration. In Section 2.4.2 the different diffusion coefficients were noted which either had a linear or exponential dependence.

The three models described in Section 2.5.2 are the Greenlaw (1997), Long (1965) and the Suzuki and Onozato (1982) models. In order to determine which of the models is most effective in describing the experimental results obtained from the pervaporation experiments, the obtained flux rates and water concentration in the feed for Nafion-212 at 55℃ are used. Figures 4.11, 4.12 and 4.13 give the results obtained for the permeate flux modeled with the Greenlaw diffusion coefficient (Eq. 2.14), Long diffusion coefficient (Eq. 2.16) and the Suzuki and Onozato diffusion coefficient (Eq. 2.18), respectively, using the computer aided program Statistica, where the sum of least squares method is used to predict the coefficients.

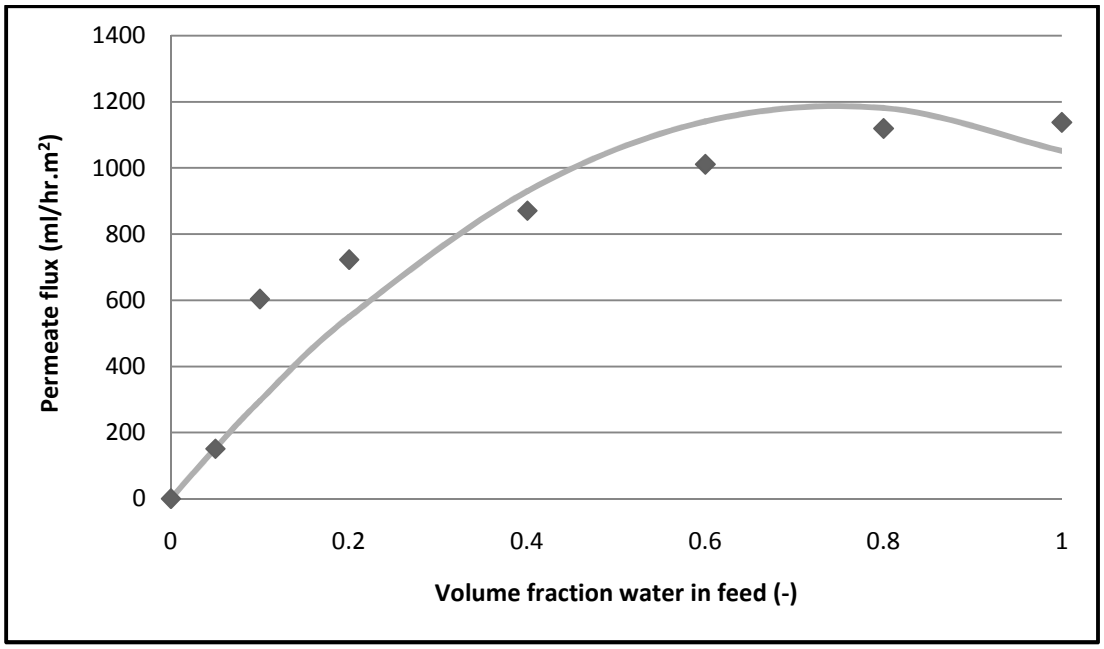

Figure 4.11: Comparison of the experimental permeate flux at 55℃ with the Greenlaw model. In the graph (♦) represents the experimental values and (--) the modeled values.

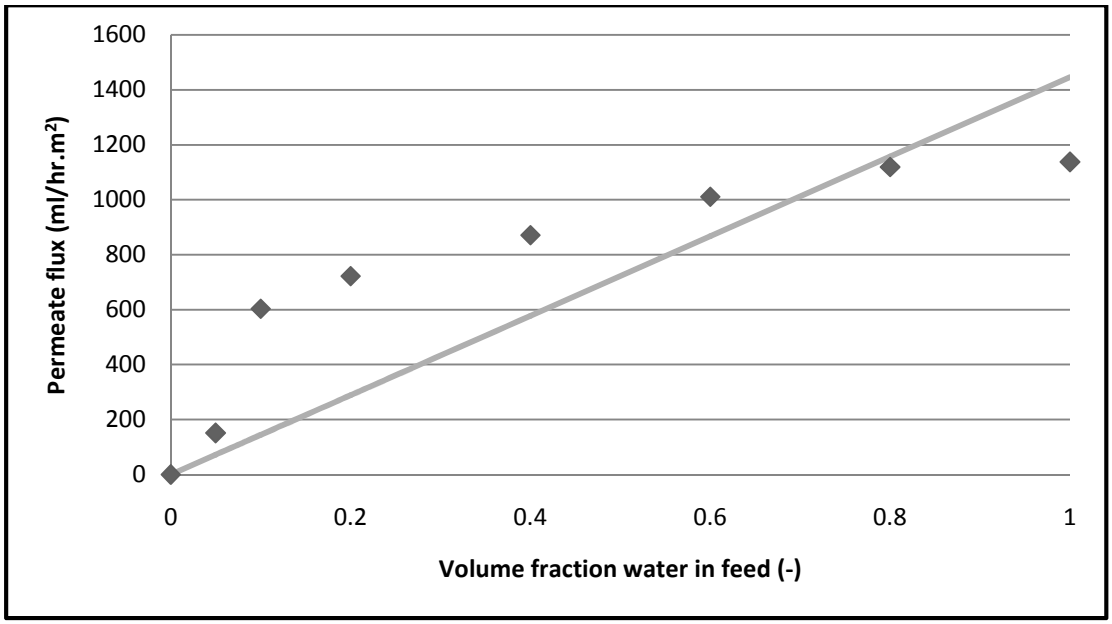

Figure 4.12: Comparison of the experimental permeate flux at 55℃ with the Long model. In the graph (♦) represents the experimental values and (--) the modeled values.

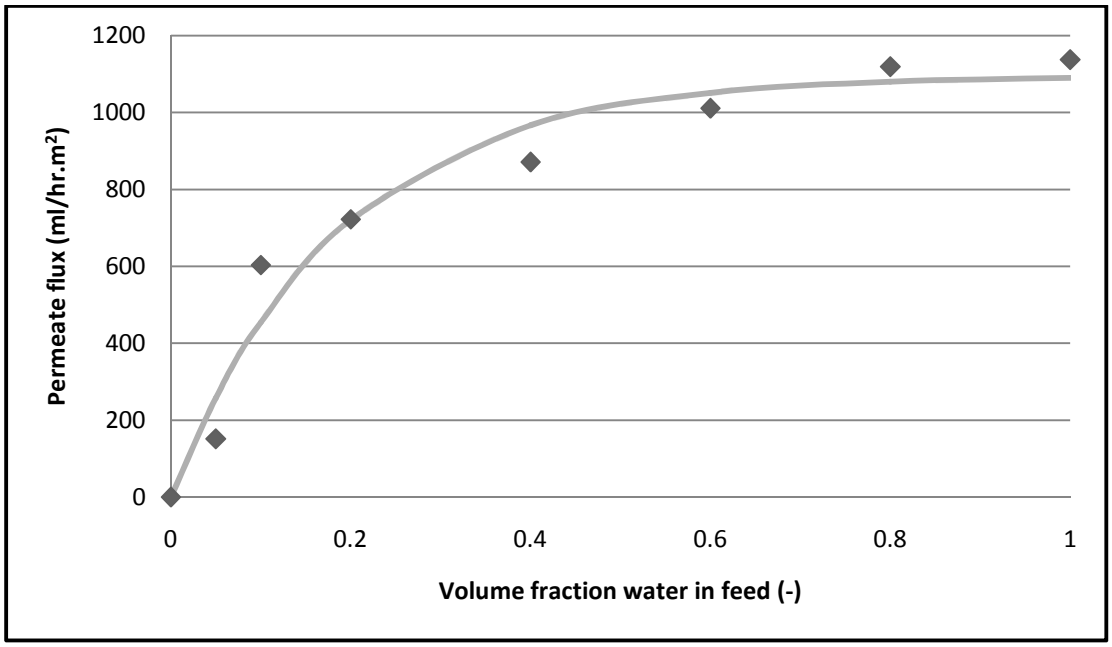

Figure 4.13: Comparison of the experimental permeate flux at 55℃ with the Suzuki and Onozato model. In the graph (♦) represents the experimental values and (--) the modeled values.

When comparing the three models with each other shown in Figures 4.11, 4.12 and 4.13 above it can be seen that the Suzuki and Onozato model seems to fit the experimental values the best with the model having an exponential dependence on the concentration. The Long-model has a linear form and fits the experimental values very loosely. In order to quantify the capability of

the applied models to represent the experimental data correctly, the models are compared by estimating the standard deviation as (Ochoa *et al.,* 2001):

$$SD = \sqrt{\frac{\sum(y_{exp} - y_{calc})^2}{N-p}} \qquad (4.2)$$

where y_{exp} and y_{calc} represent the experimentally obtained values and the calculated values, respectively, N the number of data points and p the number of fitted parameters. Table 4.1 shows the calculated standard deviation values for all the applied models, as well as the regression factor which indicates how well the applied model fits the experimental data. All the necessary calculations are shown in Appendix D.

Table 4.1: Comparison of standard deviation and R^2-values of applied models

Applied model	SD	R^2-value
Greenlaw	161.042	0.937
Long	318.828	0.728
Suzuki and Onozato	97.911	0.981

From the standard deviation values calculated it can be seen clearly that the Suzuki and Onozato model is most effective in predicting the experimental values as it has the lowest standard deviation from the experimental values. Thus, as observed from the graphs and the accompanying R-values generated, the Suzuki and Onozato model produces the best correlation between the predicted and experimental values. To verify the validity of the findings, the values calculated from the models for the limiting diffusion coefficient and the plasticization coefficients for water need to be compared to literature data. Table 4.2 gives the calculated values for each of the applied models.

Table 4.2: Calculated values of limiting diffusion coefficients and plasticization coefficients for water

Model	D_i^0 (m^2/s)	β_{ij} (-)	β_{ii} (-)
Greenlaw	5.4218E-05	1.509	-
Long	0.0502	0.00074	-
Suzuki and Onozato	1.2377E-07	0.0043	-5.353

In Table 4.3 the values obtained for the limiting diffusion coefficient and the plasticization coefficients by the Suzuki an Onozato model are compared to some values found in literature. This specific model was chosen because the standard deviation calculations showed it to be the most effective in describing the experimental results. It is difficult to compare calculated values for these parameters as each system (chemicals and membrane) is unique, but the values are given and the orders of magnitude of the values are compared.

Table 4.3: Comparison of limiting diffusion coefficients and plasticization coefficients

Model/membrane	D_i^0 (m^2/s)	β_{ij} (-)	β_{ii} (-)	Reference
Suzuki and Onozato	1.2377E-07	0.0043	-5.353	This study
Water in perfluorosulfonate ionomeric membranes	1.2E-06	-	-	Zawodzinski *et al.*, 1990
Water/ethylene glycol with PVA membrane	1.08E-14	-	-	Chen & Chen, 1997
Water and ethanol	1.36E-09	-	-	Heintz *et al.*, 2010
Ethanol/water with CS/HEC membranes		0.0452	-1.2678	Jiraratananon *et al.*, 2002
Self-diffusion of water in Nafion-117	3.87E-06	-	-	Suresh *et al.,* 2005

From the comparison with the values found in literature it can be concluded that the coefficients calculated using the Suzuki and Onozato model compare well with the order of magnitude of the limiting diffusion coefficients and the plasticization coefficients. This shows that the model can be successfully applied for the prediction of experimental results in pervaporation, but no values were found for the specific application of the separation of water and sulfuric acid.

4.4 Comparison of separation capabilities

In Section 4.1 the results obtained from the pervaporation experiments were given and discussed in detail. The results clearly indicated that effective separation of a mixture of water and sulfuric acid is obtainable using pervaporation. In the proposed design of the HyS cycle by SRNL the separation was mainly accomplished by using vapor/liquid separation techniques in the form of flash drums. As part of the objective of the research project is to determine if the proposed flash separation section can be replaced by a pervaporation process, the separation capabilities of the pervaporation process need to be compared with that of the existing flash drum design.

To investigate the capabilities of the existing flash separation section proposed in the reference design, a flash separation process was simulated using a computer aided simulation for the separation of water and sulfuric acid. The simulation was completed at atmospheric pressure. Figure 4.14 shows the resulting vapor/liquid equilibrium diagram obtained from the simulation. All the relevant data is given in Appendix E.

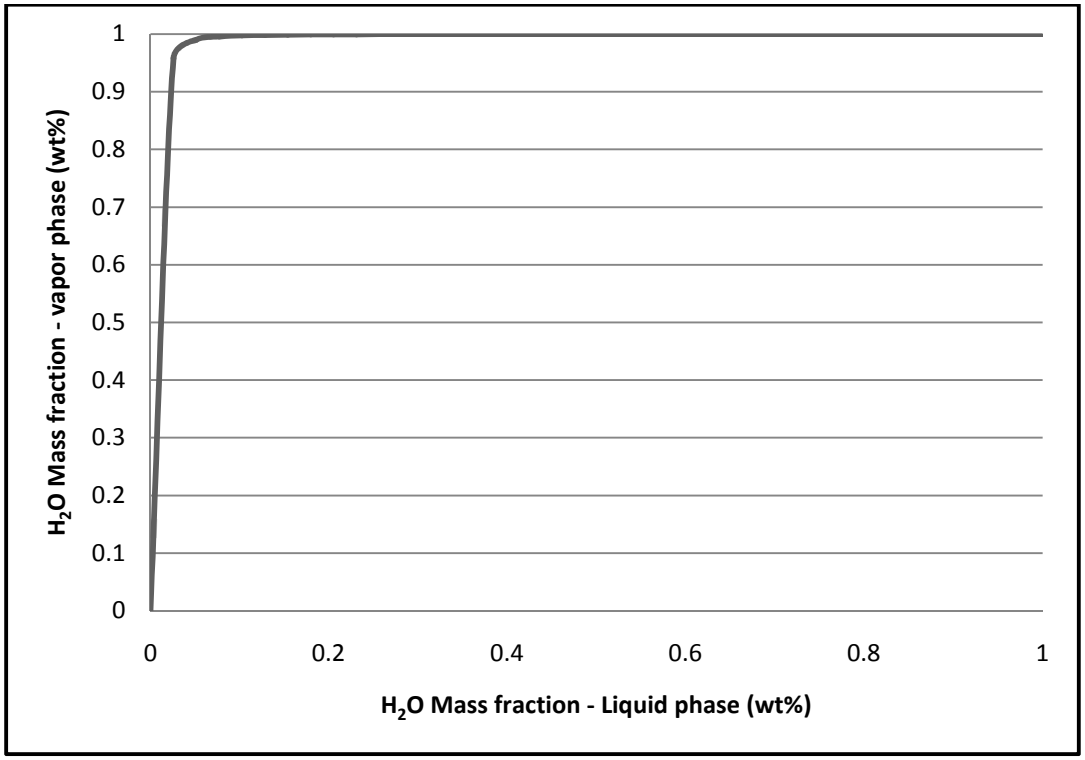

Figure 4.14: Vapor/liquid equilibrium diagram using flash separation at atmospheric pressure.

Figure 4.14 indicates that very efficient separation between water and sulfuric acid is theoretically obtainable using flash separation, as more or less all the water present in the

mixture are in the vapor phase and can be separated readily by applying flash drums or knockout drums. It should be noted that these values are obtainable theoretically under ideal conditions and that in practice the separation might not be as effective as depicted in Figure 4.14. The vapor/liquid equilibrium data also show that the sulfuric acid in the mixture remains almost completely in the liquid phase and can be recycled. Thus the flash separation process can be applied effectively for the concentration of sulfuric acid by removing the water contained in a mixture.

When examining the separation capabilities of the pervaporation process, similar results can be observed. If the permeate flux data obtained for the Nafion 212 membrane at 55˚C is taken as reference and the percentage sulfuric acid present in the permeate stream is determined, the results given in Table 4.4 are obtained. The specific operating conditions are chosen to use as an example. All the data for both Nafion membranes are given in Appendix E.

Table 4.4: Percentage sulfuric acid present in total permeate for Nafion-212 at 55˚C

20 vol% water	40 vol% water	60 vol% water	80 vol% water
0.811	0.884	0.920	1.002
0.829	0.871	0.895	1.021
0.847	0.855	0.926	1.009
0.803	0.848	0.919	1.026
0.820	0.899	0.902	1.019

The calculated percentages for the other experimental runs are given in Appendix E. In Table 4.4 it can be seen that for the entire range of water contents present in the feed, the percentage of sulfuric acid that permeated through the membrane is approximately 1%. Thus it can be concluded that pervaporation is highly effective for the removal of water from a mixture with sulfuric acid by prefferentially permeating the water. As the main purpose of the recuperation section is to concentrate the sulfuric acid before recycling to the decomposition reactor, it is important to calculate to what extent the pervaporation process is able to achieve this. For the calculations the composition of 60 vol% water is chosen (55 wt% sulfuric acid) as this fits the data from the reference design best. In Table 4.5 the calculated values are given for the concentration of the sulfuric acid stream using both the Nafion membranes at 25 and 55℃. All calculations are given in Appendix E.

Table 4.5: Concentration of sulfuric acid stream obtained for both the reference design and pervaporation process

Membrane	Temperature (℃)	Concentration obtained (wt %)
Reference design	100	75
Nafion-212	25	56.54
Nafion-212	55	82.39
Nafion-117	25	56.44
Nafion-117	55	78.69

In Table 4.5 the indicated concentration obtained, is from the feed stream to the process with a sulfuric acid concentration of 55 weight percentage. It can be seen from the results that for both membranes at the higher temperature, the pervaporation process is effective in concentrating the sulfuric acid by removing the water from the mixture. It is in accordance with the degree of concentration obtained in the reference design where flash separation was used.

Thus, theoretically, both processes are effective in the separation and can sufficiently upgrade the sulfuric acid stream and a decision cannot be made clearly as to which is practically best suited for this application. For such a comparison to be thoroughly and sensibly completed, a comparison of the involved costs need to be undergone, including both capital as well as operational costs for both processes.

Summary

In Chapter 4 the performance of the pervaporation process in the separation of water and sulfuric acid was investigated, with the following key findings from the chapter summarized as follows:

- The total flux through the membranes increases for both of the membranes as the feed temperature increases.
- The higher flux values of the Nafion-212 compared to the Nafion-117 membrane as the temperature increases may be attributed to the difference in thickness of the membranes.

- The temperature increases the pure component selectivity of both membranes decreases.
- For binary mixtures of water and sulfuric acid, the selectivity decreases as the fraction of water (preferentially permeating specie) in the feed increases.
- As the amount of water in the feed solution is increased, the amount of liquid absorbed in the membrane also increases, having the effect of higher flux values through the membrane, as well as decreasing the selectivity.
- The Suzuki and Onozato model is most effective in predicting the experimental values as it has the lowest standard deviation from the experimental values.

Chapter 5: Conclusions and recommendations

Overview

In this study commercial polymeric membranes, Nafion-212 and Nafion-117, were investigated in order to determine its pervaporation and sorption characteristics when being used for the separation of water and sulfuric acid mixtures. In Chapter 5 all the conclusions reached and forthcoming recommendations made from this study will be discussed.

The Chapter will be subdivided into 5 sections based on the scope of the investigation given in Chapter 1, including the main objective (5.1), the pervaporation (5.2) and sorption characteristics (6.3), modeling (5.4) and lastly the recommendations (5.5).

5.1 Main objective

It was shown that the proposed membrane separation process of pervaporation could be applied effectively and efficiently for the concentration of sulfuric acid by the selective removal of water from the mixture. It was shown that both Nafion membranes were effective in the separation of water and sulfuric acid mixtures and that the process could be used for this specific application.

5.2 Pervaporation characteristics

In the pervaporation experiments it was found that both the Nafion membranes were highly selective towards water, with permeate selectivities ranging from around 25 up to values of approximately 950, depending on the temperature and composition. For both the Nafion membranes the flux values increased from approximately 7 mol/(hour.m^2) at 25℃ to approximately 65 mol/(hour.m^2) at 55℃, showing an approximate increase in flux of 900% as the feed temperature of the mixture to the process is increased. This phenomenon was observed for both the pure component as well as the binary mixture experiments.

In the case of the pure component selectivity, the selectivity obtained decreased from approximately 2500 to 1000 as the temperature increases from 25 to 55℃.

The total permeate flux was found to increase, from approximately 34 mol/(hour.m^2) to 62 mol/(hour.m^2) for both membranes at a constant temperature of 55℃, as the concentration of water in the binary feed mixture increased. This amounts to an increase in total permeate flux of almost 200% as the concentration of water in the feed increases. Conversly, as the concentration of preferred permeating species, in this case water, increased, the binary selectivity decreased for both of the Nafion membranes investigated. The binary selectivity decreased from approximately 900 to 50 for both Nafion membranes at 55℃. All of the obtained results fit the hypotheses expected for this research project.

5.3 Sorption characteristics

As mentioned above in the pervaporation characteristics, both the Nafion membranes have a higher affinity for water than for sulfuric acid and thus the water is more readily and easily absorbed into the membrane. It can be observed that as the amount of water in the feed increases, the swelling ratio of the membrane increases. This increase in swelling ratio is more pronounced with the Nafion-212 membrane, where the swelling ratio increases from approximately 0.4 to 0.75, relating to an increase of almost 90%, than in the Nafion-117 membrane, where the swelling ratio increases from 0.36 to 0.65, an increase of approximately 80%.

The increase in the membrane swelling as the water concentration increases, magnifies the effect of the flux increasing, as observed in the pervaporation experiments, because the molecules diffuse more easily if the membrane is swollen. This phenomenon also helps to explain the decrease in membrane selectivity as the concentration of water increases, as the sulfuric acid is more readily transported through the membrane surface alongside the water, which is known as the coupling effect.

5.4 Modeling

Three models were considered for describing the experimental data obtained from the pervaporation experiments. The models compared are the Greenlaw, Long and the Suzuki and Onozato models. The three models are all based on the solution-diffusion mechanism. The Suzuki and Onozato model, with an exponential dependence of the diffusivity on concentration, gave the best fit for the experimental data with a standard deviation of 97, compared to that of

the Greenlaw and Long models, being 161 and 319, respectively. The limiting diffusion coefficient (D_i^0 = 1.2377e^{-7}) and plasticization coefficients (β_{ij} = 0.0043 and β_{ii} = -5.353) calculated from the model compare well with the order of magnitudes found in literature.

5.5 Recommendations

In this experimental study the focus was on separating the binary mixture of water and sulfuric acid while in reality other impurities or components like SO_2 and O_2 might be present which could affect the separation capabilities of the process. These components can be incorporated into the study to determine the effect it can have on the separation. It was proven that pervaporation is an effective method of separation for the binary mixture over a wide range of water concentrations in the feed, but it can also be recommended that further studies may focus more on the concentration range that will be present in the feed stream to the section according to the reference design, which is in the region of 60-95 vol% sulfuric acid.

Furthermore, in Chapter 4 it was shown that theoretically both processes were as effective as the other in its separation capabilities and that further investigation is necessary to distinguish between the two. It is recommended that an in-depth study should be done on the costs associated with the operation of both processes to determine which is best suited for the application. As part of this investigation I would propose that the extent of degradation of Nafion membranes be studied over a extended period of time to determine if it affects their separation capabilities in order to calculate how often the membranes should be replaced, which can have major effects on the operational costs involved.

References

Abanades, S., Charvin, P., & Flamant, G. (2005). Screening of water-splitting thermochemical cycles potentially attractive for hydrogen production by concentrated solar energy. *Energy 31* , 2805-2822.

Aminabhavi, T. M., Harlapur, S. F., Balundgi, R. H., & Ortego, J. D. (1998). Theoretical and experimental investigations of molecular migrations and diffusion kinetics of organic esters into tetrafluoroethelene/propulene copolymer membranes. Canadian Journal of Chemical Engineering 76 , 104-112.

Annual energy outlook. (2010). *US energy demand.* US Energy Information Administration.

Binning, R., Lee, R., & Jennings, J. (1961). Separation of liquid mixtures by permeation. *Industrial and engineering chemistry vol 53* , 1.

Bodderek, K. W. (1990). Terminology in pervaporation. *Journal of membrane science 51* , 259-272.

Bouallouche, R., Schaetzel, P., Amar, H., Nguyen, Q., Riffault, B., & Marais, S. (2010). Mass transfer in pervaporation: The key component approximation for the solution diffusion model. *Desalination 251* , 161-166.

Brecher, L., & Wu, C. (1975). Electrolytic decomposition of water. *US patent number 3588750* .

Brecker, L., Spewock, S., & Warde, C. (1977). The Westinghouse sulfur cycle for the thermochemical decomposition of water. *International journal of Hydrogen* .

References

Burshe, M. C., Sawant, S. B., & Pangarkar, V. G. (1999). Dehadration of glycerien-water mixtures by pervaporation. *JAOCS 76*, 209-214.

Cao, S., Shi, Y., & Chen, G. (1999). Pervaporation separation of MeOH/MTBE through CTA membranes. *Journal of Applied Polymer science* , 377-386.

Casas, J. M., Alvarez, F., & Cifuentes, L. (2000). Aqueous speciation of sulfuric acid-cupric sulfate solutions. *Chemical engineer science 55*, 6223-6234.

Charvin, P., & Abanades, S. (2008). Analysis of solar chemical processes for hydrogen production from water-splitting thermochemical cycles. *Energy conversion and management* , 1547-1556.

Charvin, P., Lemont, F., & Abanades, S. (2008). Novel two-step SnO_2/SnO water-splitting cycle for solar thermochemical production of hydrogen. *International journal of hydrogen energy* , 6021-6030.

Chen, F., & Chen, H. (1998). A diffusion model of the pervaporation separation of ethylene glycol-water mixtures through crosslinked poly(vinyl alcohol) membrane. *Journal of membrane science139*, 201-209.

Devore, J., & Farnum, N. (2005). *Appied Statistics for Engineers and Scientist.* California: Brooks and Cole.

Douglas, J. M. (1988). *Conceptual design of chemical processes.* Singapore: McGraw-Hill.

Dutta, B., JI, W., & Sikdar, S. (1997). Pervaporation: Principles and applications. *Separation and purification methods 25* , 131-224.

Farbman, G. (1976). The conceptual design of an integrated nuclear-hydrogen production pant using the sulfur cycle. *Nasa contractor report* .

References

Feng, X., & Haung, R. (1997). Liquid separation by membrane pervaporation: an overview. *Ind. Eng. Chem. Res 36* , 1048-1066.

Forsberg, C. (2007). future hydrogen markets for large-scale hedrogen production systems. *International journal of hydrogen energy* , 431-439.

Gao, Z., Yue, Y., & Li, W. (1996). Application of zeolite-filled pervaporation membrane. *Zeolites 16*, 70-74.

Ginosar, D., & Stewart, F. (2007). NHI catalyst and membrane studies for thermochemical cycles at INL. *FY annual progress report: DOE hydrogen program* , 1-4.

Goldblatt, M., & Gooding, C. (1986). An engineering analysis of membrane-aided distillation. *AIChE symposium series 82* , 51-69.

Gonzales, R., Law, V., & Prindle, J. (2009). Analysis of the hybrid copper oxide-copper sulfate cycle for the for the thermochemical splitting of water for hydrogen production. *International journal of hydrogen energy* , 4179-4188.

Gorensek, M., & Summers, W. (2009). *Hybrid sulfur process reference design and cost analysis.* Savanah rivers national laboratory.

Gosselink, J. (2002). Pathways to a more sustainable production of energy: sustainable hydrogen. *International journal of hydrogen energy* , 1125-1129.

Greenlaw, F., Shelden, R., & Thompson, E. (1977). Dependance of diffusive permeation rates on upstream and downstream pressures. *Journal of membrane science 2* , 333-348.

Heisler, E., Hunter, A., & Siciliano, J. (1956). Solute and temperature effects in the pervaporation of aqueous alcoholic solutions. *Science 77* , 24.

References

Heintz, A., Ludwig, R., & Schmidt, E. (2011). Limiting diffusion coefficients of ionic liquids in water and methanol: a combined experimental and molecular dynamics study. *Physical chemistry 13*, 3268-3273.

Heitner-Wirguin, C. (1996). Recent advances in perfluorinated ionomer membranes: structure, properties and applications. *Journal of membrane science 120*, 1-33.

Humphrey, J. L. (1997). *Separation process technology.* New York: Mcgraw and Hill.

Jiraratananon, R., Chanachai, A., & Huang, R. (2002). Pervaporation dehydration of ethanol-water mixtures with chitosan/hydroxyethylcellulose (CS/HEC) composite membranes. *Journal of membrane science 199*, 211-222.

Jonquires, A., Clement, R., Roizard, D., & Lochon, P. (1996). Pervaporative transport moddeling in a ternary system. *Journal of membrane science 109* , 65-76.

Kober, P. (1917). Pervaporation, perstillation and percrystallization. *Journal of membrane science 100* , 61-64.

Larson, J. W., Zeeb, K. G., & Hepler, L. G. (1982). Heat capacities and volumes of dissociation of phosphoric acid, bicarbonate ion and bisulfate ion in aqueous solutions. *Canadian Journal of chemistry*, 2141-2150.

Le Roux, M., & Hattingh, B. (2010). *HyS hydrogen production process development special studies: Section 4: Separation.* Potchefstroom: HyS infrastructure.

Lemort, F., Charvin, P., & Lafon, C. (2006). Technological and chemical assessment of various thermodynamical cycles: From the UT3 cycle up to the two-step iron oxide cycle. *International journal of hydrogen energy* , 2063-2075.

Leybros, J., Saturnin, A., & Mansilla, C. (2010). Plant sizing and evaluation of hydrogen production costs from advanced processes coupled to a nuclear heat source. *International journal of hydrogen energy 35* , 1019-1028.

Li, Q., He, R., Jensen, J. O., & Bjerrum, N. J. (2004). PBI-Based polymer membranes for high temperature fuel cells - Preparation, characterization and fuel cell demonstration. *Fuel cells*, 1-13.

Lipnizki, F., Field, R., & Ten, P.-K. (1999). Pervaporation-based hybrid process: a review of process design, application and economics. *Journal of membrane science 153*, 183-120.

Long, R. (1965). Liquid permeation for plastic films. *Ind. Eng. Chem. Fundam 4* , 445.

Lu, P., Ammon, R., & Parker, G. (1980). *A study on the electrolysis of sulfer dioxide and water for the sulfur cycle hydrogen production process.* Nasa contractor report.

Luo, G. S., Niang, M., & Schaetzel, P. (1997). Pervaporation separation of ethyl tert-butyl ether and ethanol mixtures with a blended membrane. *Journal of membrane science 125*, 237-244.

Majstrik, P. W., Satterfield, B., Bocarsly, A. B., & Benziger, J. B. (2007). Water sorption, desorption and transport in Nafion membranes. *Journal of membrane science 301* , 93-106.

Marx, S., van der Gryp, P., Neomagus, H., & Everson, R. (2002). Pervaporation separation of methanol from methanol/tert-amyl methyl ether mixtures with a commercial membrane. *Journal of membrane science 209* , 353-362.

Mauritz, K. A., & Moore, R. B. (2004). State of understanding of Nafion. Chem. Rev. 104 , 4535-4585.

Mulder, M. (1996). *Basic principles of membrane technology.* Dordrecht, Netherlands: Kluwer academic Publishers.

References

Mulder, M. H., Franken, T., & Smolder, C. A. (1985). Preferential sorption versus freferential permeablility in pervaporation. *Journal of membrane science 22*, 155-173.

Mulder, M., & Smolders, C. (1984). On the mechanism of separation of ethanol/water mixtures by pervaporation. *Journal of membrane science 17* , 289-307.

Nam, S., Chun, H., & Lee, Y. (1999). PErvaporation separation of water-isopropanol mixture using carboxymethylated poly(vinyl alcohol) composite membrane. *Journal of applied science 72* , 241-249.

Neel, J. (1991). Introduction to pervaporation. In R. Haung, *Pervaporation membrane separation processes* (pp. 1-109). Amsterdam: Elsevier.

Neel, J. (1995). Pervaporation. In R. D. Noble, & S. A. Stern, *Membrane Separations technology* (pp. 143-211). Amsterdam: Elsevier.

Ochoa, J., Cassanello, M. C., Bonelli, P. R., & Cukierman, A. L. (2001). CO2 gasification of Argentinean coal chars: a kinetic characterization. *Fuel processing technology 74*, 161-176.

Orhan, M., Dincer, I., & Rosen, M. (2010). An exergy-cost-energy-mass analysis of a hybrid copper-chlorine thermochemical cycle for hydrogen production. *International journal of hydrogen energy* , 4831-4838.

Orme, C., & Jones, M. (2005). Pervaporation of water from aqueous HI using Nafion-117 membranes for the sulfur-iodine thermochemical water splitting process. *Journal of membrane science* , 245-252.

Orme, C., Klaehn, J., & Stewart, F. (2009). Membrane separation processes for the benefit of the sulphur-iodine and hybrid sulphur thermochemical cycles. *International journal of hydrogen energy* , 4088-4096.

Park, H., Ramaker, N., Mulder, M., & Smolders, C. (1995). Separation of MTBE-methanol mixtures by pervaporation. *Separation science and technology, Volume 30, Issue 3* , 419-433.

Parker, G. (1983). *Solar thermal hydrogen production process.* Westinghouse electrical corporation.

Paul, D. R. (1974). Further comment on the relation between hydraulic permeation and diffusion. *Journal of polymeric science 12* , 1221.

Perry, R. H., & Green, D. H. (1997). *Perry's chemical engineers' handbook.* McGraw-Hill.

Pinto, C. G., & Laespada, E. F. (1999). Analytical applications of separation techniques through membranes. *Laboratory Automation and information management 34* , 115-130.

Randova, A., Bartovska, L., Hovorka, S., Friess, K., & Izak, P. (2009). The membranes (Nafion and and LDPE) in binary liquid mixtures benzene + methanol - sorption and swelling. *European polymer journal 45* , 2895-2901.

Schaetzel, P., Vauclair, C., Nguyen, Q., & Bouzerer, R. (2004). A simplified solution-diffusion theory in pervaporation: the total solvent volume fraction model. *Journal of membrane science 244* , 117-127.

Seader, J., & Henley, E. (2006). *Separation process principles.* Washington: Wiley and Sons.

Silberstein, M. N., & Boyce, M. (2011). Hygro-thermal mechanical behavior of Nafion during constrained swelling. *Journal of power sources 196*, 3452-3460.

South Africa. (2010, 03 18). Retrieved 02 17, 2012, from Tariff increase: http://www.southafrica.co.za/2010/03/18/tariff-increases/

Strathman, H. (2005). Synthetic membranes and their preparation. In M. Porter, *Handbook of industrial membrane technology* (pp. 1-60). New delhi: Crest publishing house.

References

Sun, Y.-M., & Haung, T.-L. (1996). Pervaporation of water-methanol mixtures through temperature sensitive poly(vinyl alcohol-g-N-isopropyacrylamide) membranes. *Journal of membrane science 110* , 211-218.

Suresh, G., Scindia, Y., Pandey, A., & Goswami, A. (2005). Self-diffusion coefficient of water in Nafion-117 membrane with different monovalent counterions: a radiotracer study. *Journal of membrane science 250*, 39-45.

Suzuki, F., & Onozato, K. (1982). Pervaporation of benzene-cyclohexane mixtures by poly (methyl-glutamate) membrane and synergistic effect of their mixture on diffusion rate. *Journal of applied polymeric science 27* , 4229-4238.

United states Department of Energy. (2006). Hydrogen posture plan: An integrated research, development and demonstration plan. 19.

Van der Gryp, P. (2003). Separation by pervaporation of Methanol from tertiary amyl methyl ether using a polymeric membrane. 24.

Vardeman, S. (1994). Statistical methods for physical science. San Diego: Academic Press.

Wijmans, J. G., & Baker, R. W. (1995). The solution diffusion model: a review. *Journal of membrane science 107* , 1-21.

Wang, K. Y., Chung, T.-S., & Qin, J.-J. (2007). Polybenzimidazole (PBI) nanofiltration hollow fibre membranes aplied in forward osmosis processes. *Journal of membrane science 300*, 6-12.

Yang, J. S., Kim, H. J., Jo, W. H., & Kang, Y. S. (1998). Analysis of pervaporation of methanol-MTBE mixtures through cellulose acetate and cellulose triacetate membranes. *Polymer 39* , 1381-1385.

Zawodzinski, T., Neeman, M., Sillerud, L., & Gottesfeld, S. (1991). Determination of water diffusion coefficients in perfluorosulfonate Ionomeric membranes. *Journal of physical chemistry 95*, 6040-6044.

Zeman, L. J., & Zydney, A. L. (1996). *Microfiltration and ultrafiltration, Principles and applications.* New York: Marcel Dekker Inc.

Zhang, S., & Drioli, E. (1995). Pervaporation membranes. *Separation science and technology* , 1.

Zhou, M., Persin, M., & Sarrazin, J. (1996). Mehanol removal from organic mixtures by pervaporation using polypyrrole membranes. *Journal of membrane science 117*, 303-309.

Appendix A: Raw data

A.1 Pure component pervaporation experiments

A.1.1 Pure water

Table A.1: Pure water data for Nafion-212 membrane

Temperature	Hours	Weight of cold trap with permeate (g)	Permeate (g)	Permeate (mol)
25˚C	2	145.540	3.966	0.220
	4	143.201	1.627	0.090
	6	143.273	1.699	0.094
	8	143.294	1.720	0.095
	10	143.252	1.678	0.093
35˚C	2	148.584	7.010	0.389
	4	144.820	3.246	0.180
	6	144.763	3.189	0.177
	8	144.536	2.962	0.164
	10	144.660	3.086	0.171
45˚C	2	153.549	11.975	0.665
	4	150.866	9.292	0.506
	6	150.642	9.068	0.513
	8	150.796	9.222	0.512
	10	150.534	8.960	0.497

55˚C	2	159.426	17.852	0.991
	4	160.219	18.645	1.035
	6	160.318	18.744	1.041
	8	160.167	18.593	1.032
	10	159.998	18.422	1.023

Table A.2: Pure water data for Nafion-117 membrane

Temperature	Hours	Weight of cold trap with permeate (g)	Permeate (g)	Permeate (mol)
25˚C	2	145.771	4.197	0.233
	4	145.010	3.436	0.190
	6	144.158	2.584	0.143
	8	143.700	2.126	0.118
	10	143.455	1.968	0.109
35˚C	2	146.892	5.318	0.295
	4	145.230	3.656	0.203
	6	145.080	3.506	0.194
	8	145.148	3.574	0.198
	10	144.976	3.402	0.189
45˚C	2	146.845	5.217	0.292
	4	146.623	5.049	0.280

	6	146.722	5.148	0.286
	8	146.720	5.146	0.285
	10	146.536	4.962	0.275
55˚C	2	159.458	17.844	0.993
	4	157.243	15.669	0.870
	6	157.161	15.587	0.865
	8	156.849	15.273	0.848
	10	156.987	15.413	0.856

A.1.2 Pure sulfuric acid

Table A.3: Pure sulfuric acid data for Nafion-212 membrane

Temperature	Hours	Weight of cold trap with permeate (g)	Permeate (g)
25˚C	2	141.584	0.010
	4	141.580	0.006
	6	141.581	0.007
	8	141.580	0.006
	10	141.579	0.005
35˚C	2	141.587	0.013
	4	141.586	0.012
	6	141.586	0.012
	8	141.585	0.011
	10	141.587	0.013

45˚C	2	141.623	0.049
	4	141.617	0.043
	6	141.620	0.046
	8	141.624	0.050
	10	141.620	0.046
55˚C	2	141.668	0.094
	4	141.659	0.085
	6	141.664	0.090
	8	141.662	0.088
	10	141.670	0.096

Table A.4: Pure sulfuric acid data for Nafion-117 membrane

Temperature	Hours	Weight of cold trap with permeate (g)	Permeate (g)
25˚C	2	141.581	0.007
	4	141.580	0.006
	6	141.581	0.007
	8	141.580	0.006
	10	141.579	0.005
35˚C	2	141.584	0.010
	4	141.585	0.011

	6	141.582	0.008
	8	141.583	0.009
	10	141.586	0.012
45˚C	2	141.623	0.049
	4	141.619	0.045
	6	141.624	0.050
	8	141.620	0.046
	10	141.622	0.048
55˚C	2	141.658	0.084
	4	141.652	0.078
	6	141.656	0.082
	8	141.652	0.078
	10	141.656	0.082

A.1.3 Proof of steady-state experiments

Table A.5: Proof of steady-state experiment for Nafion-212 membrane

Hours	Run 1 total permeate (g)	Run 2 total permeate (g)	Run 3 total permeate (g)
2	3.966	2.645	2.892
4	1.627	1.723	1.702
6	1.699	1.719	1.653
8	1.720	1.673	1.625
10	1.678	1.628	1.641

12	1.620	1.687	1.642
14	1.661	1.668	1.648

Table A.6: Proof of steady-state experiment for Nafion-117 membrane

Hours	Run 1 total permeate (g)	Run 2 total permeate (g)	Run 3 total permeate (g)
2	4.197	3.954	3.847
4	3.436	2.834	2.712
6	2.584	2.237	2.198
8	2.126	2.046	2.132
10	1.968	1.998	2.084
12	1.881	1.974	2.054
14	1.849	1.986	1.972

A.1.4 Pure component repeatability experiments

Table A.7: Repeatability experiments for Nafion-212 and pure water

Temperature	Hours	Total permeate run 1 (g)	Total permeate run 2 (g)
35˚C	2	7.010	5.142
	4	3.246	3.154
	6	3.189	3.078
	8	2.962	3.126
	10	3.086	3.119
55˚C	2	17.852	18.761
	4	18.645	18.627

	6	18.744	18.593
	8	18.593	18.648
	10	18.424	18.481

Table A.8: Repeatability experiments for Nafion-212 and pure acid

Temperature	Hours	Total permeate run 1 (g)	Total permeate run 2 (g)
25˚C	2	0.010	0.008
	4	0.006	0.005
	6	0.007	0.007
	8	0.006	0.007
	10	0.005	0.006
45˚C	2	0.049	0.050
	4	0.043	0.048
	6	0.046	0.046
	8	0.050	0.047
	10	0.046	0.045

Table A.9: Repeatability experiments for Nafion-117 and pure water

Temperature	Hours	Total permeate run 1 (g)	Total permeate run 2 (g)
25˚C	2	3.436	2.834
	4	2.584	2.147
	6	2.126	2.061
	8	1.968	2.086

	10	1.881	1.994
45˚C	2	5.271	5.214
	4	5.049	5.036
	6	5.148	5.098
	8	5.146	5.147
	10	4.962	5.109

Table A.10: Repeatability experiments for Nafion-117 and pure acid

Temperature	Hours	Total permeate run 1 (g)	Total permeate run 2 (g)
35˚C	2	0.010	0.009
	4	0.011	0.010
	6	0.008	0.008
	8	0.009	0.011
	10	0.012	0.012
55˚C	2	0.084	0.079
	4	0.078	0.082
	6	0.082	0.084
	8	0.078	0.078
	10	0.082	0.079

A.2 Binary components pervaporation experiments

Table A.11: Total permeate (g) for Nafion-212 membrane with binary components

Temperature	Hours	20vol% water	40vol% water	60vol% water	80vol% water	100vol% water
25˚C	2	1.132	1.254	1.374	1.521	1.740
	4	1.098	1.247	1.368	1.517	1.627
	6	1.104	1.244	1.370	1.513	1.699
	8	1.135	1.248	1.365	1.519	1.720
	10	1.110	1.250	1.372	1.524	1.678
55˚C	2	11.341	13.673	15.867	17.563	17.852
	4	11.338	13.658	15.852	17.527	18.645
	6	11.325	13.671	15.869	17.533	18.744
	8	11.332	13.678	15.871	17.540	18.593
	10	11.338	13.669	15.853	17.544	18.424

Table A.12: Total permeate (g) for Nafion-117 membrane with binary components

Temperature	Hours	20vol% water	40vol% water	60vol% water	80vol% water	100vol% water
25˚C	2	1.034	1.165	1.289	1.456	1.623
	4	1.042	1.158	1.279	1.462	1.627
	6	1.039	1.160	1.281	1.463	1.678
	8	1.041	1.167	1.276	1.458	1.627
	10	1.047	1.165	1.271	1.461	1.678

55˚C	2	10.854	12.987	14.342	16.248	17.968
	4	10.826	13.021	14.376	16.424	17.975
	6	10.857	12.986	14.351	16.239	17.977
	8	10.869	12.992	14.366	16.245	17.969
	10	10.855	13.007	14.358	16.244	17.972

A.2.1 Sodium hydroxide Titration

Table A.13: NaOH (g) used in sulfuric acid titration for Nafion-membrane

Temperature	Hours	20vol% water	40vol% water	60vol% water	80vol% water
25˚C	2	0.00980	0.01306	0.01796	0.02294
	4	0.00898	0.01339	0.01886	0.02335
	6	0.00898	0.01322	0.01935	0.02318
	8	0.00980	0.01290	0.01861	0.02286
	10	0.00980	0.01331	0.01918	0.02351
55˚C	2	0.07510	0.09878	0.11918	0.14367
	4	0.07673	0.09714	0.11592	0.14612
	6	0.07837	0.09551	0.12000	0.14449
	8	0.07429	0.09469	0.11918	0.14694
	10	0.07592	0.10041	0.11673	0.14612

Table A.14: NaOH (g) used in sulfuric acid titration for Nafion-membrane

Temperature	Hours	20vol% water	40vol% water	60vol% water	80vol% water
25˚C	2	0.00784	0.01135	0.01616	0.02090
	4	0.00767	0.01118	0.01567	0.02065
	6	0.00792	0.01110	0.01584	0.02024
	8	0.00776	0.01159	0.01551	0.02049
	10	0.00784	0.01143	0.01576	0.02008
55˚C	2	0.07020	0.08735	0.10122	0.12571
	4	0.06857	0.08816	0.09959	0.12735
	6	0.06939	0.08490	0.10204	0.12408
	8	0.07102	0.08735	0.01041	0.12490
	10	0.06776	0.08571	0.01122	0.12571

A.2.2 Binary mixture repeatability experiments

Table A.15: Binary mixture experiments at 40 vol% water in feed and 55˚C

Membrane	Hours	40vol% water original run	40vol% water Run 1	40vol% water Run 2	40vol% water Run 3
Nafion-212	2	13.673	13.603	13.657	13.891
	4	13.654	13.612	13.659	13.925
	6	13.671	13.589	13.662	13.973
	8	13.678	13.594	13.665	13.814
	10	13.669	13.625	13.659	13.792

Nafion-117	2	12.987	13.258	12.871	12.965
	4	13.021	13.221	12.894	12.971
	6	12.986	13.164	12.902	13.058
	8	12.992	13.297	12.876	12.847
	10	13.007	13.231	12.915	12.932

A.3 Sorption experiments

Table A.16: Measured results of sorption experiments for Nafion-212

25˚C			**55˚C**		
X_{H2O}	**W_0**	**W_∞**	**X_{H2O}**	**W_0**	**W_∞**
0	0.145	0.204	0	0.146	0.207
20	0.138	0.193	20	0.157	0.214
40	0.153	0.218	40	0.152	0.216
60	0.146	0.236	60	0.148	0.237
80	0.150	0.247	80	0.140	0.231
100	0.158	0.268	100	0.139	0.242

With x the volume fraction water in the solution, W_0 the initial mass (g) of the dry membrane strip and W_∞ the mass (g) at equilibrium.

Table A.17: Measured results of sorption experiments for Nafion-117

25°C			55°C		
X_{H2O}	W_0	W_∞	X_{H2O}	W_0	W_∞
0	0.186	0.248	0	0.178	0.243
20	0.183	0.242	20	0.183	0.244
40	0.179	0.249	40	0.184	0.261
60	0.182	0.283	60	0.183	0.287
80	0.181	0.286	80	0.180	0.291
100	0.185	0.302	100	0.182	0.301

With x the volume fraction water in the solution, W_0 the initial mass (g) of the dry membrane strip and W_∞ the mass (g) at equilibrium.

Appendix B: Calculated data

B.1 Pure component pervaporation experiments

B.1.1 Pure water

In Appendix A the permeate values obtained from the experiments were given in terms of grams and moles permeate produced. In order to determine the permeate flux values the following calculations were done:

The flux values are given in terms of (moles/hour.m^2). The membrane surface area has a diameter of 10cm – thus the surface area is

$$\text{Area} = \pi * r^2 \qquad \text{(B-1)}$$

Area = 78.5cm^2

Thus for example, calculating the flux value for the Nafion-212 membrane at 55˚C after 2 hours it will be

17.852g permeate	1 Mol water			1 cm^2
	18g	2 hours	78.5 cm^2	0.0001 m^2

If all the units are cancelled out you are left with the permeate flux value of 63.170 (mol.hr^{-1}.m^{-2}). The following table shows all the calculated flux values for the Nafion-212 membrane with pure water.

Table B.1: Calculated permeate flux for Nafion-212 membrane with pure water

Temperature	Hours	Permeate (g)	Permeate (mol)	Flux (mol/hour.m^2)
25˚C	2	3.966	0.220	14.033
	4	1.627	0.090	5.757
	6	1.699	0.094	6.012
	8	1.720	0.095	6.086

	10	1.678	0.093	5.937
35˚C	2	7.010	0.389	24.805
	4	3.246	0.180	11.486
	6	3.189	0.177	11.284
	8	2.962	0.164	10.481
	10	3.086	0.171	10.920
45˚C	2	11.975	0.665	42.374
	4	9.292	0.506	32.880
	6	9.068	0.513	32.087
	8	9.222	0.512	32.632
	10	8.960	0.497	31.705
55˚C	2	17.852	0.991	63.170
	4	18.645	1.035	65.976
	6	18.744	1.041	66.326
	8	18.593	1.032	65.792
	10	18.422	1.023	65.194

The same calculations applied for the determination of the permeate flux values for the Nafion-117 membrane with pure water, and the results are shown below.

Table B.2: Calculated permeate flux for Nafion-117 membrane with pure water

Temperature	Hours	Permeate (g)	Permeate (mol)	Flux (mol/hour.m^2)
25˚C	2	4.197	0.233	14.851
	4	3.436	0.190	12.158
	6	2.584	0.143	9.143
	8	2.126	0.118	7.523
	10	1.968	0.109	6.963
35˚C	2	5.318	0.295	18.818
	4	3.656	0.203	12.937
	6	3.506	0.194	12.406
	8	3.574	0.198	12.646
	10	3.402	0.189	12.038
45˚C	2	5.217	0.292	18.651
	4	5.049	0.280	17.866
	6	5.148	0.286	18.216
	8	5.146	0.285	18.209
	10	4.962	0.275	17.558
55˚C	2	17.844	0.993	63.282
	4	15.669	0.870	55.445
	6	15.587	0.865	55.155
	8	15.273	0.848	54.044
	10	15.413	0.856	54.539

B.1.2 Proof of Steady-state experiments

In pervaporation experiments, it is important to reach a steady-state as these values obtained are used during calculations of experimental error and all further calculations and modeling. In order to determine when steady-state is reached for both of the membranes, 3 experimental runs were completed at 25˚C using pure water as the feed. The values obtained from these experiments are given in Appendix A. The calculated flux values for the Nafion-212 membrane are given in Figure B.3 below and for the Nafion-117 membrane in Table B.4. The flux values are determined with the same calculations as for the pure water experiments above.

Table B.3: Steady-state calculations for Nafion-212 membrane at 25˚C

Hours	Run 1 total flux (mol/hour.m^2)	Run 2 total flux (mol/hour.m^2)	Run 3 total flux (mol/hour.m^2)
2	14.033	9.359	10.233
4	5.757	6.096	6.022
6	6.012	6.082	5.849
8	6.086	5.920	5.750
10	5.937	5.760	5.806
12	5.732	5.969	5.810
14	5.877	5.902	5.831

Table B.4: Steady-state calculations for Nafion-117 membrane at 25˚C

Hours	Run 1 total flux (mol/hour.m^2)	Run 2 total flux (mol/hour.m^2)	Run 3 total flux (mol/hour.m^2)
2	14.851	13.991	13.612
4	12.158	10.028	9.596
6	9.143	7.915	7.777
8	7.523	7.239	7.544
10	6.969	7.070	7.374

12	6.656	6.985	7.268
14	6.542	7.027	6.978

B.1.3 Pure Sulfuric acid

As was the case for the pure water data, the permeate flux values for pure sulfuric acid were noted in Appendix A in terms of grams. To determine the flux values in terms of (moles/hour.m^2) the following calculations were made:

For example, calculating the permeate flux values for the Nafion-212 membrane after 2 hours at 55˚C will give

0.094 permeate	1 Mol H_2SO_4			1 cm^2
	98g	2 hours	78.5 cm^2	0.0001 m^2

This gives a permeate flux value of 0.061 (mol/hour.m^2) after canceling out the units. All the calculated flux values are given in the table below for the Nafion-212 membrane.

Table B.5: Calculated permeate flux for Nafion-212 membrane with pure sulfuric acid

Temperature	Hours	Permeate (g)	Flux (mol/hour.m^2)
25˚C	2	0.010	0.00649
	4	0.006	0.00389
	6	0.007	0.00454
	8	0.006	0.00389
	10	0.005	0.00324
35˚C	2	0.013	0.00844
	4	0.012	0.00779
	6	0.012	0.00779

	8	0.011	0.00714
	10	0.013	0.00844
45˚C	2	0.049	0.03184
	4	0.043	0.02794
	6	0.046	0.02989
	8	0.050	0.03249
	10	0.046	0.02989
55˚C	2	0.094	0.06109
	4	0.085	0.05524
	6	0.090	0.05849
	8	0.088	0.05719
	10	0.096	0.06239

The same calculations applied for the determination of the permeate flux values for the Nafion117 membrane using sulfuric acid.

Table B.6: Calculated permeate flux for Nafion-117 membrane with pure sulfuric acid

Temperature	Hours	Permeate (g)	Flux (mol/hour.m^2)
25˚C	2	0.007	0.00454
	4	0.006	0.00389
	6	0.007	0.00454
	8	0.006	0.00389
	10	0.005	0.00324

35˚C	2	0.010	0.00649
	4	0.011	0.00714
	6	0.008	0.00519
	8	0.009	0.00584
	10	0.012	0.00779
45˚C	2	0.049	0.03184
	4	0.045	0.02924
	6	0.050	0.03249
	8	0.046	0.02989
	10	0.048	0.03119
55˚C	2	0.084	0.05459
	4	0.078	0.05069
	6	0.082	0.05329
	8	0.078	0.05069
	10	0.082	0.05329

B.1.4 Pure component selectivity

For the determination of the pure component selectivity, it was simply calculated by dividing the calculated water permeate value with the sulfuric acid permeate values under similar conditions. For example the pure water permeate flux value for the Nafion-212 membrane at 55˚C after 2 hours was determined as 63.170 (mol/hour.m^2) and the corresponding value for the pure sulfuric acid was calculated as 0.06109 (mol/hour.m^2). Therefore, the pure component selectivity can be calculated as

63.170/0.06109 = 1033.981

with selectivity being a dimensionless parameter. The table below gives the calculated selectivity values for the Nafion-212 membrane.

Table B.7: Pure component selectivity values for Nafion-212 membrane

Temperature	Hours	Water Flux (mol/hour.m^2)	Acid Flux (mol/hour.m^2)	Selectivity
25˚C	2	14.033	0.00649	2159.266
	4	5.757	0.00389	1476.351
	6	6.012	0.00454	1321.444
	8	6.086	0.00389	1560.740
	10	5.937	0.00324	1827.155
35˚C	2	24.805	0.00844	2935.811
	4	11.486	0.00779	1472.722
	6	11.284	0.00779	1446.861
	8	10.481	0.00714	1466.040
	10	10.920	0.00844	1292.427
45˚C	2	42.374	0.03184	1330.555
	4	32.880	0.02794	1176.506
	6	32.087	0.02989	1073.265
	8	32.632	0.03249	1004.173
	10	31.705	0.02989	1060.483
55˚C	2	63.170	0.06109	1033.981
	4	65.976	0.05524	1194.254
	6	66.326	0.05849	1133.896

	8	65.792	0.05719	1150.324
	10	65.194	0.06239	1044.879

The same calculations applied for the determination of the pure component selectivity for the Nafion-117 membrane and the results are shown below.

Table B.8: Pure component selectivity values for Nafion-117 membrane

Temperature	Hours	Water Flux (mol/hour.m^2)	Acid Flux (mol/hour.m^2)	Selectivity
25˚C	2	14.851	0.00454	3264.333
	4	12.158	0.00389	3117.851
	6	9.143	0.00454	2009.777
	8	7.523	0.00389	1929.148
	10	6.963	0.00324	2142.933
35˚C	2	18.818	0.00649	2895.355
	4	12.937	0.00714	1809.535
	6	12.406	0.00519	2386.027
	8	12.646	0.00584	2162.049
	10	12.038	0.00779	1543.500
45˚C	2	18.651	0.03184	585.666
	4	17.866	0.02924	610.866
	6	18.216	0.03249	560.560
	8	18.209	0.02989	609.067
	10	17.558	0.03119	526.819

55˚C	2	63.282	0.05459	1159.148
	4	55.445	0.05069	1093.705
	6	55.155	0.05329	1034.909
	8	54.044	0.05069	1066.064
	10	54.539	0.05329	1023.356

B.1.5 Pure component repeatability calculations

In Chapter 3 the repeatability of the pervaporation experiments were discussed. During certain pure component experiments the experimental run was repeated in order to check the validity of the pervaporation results. The data obtained from these repeated runs are given in Appendix A. The total permeate flux values were calculated in the same manner as for all the pure component experiments above, and the results for the Nafion-212 membrane is given in Table B.9 and in Table B.10 for the Nafion-117 membrane.

Table B.9: Repeatability Experiments for Nafion-212 and pure components

		Pure Water		**Pure acid**	
Temperature	**Hours**	**Flux Run 1 (mol/hour.m^2)**	**Flux Run 2 (mol/hour.m^2)**	**Flux Run 1 (mol/hour.m^2)**	**Flux Run 2 (mol/hour.m^2)**
35˚C	2	24.792	18.186	0.006	0.005
	4	11.480	11.154	0.003	0.003
	6	11.278	10.886	0.004	0.004
	8	10.475	11.055	0.003	0.004
	10	10.914	11.031	0.003	0.003
55˚C	2	63.138	66.353	0.031	0.032
	4	65.945	65.879	0.027	0.031

	6	66.293	65.759	0.029	0.029
	8	65.759	65.953	0.032	0.030
	10	65.161	65.363	0.029	0.029

Table B.10: Repeatability Experiments for Nafion-117 and pure components

		Pure Water		Pure acid	
Temperature	**Hours**	**Flux Run 1 (mol/hour.m^2)**	**Flux Run 2 (mol/hour.m^2)**	**Flux Run 1 (mol/hour.m^2)**	**Flux Run 2 (mol/hour.m^2)**
25˚C	2	12.152	10.023	0.006	0.005
	4	9.139	7.593	0.007	0.006
	6	7.519	7.289	0.005	0.005
	8	6.960	7.377	0.005	0.007
	10	6.652	7.052	0.007	0.007
45˚C	2	18.642	18.440	0.054	0.051
	4	17.857	17.811	0.050	0.053
	6	18.207	18.030	0.053	0.054
	8	18.200	18.203	0.050	0.050
	10	17.549	18.069	0.053	0.051

B.2 Binary solution pervaporation experiments

B.2.1 Flux determination

In Appendix A the data was given for the total permeate produced for the binary solution pervaporation experiments. This data was given in the form of grams permeate produced. In order to determine the binary flux in terms of (mol/hour.m^2) some calculations need to be made. Firstly, to convert the grams produced to mole values, an assumption was made that because the permeate consist predominantly of water, with only approximately 1% sulfuric acid in the permeate in all cases, the molecular weight was taken as that of water, thus 18g/mol.

Thus the flux calculations was completed as follows: For the Nafion-212 membrane with 20 vol% water at 55˚C the binary flux is determined with

11.341g permeate	1 mol water			1 cm^2
	18g	2 hours	78.5 cm^2	0.0001 m^2

which gives a flux value of 40.130 (mol/hour.m^2). The table below shows the calculated binary flux values for the Nafion-212 membrane.

Table B.11: Binary flux data for Nafion-212 membrane

Temperature	Hours	20vol% water	40vol% water	60vol% water	80vol% water	100vol% water
25˚C	2	4.005	4.437	4.861	5.382	6.157
	4	3.885	4.412	4.840	5.368	5.757
	6	3.906	4.401	4.847	5.353	6.012
	8	4.016	4.416	4.830	5.375	6.086
	10	3.927	4.423	4.854	5.392	5.937
55˚C	2	40.130	48.382	56.146	62.147	63.170
	4	40.120	48.315	56.093	62.020	65.976

	6	40.074	48.375	56.153	62.041	66.326
	8	40.099	48.400	56.160	62.066	65.792
	10	40.120	48.368	56.096	62.116	65.194

The binary flux values for the Nafion-117 membrane was similarly calculated and the results given below.

Table B.12: Binary flux data for Nafion-117 membrane

Temperature	Hours	20vol% water	40vol% water	60vol% water	80vol% water	100vol% water
25˚C	2	3.658	4.122	4.561	5.152	5.743
	4	3.687	4.097	4.525	5.173	5.757
	6	3.676	4.104	4.532	5.176	5.937
	8	3.683	4.129	4.515	5.159	5.757
	10	3.704	4.122	4.497	5.168	5.937
55˚C	2	38.407	45.955	50.750	57.494	63.581
	4	38.435	46.075	50.870	57.473	63.605
	6	38.418	45.951	50.782	57.462	63.612
	8	38.460	45.973	50.835	57.484	63.584
	10	38.411	46.026	50.806	57.480	63.595

B.2.2 Sodium Hydroxide titration

During the binary solution pervaporation experiments, a standardized sodium hydroxide titration procedure was completed in order to determine the amount sulfuric acid present in the binary flux produced. The amount of sodium hydroxide that was added before the endpoint was reached is given in Appendix A in terms of grams. As the amounts added were very small, it

was done on a lab-scale and the change in weight was noted as the sodium hydroxide solution was added.

To determine the amount of sulfuric acid present the following calculations were completed:

Firstly, the amount of sodium hydroxide added in terms of grams was divided by the molecular weight of NaOH (40g/mole) to determine the amount of moles added. According to stoichiometry in the equilibrium equation, 2 moles of sodium hydroxide reacts with one mole of sulfuric acid, thus the amount of moles is divided by 2 to give the amount of moles sulfuric acid present in the binary flux. For example taking the binary flux for the Nafion-212 membrane after 2 hours at the 20 vol% water, the calculation is as follows:

0.07510g NaOH used / 40g/mol NaOH = 0.001877 mole NaOH

0.00187mole NaOH used = 0.9387×10^{-3} mol H_2SO_4 present in binary flux.

Table B.13: H_2SO_4 (x 10^{-3} mol) present in binary permeate for Nafion-212 membrane

Temperature	Hours	20vol% water	40vol% water	60vol% water	80vol% water
25˚C	2	0.1224	0.1632	0.2244	0.2867
	4	0.1122	0.1673	0.2357	0.2918
	6	0.1122	0.1653	0.2418	0.2897
	8	0.1224	0.1612	0.2326	0.2857
	10	0.1224	0.1663	0.2397	0.2938
55˚C	2	0.9387	1.2346	1.4897	1.7959
	4	0.9591	1.2142	1.4489	1.8265
	6	0.9795	1.1938	1.5000	1.8061
	8	0.9285	1.1836	1.4897	1.8367
	10	0.9489	1.2551	1.4591	1.8265

Table B.14: H_2SO_4 (x 10^{-3} mol) present in binary permeate for Nafion-117 membrane

Temperature	Hours	20vol% water	40vol% water	60vol% water	80vol% water
25˚C	2	0.0979	0.1418	0.2020	0.2612
	4	0.0959	0.1397	0.1959	0.2581
	6	0.0989	0.1387	0.1979	0.2530
	8	0.0969	0.1448	0.1938	0.2561
	10	0.0979	0.1428	0.1969	0.2510
55˚C	2	0.8775	1.0918	1.2653	1.5714
	4	0.8571	1.1020	1.2448	1.5918
	6	0.8673	1.0612	1.2755	1.5510
	8	0.8877	1.0918	1.2551	1.5612
	10	0.8469	1.0714	1.2653	1.5714

B.2.3 Binary composition selectivity calculations

Nafion-212 membrane

To calculate the membrane selectivity when binary compositions are used, the following equation is used

$$\alpha = \frac{\mathbf{y_i}/(\mathbf{1}-\mathbf{y_i})}{\mathbf{x_i}/(\mathbf{1}-\mathbf{x_i})} \qquad \text{(B-2)}$$

In this formula i represent the preferentially permeating species, in our case water, and x and y represent the weight fraction of each of the components in the feed and permeate, respectively. Thus the weight percent water and acid should be determined for both the feed and permeate.

From the titration data calculated above, the number of moles sulfuric acid present in the permeate was determined. These values should be converted to weight values in order to use it

in the selectivity formula. To do this the number of moles is multiplied by the molecular weight of sulfuric acid, 98g/mol. This is shown in the following table

Table B.15: H_2SO_4 (g) present in binary permeate for Nafion-212 membrane

Temperature	Hours	20vol% water	40vol% water	60vol% water	80vol% water
25˚C	2	0.0120	0.0160	0.0220	0.0281
	4	0.0110	0.0164	0.0231	0.0286
	6	0.0110	0.0162	0.0237	0.0284
	8	0.0120	0.0158	0.0228	0.0280
	10	0.0120	0.0163	0.0235	0.0288
55˚C	2	0.0920	0.1210	0.1460	0.1760
	4	0.0940	0.1190	0.1420	0.1790
	6	0.0960	0.1170	0.1470	0.1770
	8	0.0910	0.1160	0.1460	0.1800
	10	0.0930	0.1230	0.1430	0.1790

To determine the amount of water in the binary permeate, the total permeate values are taken and the amount of sulfuric acid in the binary permeate is subtracted. For example to calculate the amount of water in the binary permeate at 55˚C after two hours:

11.341(g) total permeate – 0.0920(g) H_2SO_4 = 11.249(g) water in binary permeate.

Table B.16: Weight (g) of water in the binary flux for the Nafion-212 membrane

Temperature	Hours	20vol% water	40vol% water	60vol% water	80vol% water
25˚C	2	1.1200	1.2380	1.3520	1.4929
	4	1.0870	1.2306	1.3449	1.4884
	6	1.0930	1.2278	1.3463	1.4846
	8	1.1230	1.2322	1.3422	1.4910

	10	1.0980	1.2337	1.3485	1.4952
55˚C	2	11.249	13.552	15.721	17.387
	4	11.224	13.535	15.710	17.348
	6	11.229	13.554	15.722	17.356
	8	11.2451	13.562	15.725	17.360
	10	11.245	13.546	15.710	17.375

For the selectivity calculations, the weight fraction of the preferentially permeating species, thus water, should be determined in both the feed as well as the binary permeate. To calculate the weight fraction water in the feed, it should be noted that in all the experiments 2L was used and the composition was taken as volume %. For example, calculating the weight fraction water in the feed for the 40 vol% composition we have

800 ml water x 1 kg/L (density) = 800g water

1200 ml sulfuric acid x 1.83 kg/L (density) = 2196g sulfuric acid

Thus the total weight is 800g + 2196g = 2996g

Weight fraction water = 800g / 2996g = 0.2670

These calculations were completed for all the different feed compositions and the results are shown in the table below.

Table B.17: Weight fraction of water in the binary feed

Composition	Weight water (g)	Weight acid (g)	Weight fraction water	Weight fraction acid
20 vol% water	400	2928	0.1201	0.8798
40 vol% water	800	2196	0.2670	0.7329
60 vol% water	1200	1464	0.4504	0.5495
80 vol% water	1600	732	0.6861	0.3138

To determine the weight fraction water in the binary permeate, the same calculations are used as above. The weight of water in the binary permeate is divided by the total permeate to give a weight fraction. For example at 55˚C after two hours, the weight fraction water is

11.249(g) water in permeate / 11.341(g) total permeate = 0.9918 fraction water.

Table B.18: Weight fraction water in binary permeate for the Nafion-212 membrane

Temperature	Hours	20vol% water	40vol% water	60vol% water	80vol% water
25˚C	2	0.9893	0.9872	0.9839	0.9815
	4	0.9899	0.9868	0.9831	0.9811
	6	0.9900	0.9869	0.9827	0.9812
	8	0.9894	0.9873	0.9832	0.9815
	10	0.9891	0.9869	0.9828	0.9811
55˚C	2	0.9918	0.9911	0.9907	0.9899
	4	0.9917	0.9912	0.9910	0.9897
	6	0.9915	0.9914	0.9907	0.9899
	8	0.9919	0.9915	0.9908	0.9897
	10	0.9917	0.9910	0.9909	0.9898

To calculate the selectivity the formula can now be used as all the necessary data is available. For example, calculating the membrane selectivity for the 20 vol% water at 55˚C after 2 hours:

(0.9918/(1 – 0.9918)) / (0.1201/(1 – 0.1201))

= 895.0291

These selectivity calculations were completed for all the different compositions and temperatures, and the results are given in the following table.

Table B.19: Membrane selectivity for a binary solution using Nafion-212 membrane

Temperature	Hours	20vol% water	40vol% water	60vol% water	80vol% water
25˚C	2	683.200	212.394	74.974	24.306
	4	723.349	205.975	71.029	23.809
	6	727.341	208.043	69.303	23.915
	8	685.030	214.075	71.819	24.361
	10	669.780	207.761	70.007	23.751
55˚C	2	895.029	307.440	131.367	45.196
	4	875.596	312.214	134.973	454.339
	6	856.211	317.997	130.481	44.860
	8	904.221	320.928	131.40	44.123
	10	885.090	302.307	134.029	44.408

Nafion-117 membrane

All the calculations for the Nafion-117 membrane are similar to those for the Nafion-212 membrane, thus only the calculated data will be given and not all the calculations. The following table shows the amount of sulfuric acid in the binary permeate.

Table B.20: H_2SO_4 (g) present in binary permeate for Nafion-117 membrane

Temperature	Hours	20vol% water	40vol% water	60vol% water	80vol% water
25˚C	2	0.0096	0.0139	0.0198	0.0256
	4	0.0094	0.0137	0.0192	0.0253
	6	0.0097	0.0136	0.0194	0.0248
	8	0.0095	0.0142	0.0190	0.0251
	10	0.0096	0.0140	0.0193	0.0246

55˚C	2	0.0860	0.1070	0.1240	0.1540
	4	0.0840	0.1080	0.1220	0.1560
	6	0.0850	0.1040	0.1250	0.1520
	8	0.0870	0.1070	0.1230	0.1530
	10	0.0830	0.1050	0.1240	0.1540

In the table below the amount of water in the binary permeate is given in terms of grams for the Nafion-117 membrane.

Table B.21: Weight (g) of water in the binary flux for the Nafion-117 membrane

Temperature	Hours	20vol% water	40vol% water	60vol% water	80vol% water
25˚C	2	1.0244	1.1511	1.2692	1.4304
	4	1.0326	1.1443	1.2598	1.4367
	6	1.0293	1.1464	1.2616	1.4382
	8	1.0315	1.1528	1.2570	1.4329
	10	1.0374	1.1510	1.2517	1.4364
55˚C	2	10.768	12.880	14.218	16.094
	4	10.778	12.913	14.254	16.086
	6	10.772	12.882	14.226	16.087
	8	10.782	12.885	14.243	16.092
	10	10.772	12.902	14.234	16.090

Table B.22: Weight fraction water in binary permeate for the Nafion-117 membrane

Temperature	Hours	20vol% water	40vol% water	60vol% water	80vol% water
25˚C	2	0.9907	0.9880	0.9846	0.9824
	4	0.9909	0.9881	0.9849	0.9826
	6	0.9906	0.9882	0.9848	0.9830
	8	0.9908	0.9878	0.9851	0.9827
	10	0.9908	0.9879	0.9848	0.9831
55˚C	2	0.9920	0.9917	0.9913	0.9905
	4	0.9922	0.9917	0.9915	0.9903
	6	0.9921	0.9919	0.9912	0.9906
	8	0.9919	0.9917	0.9914	0.9905
	10	0.9923	0.9919	0.9913	0.9905

Table B.23: Membrane selectivity for a binary solution using Nafion-117 membrane

Temperature	Hours	20vol% water	40vol% water	60vol% water	80vol% water
25˚C	2	781.105	227.321	78.203	25.562
	4	804.109	229.277	80.049	25.979
	6	776.750	231.387	79.337	26.531
	8	794.797	222.847	80.712	26.117
	10	791.017	225.678	79.123	26.713
55˚C	2	916.532	330.426	139.886	47.811
	4	939.225	328.205	142.540	47.175
	6	927.659	340.010	138.845	48.419

	8	907.175	330.554	141.272	48.118
	10	950.012	337.295	140.044	47.799

B.2.4 Binary mixture repeatability experiments

As mentioned in chapter 3, for the binary mixture repeatability experiments it was decided to repeat the experiment for both membranes where 40vol% water is fed at 55˚C, as this scenario best fits the HyS objective . This experiment was repeated 4 times and from this the experimental error could be calculated. The flux values were calculated in the same manner as shown above for the binary mixture experiments. Table B.24 shows the obtained flux values for both the Nafion-212 and Nafion-117 membranes.

Table B.24: Flux values (mol/hour.m^2) for the repeatability experiments of the binary mixture

Membrane	Hours	40vol% water original run	40vol% water Run 1	40vol% water Run 2	40vol% water Run 3
Nafion-212	2	48.358	48.110	48.301	49.129
	4	48.291	48.142	48.308	49.249
	6	48.351	48.061	48.319	49.419
	8	48.376	48.078	48.330	48.857
	10	48.344	48.188	48.308	48.779
Nafion-117	2	45.932	46.890	45.521	45.854
	4	46.052	46.759	45.603	45.875
	6	45.928	46.558	45.631	46.183
	8	45.949	47.028	45.507	45.436
	10	46.002	46.795	45.677	45.737

B.3 Sorption experiments

In Appendix A the results obtained from the sorption experiments are given for both of the membranes. To demonstrate the calculations as example will be shown of the sequence followed to obtain the results. For this purpose the calculation for the Nafion-212 membrane will be shown at 20 vol% water in the solution at 25˚C.

The swelling ratio is a measure of the mass fraction uptake (M_t) of solvent by the membrane strips and can be calculated by the following equation

$$M_t = (W_t - W_0) / W_0 \qquad \text{(B-3)}$$

where W_0 is the initial mass of the dry membrane strip and W_t is the measured mass after an elapsed time t. To calculate the swelling ratio at equilibrium (M_∞)

$$M_\infty = (W_\infty - W_0) / W_0 \qquad \text{(B-4)}$$

$M_\infty = (0.193 - 0.138) / 0.138 = 0.398$

In Table B.25 the calculated results for the swelling ratio for the Nafion-212 membrane is given and for Nafion-117 in Table B.26.

Table B.25: Calculated swelling ratio results for Nafion-212 membrane

25˚C				**55˚C**		
X_{H2O}	**W_0**	**W_∞**	**M_∞**	**W_0**	**W_∞**	**M_∞**
0	0.145	0.204	0.403	0.146	0.207	0.417
20	0.138	0.193	0.398	0.157	0.214	0.362
40	0.153	0.218	0.422	0.152	0.216	0.415
60	0.146	0.236	0.616	0.148	0.237	0.595
80	0.150	0.247	0.639	0.140	0.231	0.651
100	0.158	0.268	0.697	0.139	0.242	0.745

With x the volume fraction water in the solution, W_0 the initial mass (g) of the dry membrane strip, W_∞ the mass (g) at equilibrium and M_∞ the swelling ratio.

Table B.26: Calculated swelling ratio results for Nafion-212 membrane

	25˚C			55˚C		
X_{H2O}	W_0	W_∞	M_∞	W_0	W_∞	M_∞
0	0.186	0.248	0.331	0.178	0.243	0.363
20	0.183	0.242	0.319	0.183	0.244	0.333
40	0.179	0.249	0.390	0.184	0.261	0.417
60	0.182	0.283	0.552	0.183	0.287	0.563
80	0.181	0.286	0.582	0.180	0.291	0.613
100	0.185	0.302	0.634	0.182	0.301	0.653

With x the volume fraction water in the solution, W_0 the initial mass (g) of the dry membrane strip, W_∞ the mass (g) at equilibrium and M_∞ the swelling ratio.

Appendix C: Statistical inference and experimental error

Overview

In this Appendix the basic terminology that is used in statistical inference will be overviewed and the experimental reproducibility and error will be calculated. In section C.1 the uncertainties and confidence intervals in measurement will be discussed with reference to the Central Limit Theorem. In section C.2 the experimental reproducibility and error of the pervaporation experiments for both the pure component and the binary mixture experiments will be calculated.

C.1 Uncertainties and confidence intervals in measurement

When conducting experiments every measurement taken of a specific quantity is subject to a degree of experimental uncertainty. This means that when a certain measurement of a specific quantity is repeated, there will be some variation in the values observed. Thus the uncertainty gives a clear indication on the amount of variation present in the measured values. The uncertainty is more commonly referred to as the experimental error. In this Appendix the variation in experimental measurements will be quantified.

When working with measured values of a particular quantity, the mean (μ) value is regarded as the best and most accurate measurement of the specific quantity (Devore & Farnum, 2005). The standard deviation, on the other hand, can be defined as a measure of the spread of the specific set of data. The Central Limit Theorem is frequently used in engineering applications when the spread of data needs to be quantified or estimated. According to Vardeman (1994), the Central Limit Theorem states that if you have values $x_1,x_2,..,x_n$ that are random variables (with mean μ and variance δ^2), for a large number of variables n, the variable $\bar{x}$ (sample mean) can be approximated as normally distributed. Thus the normal contribution with mean μ and variance δ^2 can be used for the approximation of probabilities for $\bar{x}$.

From the Central Limit Theorem it can be concluded that if the sample mean ($\bar{x}$) is approximately normal with a population mean given as μ and the standard deviation as δ, the probability that

$$\mu - z\frac{\delta}{\sqrt{n}} < \bar{x} < \mu + z\frac{\delta}{\sqrt{n}} \quad \text{(C-1)}$$

for p > 0.5, is approximately 1 – 2(1-p), where z is the p quantile of the standard normal distribution.

In other words, if

$$\bar{x} \approx N\left(\frac{\delta 2}{n}\right) \quad \text{(C-2)}$$

and

$$\frac{\bar{x}}{\delta/\sqrt{n}} \approx N(0,1) \quad \text{(C-3)}$$

Then the probability can be written as

$$P\left[-z < \frac{\bar{x}-\mu}{\delta/\sqrt{n}} < +Z\right] = 1 - 2(1-p) \quad \text{(C-4)}$$

For p > 0.5 and z the p quantile.

Equation C.1 can be rewritten as

$$\bar{x} - z\frac{\delta}{\sqrt{n}} < \mu < \bar{x} + z\frac{\delta}{\sqrt{n}} \quad \text{(C-5)}$$

Which results in the eventuality that the random interval endpoints

$$\bar{x} \pm z\frac{\delta}{\sqrt{n}} \quad \text{(C-6)}$$

brackets the unknown (μ). This equation can therefore be used to calculate the confidence interval for a population mean. For a desired confidence, the z value should be chosen in such a manner that the standard normal probability between –z and z corresponds to that confidence level. In the table below different z values is given for some commonly used confidence levels (Devore & Farnum, 2005)

Table C.1: Z-values to be used in two-sided large-n intervals for μ

Desired Confidence	z-values
80%	1.280
90%	1.654
95%	1.960
98%	2.330
99%	2.580

C.2 Calculations of pervaporation experimental error

As mentioned above in the overview, the experimental error was calculated for both the pure component and the binary mixture pervaporation experiments. For the pure component experiments the experimental error was calculated by repeating the pure water experiment at 25˚C for both membranes. This experiment was repeated three times and the results obtained for both the membranes are summarized in table C.2.

Table C.2: Pure component pervaporation experimental reproducibility data for both membranes

Experiment	Hours	Total permeate 212 (g)	Total permeate 117 (g)
Run 1	2	3.966	4.197
	4	1.627	3.436
	6	1.699	2.584
	8	1.720	2.126
	10	1.678	1.968
	12	1.620	1.881

	14	1.661	1.849
Run 2	2	2.645	3.954
	4	1.723	2.834
	6	1.719	2.237
	8	1.673	2.046
	10	1.628	1.998
	12	1.687	1.974
	14	1.668	1.986
Run 3	2	2.892	3.847
	4	1.702	2.712
	6	1.653	2.198
	8	1.625	2.132
	10	1.641	2.084
	12	1.642	2.054
	14	1.648	1.972

For the Nafion-212 membrane it was proven that it reaches steady-state after 4 hours, while for the Nafion-117 membrane it reaches steady-state after 6 hours, thus the experimental values from thereon were used in the experimental error calculations. In table C.3 below the steady-state results are given.

Table C.3: Pure component Steady-state μ results for both membranes

	Permeate μ for Nafion-212	**Permeate μ for Nafion-117**
Run 1	1.6675	2.081
Run 2	1.683	2.048
Run 3	1.651	2.088

The calculations will be shown for the Nafion 212 membrane.

Mean value = 1.667

The standard deviation is calculated by using

$$\frac{\sum(x_i - \bar{x})^2}{n-1} \qquad \text{(C-7)}$$

Which gives the standard deviation (σ) = 0.016

The 95% confidence interval = $\bar{x} \pm z\frac{\delta}{\sqrt{n}}$ = ± 1.96 x $0.024/(\sqrt{3})$ = 0.018

This produces the following limits

Upper limit = 1.685

Lower limit = 1.649

Experimental error (%) = (2 x 0.018)/1.667 x 100 = 2.1%

The same calculations were completed for the Nafion-117 membrane and it was found that the experimental error is 2.3%. For the binary mixture pervaporation experiments it was decided to repeat the experiment with 40 vol% water in the feed at 55˚C four times for both of the membranes. These specific operating conditions were chosen as it best fits the HyS objectives as described in Chapter 3. Table C.4 presents the results obtained from the repeated experiments.

Table C.4: Binary mixture pervaporation experimental reproducibility data for both membranes

Membrane	Hours	40 vol%water original	40 vol%water Run 1	40 vol%water Run 2	40 vol%water Run 3
Nafion-212	2	13.673	13.603	13.657	13.891
	4	13.654	13.612	13.659	13.952
	6	13.671	13.589	13.662	13.973
	8	13.678	13.594	13.665	13.814
	10	13.669	13.625	13.659	13.792
Nafion-117	2	12.987	13.258	12.871	12.965
	4	13.021	13.221	12.894	12.971
	6	12.986	13.164	12.902	13.058
	8	12.992	13.297	12.867	12.847
	10	13.007	13.231	12.915	12.932

Table C.5 gives the steady-state results calculated for both of the Nafion membranes.

Table C5: Binary mixture Steady-state μ results for both membranes

	Permeate μ for Nafion-212	**Permeate μ for Nafion-117**
Run 1	13.669	12.998
Run 2	13.604	13.234
Run 3	13.660	12.889
Run 4	13.879	12.954

The experimental error calculations are the same as explained above for the pure component experiments. The calculated results give an experimental error of 1.72% for the Nafion-212 membrane and 2.20% for Nafion-117.

Appendix D: Modeling of pervaporation results

The aim of the section is to determine whether a simplified model, which is based on the solution-diffusion mechanism, can be developed in order to correctly fit the experimental results obtained and predict similar pervaporation results. The three models investigated are the Greenlaw, Long and the Suzuki and Onozato models. The pervaporation results used, were those obtained from the Nafion-212 membrane using a feed concentration of 60 vol% water at 55℃, and this is shown in Table D.1.

Table D.1: Experimental results obtained from pervaporation experiments

Volume fraction water	Flux (mol/(hr.m^2))	Flux (ml/hr.m^2)
0	0	0
0.05	8.407	151.337
0.1	33.520	603.375
0.2	40.130	722.356
0.4	48.382	870.891
0.6	56.146	1010.636
0.8	62.147	1118.662
1	63.170	1137.070

The three models used, as given in Section 2.5, were fitted with the experimental data using the computer aided program Statistica, and a set of predicted values were obtained from each of the models. Table D.2 gives the predicted values calculated from the models compared to the actual observed experimental values.

Table D.2: Predicted values of the three fitted models

Observed values	Suzuki and Onozato	Long	Greenlaw
0	0	0	0
151.337	257.386	72.249	153.381
603.375	454.276	144.505	296.150
722.356	720.102	289.036	549.851
870.891	966.676	578.180	929.905
1010.636	1051.107	867.431	1140.162
1118.662	1080.018	1156.789	1180.622
1137.070	1089.917	1446.254	1051.286

These predicted values obtained from the models were used to determine which of the models gives the best fit or have the best capability to represent the experimental data the best. For this purpose the standard deviation for the three models is calculated using

$$\mathrm{SD} = \sqrt{\frac{\sum(y_{\mathrm{exp}} - y_{\mathrm{calc}})^2}{\mathrm{N}-\mathrm{p}}} \qquad \text{(D-1)}$$

where y_{exp} and y_{calc} represent the experimentally obtained values and the calculated values, respectively, N the number of data points and p the number of fitted parameters. In this calculation N is equal to 8 and the number of fitted parameters is 3 for the Suzuki and Onozato model and 2 for Long and Greenlaw. The calculated values are given in Table D.3.

In the three models a number of constant were calculated from the results obtained from the models. The constants are given in Table D.3.

Table D.3: Values for SD and modeling constants calculated for the three models

Model	SD	$D_i^0.\rho_m/L$	B_{ij} (-)	B_{ii} (-)
Suzuki and Onozato	97.911	2102.572	0.004	-5.354
Long	318.282	1946770	0.0007	-
Greenlaw	161.042	4.800	1.509	-

From the constants shown above, the limiting diffusion coefficient (D_i^0) can be calculated. The density of the membrane is given as 1970 kg/m^3 and the thickness of the membrane is 50.8 µm. Thus from the values shown in Table D.3 the limiting diffusion coefficients are calculated and the order of magnitude can be compared to values found in literature in order to validate the values obtained.

Appendix E: Separation capabilities calculations

E.1 Vapor-liquid equilibrium data

Table E.1: VLE data for the flash separation of water and sulfuric acid

Mass fraction H_2O	Total Temperature	Vapor mass fraction H_2O	Vapor mass fraction H_2SO_4	Liquid mass fraction H_2O	Liquid mass fraction H_2SO_4
0	274.802	0	1	0	1
0.025	170.607	0.957601	0.042398	0.025641	0.974359
0.051	147.557	0.989839	0.010160	0.051282	0.948717
0.076	136.283	0.995500	0.004499	0.076923	0.923076
0.102	129.292	0.997437	0.002562	0.102564	0.897435
0.128	124.441	0.998329	0.001670	0.128205	0.871794
0.153	120.844	0.998817	0.001182	0.153846	0.846153
0.179	118.054	0.999114	0.000885	0.179487	0.820512
0.205	115.819	0.999310	0.000689	0.205128	0.794871
0.230	113.983	0.999447	0.000552	0.230769	0.769230
0.256	112.447	0.999546	0.000453	0.256410	0.743589
0.282	111.140	0.999621	0.000378	0.282051	0.717948
0.307	110.014	0.999679	0.000320	0.307692	0.692307
0.333	109.033	0.999726	0.000273	0.333333	0.666666
0.358	108.170	0.999763	0.000236	0.358974	0.641025
0.384	107.406	0.999794	0.000205	0.384615	0.615384
0.410	106.723	0.999820	0.000179	0.410256	0.589743
0.435	106.109	0.999842	0.000157	0.435897	0.564102
0.461	105.554	0.999860	0.000139	0.461538	0.538461
0.487	105.050	0.999876	0.000123	0.487179	0.512820
0.512	104.591	0.999890	0.000109	0.512820	0.487179
0.538	104.169	0.999903	9.68E-05	0.538461	0.461538
0.564	103.782	0.999914	8.59E-05	0.564102	0.435897
0.589	103.424	0.999923	7.62E-05	0.589743	0.410256

0.615	103.093	0.999932	6.76E-05	0.615384	0.384615
0.641	102.786	0.999940	5.98E-05	0.641025	0.358974
0.666	102.500	0.999947	5.28E-05	0.666666	0.333333
0.692	102.233	0.999953	4.64E-05	0.692307	0.307692
0.717	101.983	0.999959	4.06E-05	0.717948	0.282051
0.743	101.749	0.999964	3.53E-05	0.743589	0.256410
0.769	101.528	0.999969	3.05E-05	0.769230	0.230769
0.794	101.321	0.999974	2.60E-05	0.794871	0.205128
0.820	101.126	0.999978	2.19E-05	0.820512	0.179487
0.846	100.941	0.999982	1.80E-05	0.846153	0.153846
0.871	100.766	0.999985	1.45E-05	0.871794	0.128205
0.897	100.601	0.999988	1.12E-05	0.897435	0.102564
0.923	100.444	0.999991	8.10E-06	0.923076	0.076923
0.948	100.295	0.999994	5.22E-06	0.948717	0.051282
0.974	100.153	0.999997	2.53E-06	0.974359	0.025641
1	100.017	1	0	1	0

E.2 Pervaporation efficiency data

Table E.2: Percentage sulfuric acid present in total permeate for Nafion-212 at 25˚C

20 vol% water	40 vol% water	60 vol% water	80 vol% water
1.060	1.275	1.601	1.847
1.001	1.315	1.688	1.885
0.996	1.302	1.729	1.877
1.057	1.266	1.670	1.843
1.081	1.304	1.712	1.889

Table E.3: Percentage sulfuric acid present in total permeate for Nafion-212 at 55˚C

20 vol% water	40 vol% water	60 vol% water	80 vol% water
0.811	0.884	0.920	1.002
0.829	0.871	0.895	1.021
0.847	0.855	0.926	1.009
0.803	0.848	0.919	1.026
0.820	0.899	0.902	1.019

Table E.4: Percentage sulfuric acid present in total permeate for Nafion-117 at 25˚C

20 vol% water	40 vol% water	60 vol% water	80 vol% water
0.928	1.193	1.536	1.758
0.902	1.183	1.501	1.730
0.933	1.172	1.514	1.695
0.912	1.216	1.489	1.721
0.916	1.201	1.518	1.683

Table E.5: Percentage sulfuric acid present in total permeate for Nafion-117 at 55˚C

20 vol% water	40 vol% water	60 vol% water	80 vol% water
0.792	0.823	0.864	0.947
0.773	0.829	0.848	0.960
0.782	0.800	0.871	0.936
0.800	0.823	0.856	0.941
0.764	0.807	0.863	0.948

E.3 Concentration of sulfuric acid

For the calculations of the concentration of sulfuric acid in the pervaporation process, a simple mass balance was completed over the process unit. For the calculations the feed concentration of 60 vol% water (approximately 55 wt% sulfuric acid) was used as this best fits the scenario simulated in the reference design. The feed to the pervaporation process was measured as 50 ml/min, which is converted to 3 000 g/hr. The obtainable permeate flux values were then used for both of the Nafion membranes at the two different temperatures to determine the flux mass flow of the permeate stream. The concentration of sulfuric acid in the stream during the pervaporation experiments was also used to calculate the amount of sulfuric acid leaving the system as permeate.

The retentate stream was then calculated as the feed mass flow rate minus the permeate mass flow rate, and the component balance of the water and sulfuric acid was used to determine the concentration of the retentate stream. Table E.6 and E.7 give the mass balance data for Nafion-212 at 25℃ and 55℃, respectively.

Table E.6: Mass balance calculation for Nafion-212 at 25℃

	Total (g)	Water (g)	Sulfuric acid (g)
Feed	3000	1351.35	1648.64
Permeate	87.21	85.70	1.50
Retentate	2912.78	1254.64	1647.13

Table E.7: Mass balance calculation for Nafion-212 at 55℃

	Total (g)	Water (g)	Sulfuric acid (g)
Feed	3000	1351.35	1648.64
Permeate	1010.25	1000.95	9.29
Retentate	1989.74	350.394	1639.35

Table E.8 and E.9 gives the calculated mass balance data for Nafion-117 at 25℃ and 55℃, respectively.

Table E.8: Mass balance calculation for Nafion-117 at 25℃

	Total (g)	Water (g)	Sulfuric acid (g)
Feed	3000	1351.35	1648.64
Permeate	81.55	80.31	1.23
Retentate	2918.44	1271.03	1647.41

Table E.9: Mass balance calculation for Nafion-117 at 55℃

	Total (g)	Water (g)	Sulfuric acid (g)
Feed	3000	1351.35	1648.64
Permeate	915.20	907.24	7.95
Retentate	2084.79	444.10	1640.69